

Tumor-inducing signal transduction of the heme oxygenase 1 product carbon monoxide

Dissertation

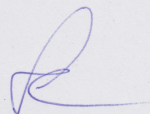
Zur Erlangung der Würde des Doktors der Naturwissenschaften
des Fachbereichs Biologie, der Fakultät für Mathematik,
Informatik und Naturwissenschaften
der Universität Hamburg

vorgelegt von
Julia Schildgen
aus Tallinn

Hamburg Januar 2014

Genehmigt vom Fachbereich Biologie
der Fakultät für Mathematik, Informatik und Naturwissenschaften
an der Universität Hamburg
auf Antrag von Frau Professor Dr. G. TIEGS
Weiterer Gutachter der Dissertation:
Professor Dr. T. DOBNER
Tag der Disputation: 17. Januar 2014

Hamburg, den 02. Januar 2014

A handwritten signature in blue ink, consisting of a stylized 'L' followed by a horizontal stroke.

Professor Dr. C. Lohr
Vorsitzender des
Fach-Promotionsausschusses Biologie

Meinem Mann Markus



Heinrich-Pette-Institut
Leibniz-Institut für Experimentelle Virologie

Carol Stocking, Ph.D.
Retrovirus Pathogenesis, Head
Phone: +49-40-48051 273
Fax: +49-40-48051 187
Email: stocking@hpi.uni-hamburg.de

Studienbüro Biologie
z.H. Frau Sült-Wüpping
MIN Fakultät
Universität Hamburg
Biozentrum Klein Flottbek
Ohnhorststr. 18
22609 Hamburg

12. November 2013

Sehr geehrte Damen und Herrn,

hiermit bestätige ich, dass die von Frau Julia Schildgen mit dem Titel " Tumor-inducing signal transduction of the heme oxygenase 1 product carbon monoxide " vorgelegte Doktorarbeit in korrektem Englisch geschrieben ist.

Mit freundlichen Grüßen,

Dr. Carol Stocking

Leiterin der FG Retrovirus Pathogenesis
Heinrich-Pette-Institut
(Amerikanerin)

Heinrich-Pette-Institut
Leibniz-Institut für
Experimentelle Virologie

Martinistrasse 52-20251 Hamburg
Telefon +49 (0) 40 480 51-0
Telefax +49 (0) 40 48051-103
hpi@hpi.uni-hamburg.de

Bankverbindung
Haspa (200 505 50)
Konto 1001 315 959
www.hpi-hamburg.de

Mitglied der



Abstract

Chronic inflammation of the liver, which is characterized by repetitive cycles of cell death and regeneration thus promoting the accumulation of genetic mutations, is responsible for the development of more than 90% of hepatocellular carcinoma (HCC). Among others the heme-degrading enzyme heme oxygenase 1 (HO-1/*HMOX1*) is overexpressed in HCC. In general, HO-1 has anti-inflammatory, anti-viral, anti-oxidative, and anti-apoptotic properties, whereas the latter point can be attributed to its catalytic product carbon monoxide (CO). It was shown that knock-down of HO-1 results in reduced tumor mass and increased apoptotic rates of tumor cells, whereas the induction of HO-1 during early steps of inflammation interferes with chronic inflammation and fibrogenesis.

One hallmark of cancer, including HCC, is the resistance against apoptosis. We hypothesized that HCC cells, which overexpress HO-1, have advantage in contrast to healthy cells because of CO-mediated anti-apoptotic signaling. This thesis focuses on the cytoprotective anti-apoptotic effects of CO against induced cellular damage in primary murine hepatocytes. The aim of the study was to investigate CO-dependent signal transduction and the effectors, which mediate this protective effect. By specifically inhibiting identified signaling pathways and effectors in the next step, HCC therapy could be improved, as tumor cells would be sensitized to apoptotic signaling and therapy.

In order to mimic the *in vivo* situation of a hepatocyte overexpressing HO-1 and being flushed with CO, primary murine hepatocytes were isolated and incubated with the CO donor methylene chloride (MC) *in vitro*. Apoptotic signaling was mediated by cell damage induction with Actinomycin D and tumor necrosis factor alpha (TNF α) (Act.D/TNF α model). CO-dependent cellular changes were determined on RNA and protein level via RT² ProfilerTM PCR Array and 2-dimensional gel electrophoresis (2D PAGE) with subsequent mass spectrometry analysis, respectively. Putative anti-apoptotic gene products of the investigated signaling pathways were further

analyzed via quantitative reverse-transcription polymerase chain reaction (qRT-PCR), Western Blot analysis, and in the Act.D/TNF α model.

The results show that CO inhibited apoptosis, activated survival and proliferative signaling, and modified the mRNA expression of tumor-promoting genes in primary murine hepatocytes. Further, it could be demonstrated that CO activated a positive feedback loop by inducing the expression of HO-1 via nitric oxide (NO) signaling for a permanent elevated CO level.

In summary, this thesis (i) demonstrates CO-dependent anti-apoptotic mechanisms; (ii) provides evidence on multiple CO-mediated proliferative and tumor-promoting signaling pathways and genes; and (iii) depicts the formation of an enhancing positive feedback-loop for sustained HO-1 expression and CO production. This leads to the assumption that CO has a carcinogenic character providing cells with anti-apoptotic and proliferative properties, thus rendering HO-1-overexpressing HCC cells resistant to apoptotic signaling and therapy.

Zusammenfassung

Die chronische Entzündung der Leber, welche sich durch wiederholte Zyklen von Zelltod und Regeneration mit anschließender Akkumulation von Mutationen charakterisiert, ist die Ursache für 90% aller Hepatozellulären Karzinome (HCC).

So wurde bei HCC unter anderem das Häm-abbauende induzierbare Enzym Hämoxygenase 1 (HO-1/*HMOX1*) überexprimiert nachgewiesen. HO-1 hat anti-inflammatorische, anti-virale und anti-apoptotische Eigenschaften, wobei letztere dem katalytischen Abbauprodukt Kohlenstoffmonoxid (CO) zugeschrieben werden kann. Es konnte gezeigt werden, dass eine Hemmung der HO-1 Expression zu reduziertem Wachstum der Tumormasse führt. Gleichzeitig verhindert die Induktion des Enzyms während der frühen, akuten Entzündung die Weiterentwicklung zur chronischen Entzündung und zur Fibrose.

Ein Kernmerkmal von Tumoren, einschließlich des HCCs, ist die Resistenz gegenüber Apoptose. Unserer Hypothese nach sind HO-1 exprimierende HCC-Zellen aufgrund CO-vermittelter anti-apoptotischer Effekte im Vorteil gegenüber gesunden Hepatozyten. Die vorliegende Dissertation fokussiert auf die Untersuchung anti-apoptotischer und damit zellschützender Effekte des CO gegenüber induziertem Zellschaden in primären Hepatozyten der Maus. Zielstellung der Arbeit ist die Erforschung CO-abhängiger Signaltransduktionen und deren Effektoren, die für diesen protektiven Effekt verantwortlich sind. Weiterhin soll die spezifische Hemmung der identifizierten Gene und Proteine erfolgen. Dadurch würde die Tumorzelle gegenüber apoptotischen Signalen sensibilisiert, wodurch sich Verbesserungen in der Therapie ergeben könnten.

Um den *in vivo*-Effekt eines HO-1-exprimierenden Hepatozyten bei Exposition gegenüber CO nachzuahmen, wurden isolierte Hepatozyten der Maus mit dem CO-Donor Methylenchlorid (MC) *in vitro* behandelt. Die Induktion des Zellschadens und damit der Apoptose erfolgte mittels Actinomycin D (Act.D) und des Tumornekrosefaktors alpha (TNF α) (Act.D/TNF α -Modell). CO-abhängige, zelluläre

Veränderungen wurden auf RNA- und Proteinebene mit Hilfe des *RT² ProfilerTM PCR Arrays* sowie der 2-dimensionalen Gelelektrophorese mit anschließender massenspektrometrischer Analyse (2D PAGE) detektiert. Potentielle anti-apoptotische Genprodukte der Signalwege wurden anschließend mit Hilfe der qRT-PCR, der Western Blot Analyse und des Act.D/TNF α -Modells detailliert untersucht.

Die Ergebnisse in primären Hepatozyten zeigen, dass CO die Apoptose verhindert, Überlebens- und Proliferationssignalwege aktiviert, als auch die Expression tumorpromovierender Gene verändert hat. Im Weiteren konnte gezeigt werden, dass CO eine verstärkende Feedback-Schleife aktiviert. In dieser wird die HO-1 Expression über Stickstoffmonoxid (NO)-vermittelte Signalwege induziert und dadurch ein permanent erhöhter CO-Level beibehalten.

Zusammenfassend beschreibt diese Arbeit (i) CO-abhängige anti-apoptotische Mechanismen, (ii) zeigt mehrere proliferations- und tumorpromovierende CO-vermittelte Signalwege und Gene auf und (iii) skizziert den Aufbau einer verstärkenden Feedback-Schleife zur anhaltenden HO-1 Expression und damit zur CO-Erzeugung. Dies führt zu der Annahme, dass CO karzinogene Eigenschaften besitzt, welche einer HO-1-überexprimierten HCC-Zelle nicht nur Überlebens- sondern auch Ausbreitungsvorteile verschaffen, indem diese resistent gegenüber apoptotischen Signalen und damit der Therapie wird.

Contents

1. Introduction	1
1.1. Liver anatomy and function	1
1.2. Liver damage and progression to hepatocellular carcinoma	3
1.3. Heme/heme oxygenase 1 (HO-1) system	7
1.4. CO and CO-dependent cytoprotection	9
1.5. Urea cycle and nitric oxide (NO) metabolism	11
1.6. Aim of the thesis	13
2. Materials and methods	15
2.1. Materials	15
2.1.1. Technical equipment	15
2.1.2. Consumables	16
2.1.3. Reagents and Kits	17
2.1.4. Western Blot Antibodies	21
2.1.5. Oligonucleotides	22
2.1.6. siRNA variants and plasmid DNA	23
2.1.7. Buffers and solutions	23
2.1.8. Software and online databases	26
2.2. Methods	27
2.2.1. Animals and cell lines	27
2.2.2. Isolation of primary murine hepatocytes	27
2.2.3. Dosage and incubation protocols	28
2.2.4. Cell damage measurement	29
2.2.5. Transfection of siRNA and plasmid DNA	29
2.2.6. Luciferase reporter assay	30
2.2.7. Nitric oxide (NO) measurement	30

2.2.8. Quantitative Reverse-Transcription Polymerase Chain Reaction (qRT-PCR).....	30
2.2.9. RT ² Profiler TM PCR Array: PAMM-014D.....	31
2.2.10. Protein isolation and Western Blot analysis.....	32
2.2.11. Two-dimensional polyacrylamide gel electrophoresis (2D PAGE) and protein identification by Liquid chromatography (LC) – Electrospray Ionization (ESI) – Ion trap analysis.....	33
2.2.12. Statistical analysis	34
3. Results.....	35
3.1. Carbon monoxide protects primary mouse hepatocytes from induced cellular damage	35
3.2. CO protection is independent from HO-1	38
3.3. Proteomic analysis of murine primary hepatocytes upon MC via 2D PAGE.....	40
3.4. CO-incubation induced the nitric oxide pathway.....	46
3.5. NO induced <i>Hmox1</i> expression	51
3.6. Carbon monoxide activates the anti-apoptotic sGC-PKG cascade.....	53
3.7. RT ² Profiler TM PCR Array	57
3.8. CO activates the STAT3 signaling pathway.....	62
4. Discussion	64
5. Outlook	77
6. References	78
Eidesstattliche Versicherung	XVII
Danksagung.....	XVIII
Author's contact data.....	XX

Figures

Fig. 1.1	Anatomy of the liver (Gray 1918).	2
Fig. 1.2	Multistep progress of hepatocarcinogenesis (Wong and Ng 2008). ...	4
Fig. 1.3	10 Hallmarks of cancer development and progression (Hanahan and Weinberg 2011).....	5
Fig. 1.4	Schematic representation of heme degradation pathway (Abraham and Kappas 2008).....	8
Fig. 1.5	The urea cycle with incorporated citrulline-NO cycle (modified from Lanpher 2003).....	11
Fig. 3.1	CO-dependent protection of primary mouse hepatocytes (PH) against induced cellular damage.	36
Fig. 3.2	CO-dependent protection against induced cell damage is independent from HO-1 induction in primary hepatocytes (PH)...	39
Fig. 3.3 A	False color representation of overlaid pictures of the first approach of 2D-PAGE.	41
Fig. 3.3 B	False color representation of overlaid pictures of the second approach of the 2D-PAGE.....	42
Fig. 3.4	CO-regulated proteins, which were identified by 2D PAGE, were further summarized from both approaches (A+B) and categorized by their cellular function (see also Tab. 3.1).....	45
Fig. 3.5	MC interacts with the urea/NO cycle.	47
Fig. 3.6	Influence of MC on activation and expression of transcription factors (i.e. NFkB, AP-1, and Hif-1α) of iNOS.....	48
Fig. 3.7	NO-dependent protection of PHs against Act.D/TNFα-induced cellular damage.....	49
Fig. 3.8	Efficiency test of siRNA (iNOS-a and iNOS-b) in Hepa 1-6 cells. ..	50

Fig. 3.9	CO-dependent protection against Act.D/TNFα-induced cell damage is independent from NO as assessed by knock-down and knock-out experiments.	51
Fig. 3.10	Nitric oxide induced the expression of HO-1.	52
Fig. 3.11	Inhibitors of sGC and PKG abrogated MC-dependent protective effect against induced cellular damage in primary murine hepatocytes.	54
Fig. 3.12	Phosphorylation status of kinases ERK1/2 and GSK3-β upon MC incubation in primary hepatocytes.....	55
Fig. 3.13	Possible anti-apoptotic effects of MC concerning the kinase JNK and Bcl-2 in primary hepatocytes.	57
Fig. 3.14	RT² ProfilerTM PCR Array and verification.....	59
Fig. 3.15	Activation of STAT3 signaling upon MC incubation.....	63
Fig. 4.1	Scheme of CO-dependent anti-apoptotic and tumor-promoting mechanisms and the positive feedback loop.....	74

Abbreviations

2D	two-dimensional
Act.D	Actinomycin D
Actb	actin, beta
ad	fill-up to
ANGPT2	angiopoietin 2
ANOVA	analysis of variance
AP-1	activator protein 1
ARG	arginase
ASL/ARLY	argininosuccinate lyase
ASS	argininosuccinate synthase
BCL-2	B cell leukemia/lymphoma 2
BCL-XL	BCL2-like 1
Birc	baculoviral IAP (inhibitor of apoptosis) repeat-containing
BL/6	C57BL/6J
bp	base pairs
Brk	breast cancer kinase
BSA	bovine serum albumin
CaMP	Ca ²⁺ /calmodulin-dependent protein kinase
CASP-3	CASPASE-3
CASP-8	CASPASE-8
cDNA	complementary DNA
cGMP	cyclic guanosine monophosphate
C/EBP	CCAAT-enhancer-binding protein
CoPP	cobalt protoporphyrine IX
CPS1	carbamoylphosphate synthetase 1
CREB	cAMP response element-binding protein
c-Src	(Rous sarcoma oncogene) tyrosine kinase
Cxcl	chemokine (CXC-motif) ligand
DAF-FM	4-Amino-5-Methylamino-2',7'-Difluorofluorescein Diacetate
ECL	enhanced chemiluminescence
EGF	epidermal growth factor
ERK1/2	extracellular-signal-regulated kinases 1/2
ESI	electrospray ionization
Fas(r)	Fas receptor
Fos	FBJ (Finkel–Biskis–Jinkins) osteosarcoma oncogene
GAPDH	glyceraldehyde-3-phosphate dehydrogenase
GROα	growth-related oncogene alpha
GSK-3β	glycogen synthase kinase 3 beta

Gusb	glucuronidase beta
h	hours
HbCO	carboxyhaemoglobin
HBSS	Hanks balanced salt solution
HBV	hepatitis B virus
HCC	hepatocellular carcinoma
HCV	hepatitis C virus
HGF	hepatocyte growth factor
HIF	hypoxia induced factor
HO	heme oxygenase
Hprt1	hypoxanthine guanine phosphoribosyl transferase 1
HSC	hepatic stellate cell
Hsp90ab1	heat shock protein 90 alpha
c-IAP1	inhibitor of apoptosis 1
IL	interleukin
IRF	interferon regulatory factor
JAK	Janus kinase
JNK	c-Jun N-terminal kinase
Jun	Jun oncogene
KC	Kupffer cell
KO	knock-out
L-Arg	L-Arginine
LC	liquid chromatography
LDH	lactate dehydrogenase
MAPK	mitogen-activated protein kinase
MC	methylene chloride
MCL-1	myeloid cell leukemia sequence 1
MGSA	melanoma growth-stimulatory activity
MS/MS	tandem mass spectrometry
Myc	myelocytomatosis oncogene
NAFLD	non-alcoholic fatty liver disease
NADP(H)	Nicotinamide adenine dinucleotide phosphate
NASH	non-alcoholic steatohepatitis
NFκB	nuclear factor kappa B
(i)NOS	(inducible) nitric oxide synthase
ORNT1	ornithine translocase 1
OTC	ornithine transcarbamoylase
PAGE	polyacrylamid gel electrophoresis
pB2luc	pBIIIX-luciferase vector
PH	primary hepatocyte

PI3K	phosphatidylinositide 3-kinase
PIM3	PIM3 oncogene (Provirus integrating site Moloney murine leukemia virus)
PKG	protein kinase G
PLAU	plasminogen activator, urokinase
PM	perfusion medium
PPML	pre-perfusion buffer
PTK6	protein tyrosine kinase 6
Ras	resistance to audiogenic seizures
ROS	reactive oxygen species
SEM	standard error of the mean
sGC	soluble guanylyl cyclase
SNAP	S-Nitroso-N-Acetylpenicillamine
STAT	signal transducer and activator of transcription
TGFα	transforming growth factor alpha
TNF	tumor necrosis factor
VEGF (A)	Vascular endothelial growth factor (alpha)
VEGFR	Vascular endothelial growth factor receptor
VSMC	vascular smooth muscle cell
wt	wild-type
XIAP	X-linked inhibitor of apoptosis

Poster presentations

Julia Solomentsew (birth name), Gabriele Sass and Gisa Tiegs. Carbon monoxide protects primary mouse hepatocytes from induced apoptosis by activating the nitric oxide pathway. 27. Jahrestagung der Deutschen Arbeitsgemeinschaft zum Studium der Leber (GASL) 2011, Regensburg, Germany

Julia Schildgen, Gabriele Sass, Hartmut Schlüter, Gisa Tiegs. Nitric oxide supports carbon monoxide-induced protection from apoptosis in isolated primary mouse hepatocytes. 28. Jahrestagung der Deutschen Arbeitsgemeinschaft zum Studium der Leber (GASL) 2012, Hamburg, Germany

1. Introduction

1.1. Liver anatomy and function

The liver is one of the largest organs in the body and receives 25% of the cardiac output, although it constitutes only 2.5% of body weight (Gray 1918; Lautt 2009). It interacts with the cardiovascular and immune systems, secretes important substances into the gastro-intestinal tract, and stores, degrades, and detoxifies many substrates (Tso and McGill 2004).

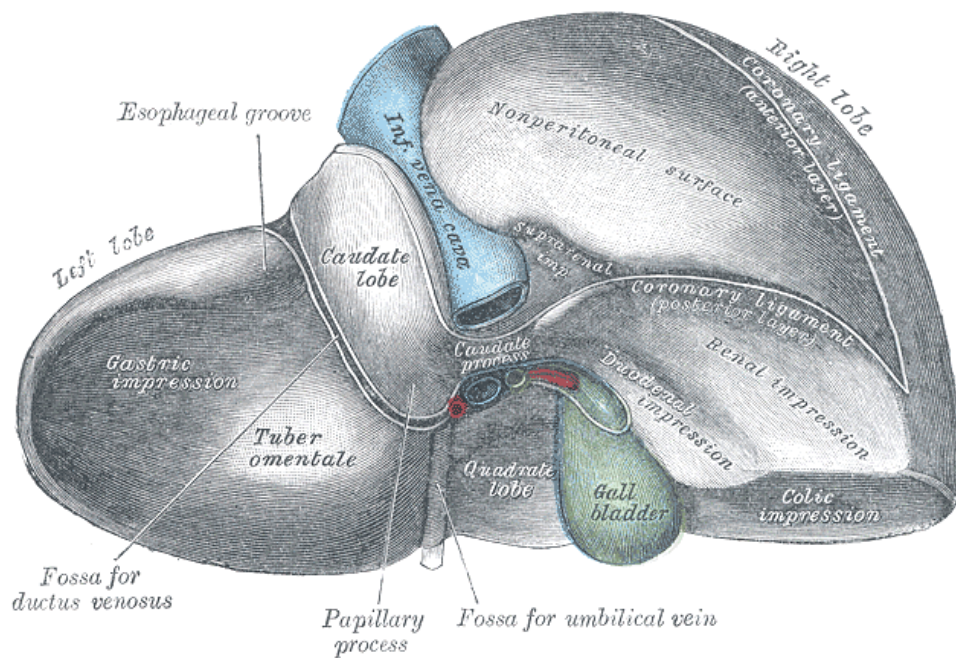
From an anatomical point of view, the liver is divided into four parts, termed the right (*lobus hepatis dexter*), left (*lobus hepatis sinister*), caudate (*lobus caudatus*), and the quadrate lobe (*lobus quadratus*) (Gray 1918) (Fig. 1.1 A). Furthermore, the lobes are subdivided into smaller lobules, which form the general mass of the hepatic substance (Gray 1918) (Fig. 1.1 B). The exchange of gases, i.e. oxygen and carbon dioxide, and the supply with nutrients is carried out by the hepatic portal vein and the hepatic artery.

The lobules, measuring from 1 to 2.5 mm in diameter, consist of a mass of parenchymal cells (i.e. hepatocytes), arranged in irregular radiating columns around blood channels (*sinusoids*) (Fig. 1.1 C). The liver sinusoid is lined with sinusoidal cells (endothelial cells), Kupffer cells, and fat storage cells (also called stellate or Ito cells), which perform important metabolic functions, such as vitamin A storage, collagen secretion, and regulation of sinusoidal portal pressure (Tso and McGill 2004).

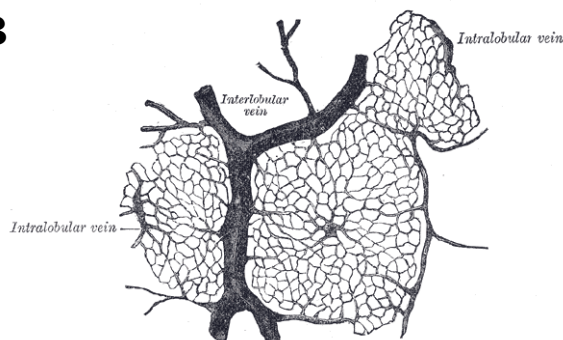
Physiologically the liver is responsible for the synthesis of plasma proteins, growth factors, the bile, lipids, and the degradation of nitrogenous products of amino acids and nucleotides (see section 1.5). Furthermore, multiple lipophilic vitamins, iron, and glycogen are stored in the liver.

The liver is also important for the metabolism of both, nitrogenous and carbohydrate materials, recycling of erythrocyte components, and detoxification of alcohol and drugs (Campbell 2000; Gray 1918).

A



B



C

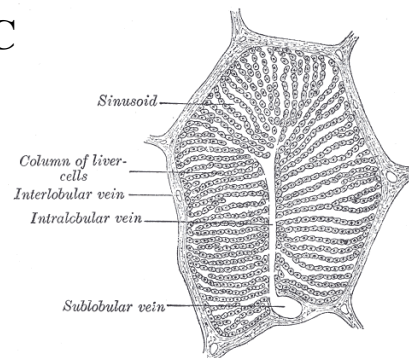


Fig. 1.1 Anatomy of the liver (Gray 1918).

A: Posterior and anterior surfaces. **B:** Section of lobules and vein (dog).
C: Single lobule (pig).

One important and unique feature of the liver is its ability to regenerate. There seems to be a critical ratio between functional liver mass and body mass. Deviations in this ratio trigger a modulation of either hepatocyte proliferation or apoptosis, in order to

maintain the liver's optimal size (Tso and McGill 2004). Besides peptide growth factors, such as transforming growth factor alpha (TGF- α), hepatocyte growth factor (HGF), and epidermal growth factor (EGF), signal transduction pathways including transcription factors, such as nuclear factor kappa B (NF κ B), signal transducer and activator of transcription 3 (STAT3), and activator protein 1 (AP-1), are the regulators for an effective regeneration process (Kurinna and Barton 2011; Tso and McGill 2004).

1.2. Liver damage and progression to hepatocellular carcinoma

Accordingly to the unique ability of the liver to regenerate, there are disadvantageous effects of this property. By providing an inflammatory response towards antigens, such as viruses, drugs, or cellular debris, the organism maintains its health. Under some conditions, it is not possible to clear the antigen completely resulting in chronic infection with inflammation as a major component. This state can progress to fibrosis and malignancy of the tissue. In fact, it was in 1863 that Rudolf Virchow noted leucocytes in neoplastic tissues and established a connection between inflammation and cancer (Balkwill and Mantovani 2001; Virchow 1863).

Regarding the epidemiology of human cancer, hepatocellular carcinoma (HCC) is the fifth most common cancer worldwide and the third most common cause of cancer mortality (Parkin 2001). HCC has several epidemiologic features including marked variations among geographic regions, racial and ethnic groups, and between men and women (El-Serag and Rudolph 2007). For example, most HCC cases (>80%) occur in either sub-Saharan Africa or in Eastern Asia. China alone accounts for more than 50% of the world's cases with higher incidence of men than women (2-4:1) (El-Serag and Rudolph 2007; El-Serag, White, and Nurgalieva 2008).

Regarding carcinogenesis, there are several reported factors, which favor the development of chronic inflammation, fibrosis, cirrhosis, and finally HCC, which is

believed to be a multistep process (Wong and Ng 2008) (Fig. 1.2). The main cause of HCC is viral hepatitis caused by the hepatitis B virus (HBV) or hepatitis C virus (HCV); other major etiologies include hemochromatosis, alcoholic hepatitis, and non-alcoholic steatohepatitis (NASH) (Nakagawa and Maeda 2012). In case of these diseases, the liver undergoes a chronic stimulation due to an antigen-specific immune response, thus triggering the production of various cytokines and growth factors and subsequently inducing compensatory hepatocyte regeneration. This persistent cycle of necro-inflammation and hepatocyte regeneration is thought to increase the risk of genetic mutation in hepatocytes, and, furthermore, to promote survival and expansion of altered cells leading to carcinogenesis (Nakagawa and Maeda 2012). There are several important hallmarks of cancer, such as sustained proliferative signaling, resistance towards cell death, genome instability and mutations, which can be applied to HCC (Fig. 1.3).

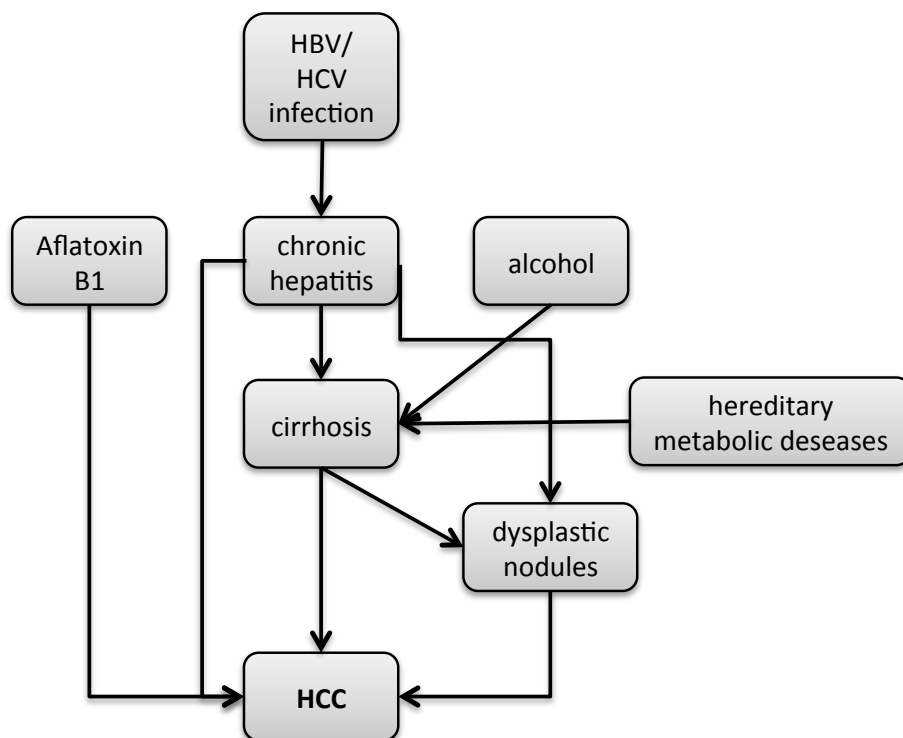


Fig. 1.2 Multistep progress of hepatocarcinogenesis (Wong and Ng 2008).

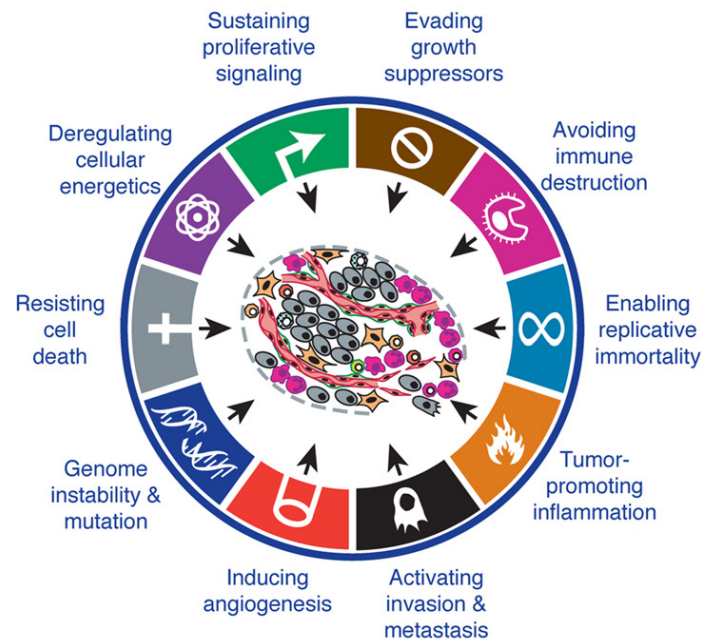


Fig. 1.3 10 Hallmarks of cancer development and progression (Hanahan and Weinberg 2011).

Some of these hallmarks, which are important for this thesis, are described here in more detail: With regard to tumor-promoting inflammation caused by viral hepatitis or other chronic diseases of the liver, various inflammatory cytokines, including tumor necrosis factor alpha (TNF- α), interleukin 1 α (IL-1 α), IL-1 β , IL-6, and IL-8, have been implicated to play an important role. Among these, IL-6 is thought to be one of the most important cytokines (Nakagawa and Maeda 2012).

A further indication is the induction of angiogenesis. In general, angiogenesis occurs under physiological conditions, such as during embryonic development, wound healing, and regeneration processes (Sato et al. 2001), but can also take place under pathophysiological conditions, such as the end-stage of liver cirrhosis and in all stages of human HCC (Kimura et al. 1998; Paternostro 2010). Angiogenesis plays two roles in HCC development: on the one hand, the initial tumor mass has to be provided with nutrients and oxygen for further growth, on the other hand, it favors metastasis formation by shedding and transporting cells from the primary tumor to other organs (Folkman 1990). There are also two important molecular factors for

angiogenesis in the liver: vascular endothelial growth factor A (Vegfa) and angiopoietin 2 (Angpt2) (Fang et al. 2012; Medina et al. 2004; Taura et al. 2008). Blocking each factor separately or simultaneously was reported to suppress angiogenesis and thus increase the efficiency of anti-angiogenic cancer therapy (Fang et al. 2012; Hashizume et al. 2010; Oliner et al. 2004).

Regarding genome instability and mutation it is now widely accepted that stepwise accumulation of mutations in cancer-related genes as well as chromosomal alterations are involved in carcinogenesis (Nishida and Goel 2011). Although the specifics of genome alteration vary immensely between different tumor types, there is a large number of equal genome maintenance and repair defects that have already been documented in human tumors (Hanahan and Weinberg 2011). These are, for example, defects in main biological processes including regulation of p53/ARF, RB/INK4A, and Wnt/ β -catenin pathway (Nishida and Goel 2011). In more detail, 30-60% of HCC carry mutations in the *p53* gene (Nishida and Goel 2011). Associated to this pathway regulating cell cycle, apoptosis, and DNA repair, further mutations of *p14^{ARF}*, *p16^{INK4a}*, *p21^{WAF1}*, and *p27^{KIP1}* genes are known (El-Serag and Rudolph 2007; Nishida and Goel 2011). Deregulation of this pathway and corresponding effectors leads to elevated cell division rates and reduced apoptosis rates.

Another signaling pathway, which is frequently activated (i.e. in 33-67%) in human HCC, is the Wnt/ β -catenin pathway that regulates the expression of several genes indispensable for cell growth, such as *MYC* and *CCND1* (cyclin D1) (Nishida and Goel 2011; Zulehner et al. 2010). While mutations of *CTNNB1* (β -catenin) are rather rare, i.e. 10-30% of HCC with verified activated signaling, other mechanisms activating Wnt signaling, such as secretion of the receptor Frizzled7, contribute to nuclear accumulation of β -catenin (Lee, Kim, and Wands 2006; Zulehner et al. 2010). A further sign of cancer is resistance to cell death. Deregulation of the balance between proliferation and apoptosis is a typical marker for HCC. Many studies are elucidating molecular anti-apoptotic mechanisms, which provide benefit for malignant cells. For example, alterations in the expression and/or activation of p53,

which are frequent in HCC cells, confer them on resistance to chemotherapeutic drugs, such as Sorafenib (Fabregat 2009). Furthermore, many HCCs show activation of anti-apoptotic pathways due to overexpression of anti-apoptotic molecules, such as *BCL2-like 1* (also known as Bcl-XL), *MCL1*, *BIRC2* (also known as c-IAP1), *XIAP* or survivin. Additionally, the expression and/or activation of the JAK/STAT, PI3K/AKT and RAS/ERKs pathways is enhanced in many HCC cells, conferring them on resistance to apoptotic stimuli (Fabregat, Roncero, and Fernandez 2007; Fabregat 2009).

Finally, cancer cells show sustaining proliferative signaling. Normal tissues carefully control the production and release of growth-promoting signals in contrary to cancer cells, which, by deregulating these signals, become masters of their own destinies (Hanahan and Weinberg 2011). Among the most important survival factors are several receptors of tyrosine kinases activated by growth factors, such as epidermal growth factor (EGF), fibroblast growth factors (FGFs) or hepatocyte growth factor (HGF). Their activation triggers the Ras/Raf/MEK1-2/ERK (extracellular signal-regulated protein kinases) pathway and functional transcription factors, such as AP-1, with the consequent induction of cell proliferating gene transcription (Fabregat et al. 2007).

In conclusion, HCC is a heterogeneous type of cancer with bad prognosis and high recurrence rates. The treatment of HCC is difficult because most patients are diagnosed when the tumor is in an advanced stage and is not amenable to potential curative therapy. Thus, improvement of anti-cancer therapy and prevention are the keys to reduce HCC development and its related morbidity and mortality (Lodato et al. 2006).

1.3. Heme/heme oxygenase 1 (HO-1) system

Heme (i.e. iron protoporphyrine IX) is a metal incorporating molecule, which represents the prosthetic group of many enzymes involved in cell respiration, electron

transport chain, and drug detoxification (Graca-Souza 2005). Besides, heme is part of the blood hemoglobin of erythrocytes and is responsible for the gas exchange of the organism. During the degradation process of erythrocytes and hemoproteins, which mainly takes place in the liver, heme is degraded by the rate-limiting enzyme heme oxygenase (HO) producing equal amounts of iron, carbon monoxide (CO), and biliverdin, which is subsequently reduced to bilirubin (Maines 1988) (Fig. 1.4). The degrading function provides the HO enzymes with anti-inflammatory, anti-viral, anti-apoptotic, and anti-oxidative properties, thus being center of intense medical interest (Sass, Barikbin, and Tiegs 2012). The family of HO consists of three isoforms and is encoded by the genes *Hmox1*, *Hmox2*, and *Hmox3*. While two isoforms, HO-1 (*Hmox1*) and HO-2 (*Hmox2*), are well described and investigated, the function of the third isoform, HO-3 (*Hmox3*), is still poorly understood (McCoubrey, Huang, and Maines 1997; Sass et al. 2012). *Hmox2* is constitutively expressed, whereas *Hmox1* is inducible by a variety of stimuli, like heme, metalloporphyrins, cell stress, cytokines, and reactive oxygen species (ROS) (Abraham and Kappas 2008) (Fig. 1.4).

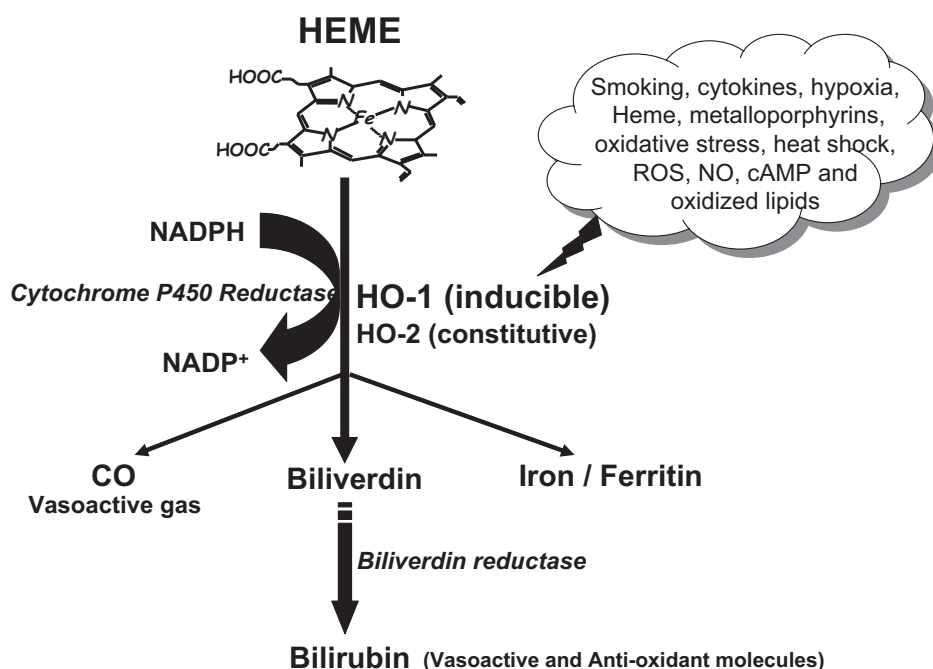


Fig. 1.4 Schematic representation of heme degradation pathway (Abraham and Kappas 2008).

It is supposed that biliverdin/bilirubin is responsible for the anti-oxidative effect of HO, while CO is responsible for the anti-apoptotic effect, thus contributing to the protective property of HO. As HO-1 is a heat shock protein, which is inducible by many cell damaging mechanisms, it might represent an important cell protective tool during acute injury (Abraham and Kappas 2008; Gozzelino, Jeney, and Soares 2010). Endogenous CO is a gasotransmitter and acts as a second messenger, similar to nitric oxide (NO) or hydrogen sulfide (H₂S), but with lower reactivity potential (Gozzelino et al. 2010). It was shown in multiple animal models that either exogenously applied CO or the induction of HO-1 protects the investigated tissue against cellular damage in ischemia-reperfusion models, transplantation experiments, and TNF α -induced apoptosis models (Kim et al. 2008; Wegiel, Chin, and Otterbein 2008; Gozzelino et al. 2010; Wen et al. 2012).

1.4. CO and CO-dependent cytoprotection

For a long time CO was regarded as a hazardous gas, which is generated during incomplete combustion of organic materials, leading to acute and chronic toxicity of the organism (Bauer and Pannen 2009). Indeed, high concentrations of this odorless and colorless gas are detrimental for the organism. The poisoning is diagnosed by measurement and expression of the percentage of carboxyhaemoglobin (HbCO) levels in the blood (Smollin and Olson 2010). Mild poisoning is assumed at 10% of HbCO level and severe poisoning is asserted with levels over 20–25% (Smollin and Olson 2010). CO-mediated intoxication is characterized by vertigo, vomiting, headache, loss of consciousness, and can ultimately result in death (Ryter, Alam, and Choi 2006).

Since the last 40 years, when CO was found to be endogenously generated by HO (Tenhunen, Marver, and Schmid 1969), it remains under investigation because of its unique characteristics and putative therapeutic options. In particular, CO was reported to possess vasoactive, anti-proliferative, anti-oxidant, anti-inflammatory and

anti-apoptotic effects (Bauer and Pannen 2009). In general, these effects result from CO-mediated influence on cell signaling at various points either directly binding to proteins containing a prosthetic heme group or indirectly by yet unknown mechanisms (Gozzelino et al. 2010). Due to these facts, CO is regarded and already tested in clinical trials as a therapeutic agent (Foresti, Bani-Hani, and Motterlini 2008; Hoetzel and Schmidt 2006).

One direct effect of CO is the modulation of soluble guanylyl cyclase (sGC) activity and subsequent stimulation of cyclic guanosine monophosphate (cGMP) production (Hoetzel and Schmidt 2006; Motterlini and Otterbein 2010; Ryter et al. 2006). CO binds to the heme group of sGC and activates the enzyme thus elevating cellular cGMP levels. The second messenger cGMP further modulates a variety of downstream signaling, such as vascular relaxation, immune suppression of platelet aggregation, and neurotransmission (Chung et al. 2008; Francis, Busch, and Corbin 2010).

The indirect effects of CO are quite diverse and not fully understood yet. There is a high evidence that CO activates mitogen-activated protein kinases (MAPK), such as p38, ERK1/2, and JNK1/2, without directly binding to the enzymes (Ryter et al. 2006). Additionally, other signaling pathways are influenced by CO, e.g. the Akt, NF κ B, and STAT pathways (Wegiel, Hanto, and Otterbein 2013). As CO acts via generation of reactive oxygen species (ROS), these important regulators of eukaryotic signal transduction, mentioned above, regulate many biological processes, such as proliferation and apoptosis (Bilban et al. 2008; Gozzelino et al. 2010). These signal transducing pathways and their effectors might be responsible for CO-dependent cytoprotective mechanisms.

1.5. Urea cycle and nitric oxide (NO) metabolism

As previously mentioned, the liver is responsible for detoxification of the organism. One mechanism to dispose of, for example, nitrogenous waste is to incorporate the toxic ammonia group into harmless urea, which is then excreted. This enzymatic process is called the urea cycle, which takes place exclusively in the liver of terrestrial vertebrates, and was discovered by Hans Krebs and Kurt Henseleit in 1932 (Krebs and Henseleit 1932; Shambaugh 1977) (Fig. 1.5). The cycle consists of five steps, which are catalyzed by the two mitochondrial enzymes, Carbamoylphosphate synthetase 1 (CPS I) and Ornithine transcarbamylase (OTC), and the three cytosolic enzymes, Argininosuccinate synthetase (ASS), Argininosuccinate lyase (ASL), and Arginase (ARG) (Lanpher 2003).

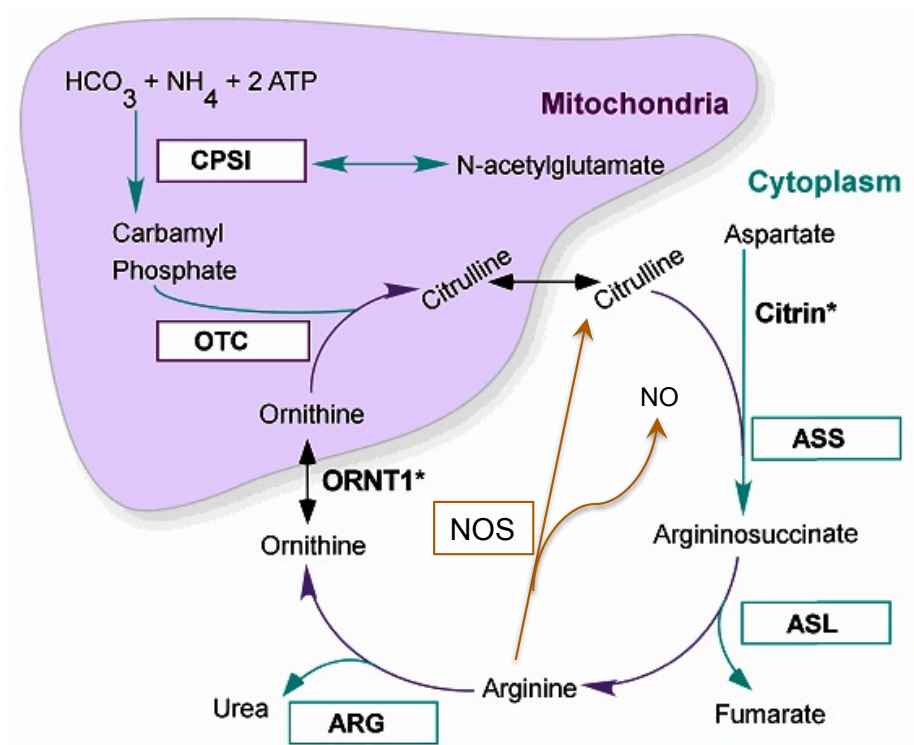


Fig. 1.5 The urea cycle with incorporated citrulline-NO cycle (modified from Lanpher 2003).

CPSI = Carbamoylphosphate synthetase 1; OTC = Ornithine transcarbamylase;
 ASS = Argininosuccinate synthetase; ASL = Argininosuccinate lyase; ARG = Arginase;
 NOS = Nitric oxide synthase; *transporter: ORNT1 = Ornithine translocase; Citrin

Incorporated into the urea cycle is the Citrulline-NO cycle, which is not limited to the hepatocytes but was also detected in other cell types (Morris 2002). This cycle converts Citrulline to L-Arginine (L-Arg), the substrate for nitric oxide synthase (NOS), and thus represents the check point for NO synthesis (Morris 2002). The semi-essential amino acid L-Arg plays an important regulating role for both metabolic cycles, as it is the substrate for both enzymes NOS as well as for ARG (Fig. 1.5). Moreover, L-Arg is the precursor for protein, polyamine, and creatine biosynthesis (Lind 2004). L-Arg metabolism is effectively studied in the context of cancer. Some cancer types, such as melanoma and HCC, are auxotrophic for this amino acid due to the lack of enzymes required for L-Arg synthesis (Lind 2004). Therefore, several clinical studies aim to inhibit tumor growth by degrading L-Arg selectively in malignant cells. L-Arg degrading enzymes, such as arginine deiminase and ARG, were shown to successfully reduce tumor growth and induce apoptosis in animal models and in phase I/II studies (Glazer et al. 2010; Kuo, Savaraj, and Feun 2010; Lind 2004).

Nevertheless, the second messenger NO plays also a role in carcinogenesis by directly modifying DNA and proteins, inhibiting programmed cell death, thus leading to abnormal cell growth (Lind 2004). The family of NOS isoenzymes consists of three members, encoded by distinct genes: inducible NOS (iNOS; *Nos2*), neuronal NOS (nNOS; *Nos1*) and endothelial NOS (eNOS; *Nos3*). *Nos1* and *Nos3* are constitutively expressed at low levels in a variety of cell types and their activity is dynamically regulated by Ca^{2+} /calmodulin. On the contrary, *Nos2* expression is inducible by external stimuli, such as inflammatory cytokines. Once expressed, iNOS is constitutively active (Wu and Morris 1998).

The effects of NO are diverse and depend on the concentration, cell type and other co-induced factors. In general, NO contribute to vasodilation, respiration, cell migration, immune response and apoptosis (Muntané and De la Mata 2010). These effects are classified by cGMP-dependent and cGMP-independent pathways, whereas the latter reaction generates stable nitrosothiols, i.e. posttranscriptional modification

of cysteine residues of proteins (Muntané and De la Mata 2010). In regard to NO signaling and carcinogenesis, there are multiple studies presenting its contrary character: NO can cause DNA damage and protect from cytotoxicity, inhibit and stimulate cell proliferation, and activate anti- and pro-apoptotic signaling (Allen, Demchenko, and Piantadosi 2009; Muntané and De la Mata 2010; Olson and Garbán 2008).

1.6. Aim of the thesis

Chronic inflammation of the liver results in repetitive cycles of cell death and regeneration, thus promoting the accumulation of genetic mutations, which finally can lead to malignant transformation and cancer.

In case of HCC, the heme-degrading enzyme HO-1 was ascertained over-expressed (Abdel Aziz et al. 2008; Calvisi et al. 2007; Sass et al. 2008). HO-1 catabolizes the cleavage of heme to iron, biliverdin, and CO (Maines 1988). In general, HO-1 has anti-inflammatory, anti-viral, anti-oxidative, and anti-apoptotic properties, whereas the latter point can be attributed to CO. It was previously shown that knock-down of *Hmox1* results in reduced tumor mass and increased apoptotic rates of tumor cells (Sass et al. 2008), which indicates its protective effect in tumor cells. On the contrary, induction of *Hmox1* during early steps of inflammation interferes with chronic inflammation, fibrogenesis, and signs of hepatic dysplasia (Barikbin et al. 2012).

One hallmark of cancer, including HCC, is the resistance against apoptosis (Hanahan and Weinberg 2011). Via multiple mechanisms cancer cells gain the ability to circumvent intrinsic as well as extrinsic apoptotic signaling. We hypothesize that HCC cells, overexpressing HO-1, are advantageous in contrast to healthy cells because of CO-mediated anti-apoptotic signaling.

In this thesis, I focused on the protective anti-apoptotic effects of CO against induced cellular damage in primary murine hepatocytes. The aim of the study was to investigate CO-dependent signal transduction pathways and effectors, which mediate the protective effect in order to inhibit them specifically in the next step. Inhibition of these pathways would sensitize tumor cells for apoptotic stimuli and subsequently for therapeutic treatment without influencing healthy cells, which do not express HO-1.

2. Materials and methods

2.1. Materials

2.1.1. Technical equipment

Equipment	Supplier
ATILON ATL-423-I	Acculab Sartorius group, Göttingen, Germany
C1000 Thermal Cycler + CFX 96 Real-Time System	BioRad, Hercules, USA
Casy	Roche, Basel, Switzerland
Centrifuge 5417	Eppendorf, Hamburg, Germany
Centrifuge 5430 R	Eppendorf, Hamburg, Germany
Centrifuge 5810 R	Eppendorf, Hamburg, Germany
Cobas Integra 400 Plus	Roche, Basel, Switzerland
Cobas Mira	Roche, Basel, Switzerland
Eppendorf Research® Plus Pipettes	Eppendorf, Hamburg, Germany
HandyStep® electronic	BRAND GmbH, Wertheim, Germany
Hera Cell 240 Incubator	Thermo Fisher Scientific, Waltham, USA
HERA Safe Clean Bench	Heraeus Instruments, Hanau, Germany
Infinite M200 Photometer	Tecan, Crailsheim, Germany
Innova CO-48 Incubator	New Brunswick Scientific, Nürtingen, Germany
IKAMAGR RCT magnetic stirrer	Janke und Kunkel, Staufen, Germany
Mini-PROTEAN® Cell	Bio-Rad, Hercules, USA
Mini Trans-Blot® Cell	Bio-Rad, Hercules, USA
MSC Advantag, Clean Bench	Thermo Fisher Scientific, Waltham, USA
MyCycler™ Thermal Cycler	Bio-Rad, Hercules, USA
NanoDrop ND-1000	Peqlab, Erlangen, Germany

Neubauer Improved Chamber	Roth, Karlsruhe, Germany
Primus 96 plus	Eurofins MWG, Ebersberg, Germany
PowerPac™ HC Power Supply	Bio-Rad, Hercules, USA
Schlauchpumpe TL/150	Medorex, Nörten-Hardenberg, Germany
Sonorex RK 102H	Bandelin electronics, Berlin, Germany
TE124S scale	Sartorius, Göttingen, Germany
Thermoleader Dry Block Heat Bath	Uniequip, Martinsried, Germany
VersaDoc™ Imaging System 4000 MP	Bio-Rad, Hercules, USA
Vortexer	Heidolph, Schwabach, Germany

2.1.2. Consumables

Consumable	Supplier
Abgene PCR tubes	Thermo Fisher Scientific, Waltham, USA
Cell culture flask	Sarstedt, Nümbrecht, Germany
Cell culture plates, flat or round bottom	Thermo Fisher Scientific, Waltham, USA
Hollow needles/cannulas	B. Braun, Melsungen AG, Melsungen, Germany
Microlon 600 high binding plates	Greiner Bio-one GmbH, Frickenhausen, Germany
MicroWell™ 96-Well Optical-Bottom Plates	Nunc A/S, Roskilde, Denmark
Nylon meshes (100 µm)	BD Falcon, Heidelberg, Germany
Parafilm M	Brand, Wertheim, Germany
PCR tubes	Kisker Biotech GmbH, Steinfurt, Germany
Petridishes	Greiner Bio-One, Solingen, Germany
Pipette tips (10 µl, 200 µl, 1000 µl)	Sarstedt, Nümbrecht, Germany
Pipette tips, sterile and RNase free (10 µl, 20 µl, 200 µl, 1000 µl)	Sarstedt, Nümbrecht, Germany

Pipettes (2 ml, 5 ml, 10 ml, 25 ml)	Sarstedt, Nümbrecht, Germany
Reaction tubes (1.5 ml, 2 ml)	Sarstedt, Nümbrecht, Germany
Reaction tubes (15 ml, 50 ml)	Sarstedt, Nümbrecht, Germany
Reaction tubes, sterile and RNase free (1.5 ml, 2 ml)	Sarstedt, Nümbrecht, Germany
Syringes	B.Braun, Melsungen, Germany
White Microwells 96 Well	Nunc A/S, Roskilde, Denmark

2.1.3. Reagents and Kits

Reagents and Kits	Supplier
Acetic acid (C ₂ H ₄ O ₂)	Roth, Karlsruhe, Germany
Actinomycin D	Sigma-Aldrich, St Louis, USA
Acrylamid/Bis-Acrylamid 28-40%	AppliChem, Darmstadt, Germany
Agarose	Serva, Heidelberg, Germany
Amoniumpersulfat (APS)	Sigma-Aldrich, St Louis, USA
Antibiotic + Antimycotic Mix	Gibco®, Invitrogen, Darmstadt, Germany
Bromophenol blue	Sigma-Aldrich, St Louis, USA
Bovine serum albumin (BSA)	Serva, Heidelberg, Germany
Calcium chlorid (CaCl ₂)	Merck, Whitehouse Station, USA
Co-(III)-Protoporphyrin IX chloride	Frontier Scientific, Utah, USA
Chloramine T hydrate	Roth, Karlsruhe, Germany
Chloroform	Roth, Karlsruhe, Germany
Collagenase D	Roche, Basel, Switzerland
Deoxyribonuclease I (DNase I)	Roche, Basel, Switzerland
Deoxynucleotidetriphosphates (dNTPs, 10mM)	Invitrogen GmbH, Darmstadt, Germany
Dulbecco's modified Eagles Medium (DMEM)	Gibco®, Invitrogen, Darmstadt, Germany
Dichloromethane (Methylene chloride, MC)	Sigma-Aldrich, St Louis, USA

Diethylpyrocarbonate (DEPC)	Sigma-Aldrich, St Louis, USA
D-glucose	Roth, Karlsruhe, Germany
Dimethyl sulfoxide (DMSO)	Sigma-Aldrich, St Louis, USA
Diaminofluorescein-FM (DAF-FM)	Calbiochem, Merck, Darmstadt, Germany
4-Dimethylamino benzaldehyde	Merck, Whitehouse Station, USA
di-sodiumhydrogenphosphatlydrate (Na ₂ HPO ₄)	Roth, Karlsruhe, Germany
Distilled water, RNase free	Thermo Fisher Scientific, Waltham, USA
10x DPBS	Gibco®, Invitrogen, Darmstadt, Germany
ECL Prime Western Blotting Detection Reagent	Amersham Biosciences, GE Healthcare, Uppsala, Sweden
Ethylenediaminetetraacetic acid (EDTA)	Roth, Karlsruhe, Germany
Ethylene glycol tetraacetic acid (EGTA)	Roth, Karlsruhe, Germany
Ethanol	Chemsolute, Th. Geyer, Renningen, Germany
Fetal calf serum (FCS)	Invitrogen, Darmstadt, Germany
Glycerine	Roth, Karlsruhe, Germany
Heparin 5000 (IU/mL)	Sigma-Aldrich, St. Louis, USA
4-(2-hydroxyethyl)-1-piperazineethane sulfonic acid (HEPES)	Roth, Karlsruhe, Germany
Hydrochloric acid (HCL)	Roth, Karlsruhe, Germany
Hydrogen peroxide (H ₂ O ₂)	Roth, Karlsruhe, Germany
Isopropanol	Roth, Karlsruhe, Germany
Ketamin Gräub	Albrecht, Aulendorf, Germany
2,3,9,10,11,12-hexahydro-10R-methoxy- 2,9-dimethyl-1-oxo-9S,12R-epoxy-1H- diindolo[1,2,3-fg:3',2',1'-kl]pyrrolo[3,4-i] [1,6]benzodiazocine-10-carboxylic acid, methyl ester (KT5823)	Tocris Bioscience, Bristol, UK

Lactate dehydrogenase reagents (kit)	Roche, Basel, Switzerland
L-glutamine	Invitrogen, Darmstadt, Germany
Liberase	Roche, Basel, Switzerland
Lipofectamine™ 2000	Invitrogen GmbH, Karlsruhe, Germany
Luminol sodium salt	Sigma-Aldrich, St Louis, USA
Luciferase Assay System	Promega, Mannheim, Germany
Magnesium sulfate heptahydrate (MgSO ₄ ·7 H ₂ O)	Merck, Whitehouse Station, USA
Magnesium chloride hexahydrate (MgCl ₂ ·6 H ₂ O)	Roth, Karlsruhe, Germany
Maxima SYBR green/ROX qPCR Master mix (2x)	Thermo Fisher Scientific, Waltham, USA
2-Mercaptoethanol	Gibco®, Invitrogen, Darmstadt, Germany
Methanol	Roth, Karlsruhe, Germany
(3-(4,5-Dimethylthiazol-2-yl)-2,5-diphenyl- Tetrazolium bromide (MTT)	Sigma-Aldrich, St Louis, USA
N-[2-(methylamino)ethyl]-5-isoquinolinesulfonamide, dihydrochloride (H-8)	Cayman, Tallinn, Estonia
Non-Fat Dry Milk	Bio-Rad, Hercules, USA
NP-40	Sigma-Aldrich, St Louis, USA
Opti-MEM (1X)	Gibco®, Invitrogen, Darmstadt, Germany
ODQ (1H-[1,2,4]oxadiazolo[4,3-a]quinoxalin -1-one)	Cayman, Tallinn, Estonia
RT ² Profiler™ PCR Array: PAMM-014D	SABiosciences, Qiagen GmbH, Hilden, Germany
rDNase Kit	Macherey-Nagel, Düren, Germany
Para-hydroxy coumaric acid	Sigma-Aldrich, St Louis, USA
Penicillin/streptomycin (100 U/mL)	Gibco®, Invitrogen, Darmstadt, Germany
Percoll	GE Healthcare, Chalfont St. Giles, UK

PhosSTOP	Roche, Basel, Switzerland
Ponceau S	Sigma-Aldrich, St Louis, USA
Precesion Plus Protein TM WesternC TM Standard	Bio-Rad, Hercules, USA
1-Propanol	Roth, Karlsruhe, Germany
Protease inhibitor cocktail	Sigma-Aldrich, St Louis, USA
Precision Protein TM StrepTactin Conjugate	Bio-Rad, Hercules, USA
Protein Assay Dye Reagent Concentrate	Bio-Rad, Hercules, USA
Potassium dihydrogen phosphate (KH ₂ PO ₄)	Fluka, Sigma-Aldrich, St Louis, USA
Potassium chloride (KCl)	Roth, Karlsruhe, Germany
Recombinant DNase	Macherey & Nagel, Düren, Germany
Recombinant murine tumor necrosis factor alpha (TNF α)	Innogenetics, Ghent, Belgium
RPMI 1640 (1X) + GlutaMAX TM -I	Gibco®, Invitrogen, Darmstadt, Germany
Sedaxylan	WDT, Gabsen, Germany
S-Nitroso-N-acetylpenicillamine (SNAP)	Calbiochem, Merck, Darmstadt, Germany
Sodium chloride (NaCl)	AppliChem, Darmstadt, Germany
Sodium dodecyl sulfate (SDS)	AppliChem, Darmstadt, Germany
Sodium hydrogen carbonate (NaHCO ₃)	Roth, Karlsruhe, Germany
Sodium hydroxide (NaOH)	Roth, Karlsruhe, Germany
Sodium hydrogen phosphate dihydrate (NaHPO ₄ x2 H ₂ O)	Roth, Karlsruhe, Germany
SP600125 (1,9-Pyrazoloanthrone)	Biaffin GmbH & Co KG, Kassel, Germany
Streptavidin horseradish peroxidase (HRP)	R&D, Minneapolis, USA
Sucrose	Roth, Karlsruhe, Germany
Tetrmethylethylenediamine (TEMED)	Sigma-Aldrich, Taufkirchen, Germany

Tris-Base	Sigma-Aldrich, Taufkirchen, Germany
Tris-HCl	Roth, Karlsruhe, Germany
Triton X-100	Fluka, Sigma-Aldrich, St Louis, USA
TRIzol Reagent	Invitrogen, Karlsruhe, Germany
Trypan blue	Sigma-Aldrich, St Louis, USA
Tween-20	Roth, Karlsruhe, Germany
Verso™ cDNA Kit	Thermo Fisher Scientific, Waltham, USA
William's medium E (1X) + GlutaMAX™-I	Gibco®, Invitrogen, Darmstadt, Germany

2.1.4. Western Blot Antibodies

Protein name & origin	Dilution	Supplier
BAX (Δ 21) rabbit	1:200	Santa Cruz Biotechnology, Texas, USA
BID rabbit	1:500	MBL, Woburn, USA
CASPASE-3 rabbit	1:400	Cell Signaling Technology Inc., Danvers, USA
CASPASE-8 rabbit	1:350	Cell Signaling Technology Inc., Danvers, USA
GAPDH mouse	1:1000	5G4, HyTest, Turku, Finland
GSK3- β rabbit	1:1000	Cell Signaling Technology Inc., Danvers, USA
phospho-GSK3- β rabbit	1:1000	Cell Signaling Technology Inc., Danvers, USA
HO-1 rabbit	1:1000	Epitomics, Burlingame, USA
p44/42 (ERK1/2) rabbit	1:1000	Cell Signaling Technology Inc., Danvers, USA
phospho-p44/42 (p-ERK1/2) mouse	1:500	Cell Signaling Technology Inc., Danvers, USA
STAT3 mouse	1:500	Cell Signaling Technology Inc., Danvers, USA

phospho-STAT3 rabbit	1:500	Cell Signaling Technology Inc., Danvers, USA
anti-mouse goat HRP	1:5000	Bio-Rad, Hercules, USA
anti-rabbit goat POD	1:5000	Jackson ImmunoResearch Laboratories Inc., Suffolk, UK

2.1.5. Oligonucleotides

All nucleotides were purchased from Invitrogen, Darmstadt, Germany. The reference number indicates the mRNA number of the NCBI gene bank.

Target gene	Forward primer 5'-3'	Reverse primer 3'-5'	Reference
<i>Arg1</i>	GGAAAGCCAATGAAGAGCTG	CTGGTTGTCAGGGGAGTGTT	NM_007482.3
<i>Asl</i>	TACTACCTGGTCCGCAAAGG	CTGTCCACGCTGTGACTGT	BC016670
<i>Atp5b</i> (mitochondrial ATP Synthase, beta subunit)	ATTGCCATCTTGGGTATGGA	AATGGGTCCCACCATGTAGA	NM_016774
<i>Bcl2</i>	CTGAAGTCATACTTGGATGAC	TTGTTTGAAGCACATACATCC	NM_007536
<i>Birc5</i>	ATCGCCACCTTCAAGAACTG	CAGGGGAGTGCTTTCTATGC	BC004702.1
<i>Ccnd1</i> (Cyclin D1)	AGTGCCTGCAGAAGGAGATT	CACAACTTCTCGGCAGTCAA	NM_007631
<i>Cxcl1</i>	GCTGGGATTACCTCAAGAA	TGGGGACACCTTTTAGCATC	NM_008176
<i>Nos3</i>	TACGCACCCAGAGCTTTTCT	GCAGGATGCCCTAACTACCA	NM_008713
<i>Fas</i> (Fas receptor)	CTGAAGAGCCTGGAAGATCG	GTCACACACCTGGGAGAGGT	NM_007988.3
<i>Fosl1</i>	GAGACCGACAAATTGGAGGA	CAAGTACGGGTCTGGAGAA	NM_010235
<i>Hif1a</i>	CAAGGAGCCTTAAGCTGTC	CTTCACAATCGTAACTGGTC	AF003695
<i>Hmox1</i>	GAGATAGAGCGCAACAAGCAG	CTTGACCTCAGGTGTCATCTC	NM_010442
<i>Nos2</i>	TGGTGGTGACAAGCACATTT	AAGGCCAAACACAGCATACC	NM_010927.3
<i>Jun</i>	TCCCTATCGACATGGAGTC	TGAGTTGGCACCCACTGTTA	NM_010591
<i>Myc</i>	CAACGTCTTGAACGTCAGA	TCGTCTGCTTGAATGGACAG	NM_010849

<i>Cdkn2b</i> (p15)	TTACCAGACCTGTGCACGAC	GCAGATACCTCGCAATGTCA	NM_007670.4
<i>Cdkn1a</i> (p21)	CGGTGGAACCTTGACTTCGT	CAGGGCAGAGGAAGTACTGG	NM_007669
<i>Pim3</i>	CCTTTGAGCAGGATGAGGAG	ACAAAGCCGAAGGTCACAGT	NM_145478
<i>Plau</i>	CCTACAATGCCACAGACCT	TAGAGCCTTCTGGCCACACT	NM_008873.3
<i>Ptk6</i>	AAGACCCAGAGCCTGTCTCA	CCTGAATCTCAGCCTGGAAG	NM_009184.2
<i>Vegfa</i>	CAGGCTGCTGTAACGATGAA	TTTGACCCTTTCCTTTCCT	NM_001025250

2.1.6. siRNA variants and plasmid DNA

siRNA gene target	5'-3' sequence	Supplier
siControl	CGAAUCCUACAAGCGCdTdT	Eurogentec, Cologne, Germany
<i>Hmox1</i>	GCCGAGAATGCTGAGTTCA	Eurogentec, Cologne, Germany
<i>Nos2-a</i>	CCGATTTAGAGTCTTGGTGAA	QIAGEN, Hilden, Germany
<i>Nos2-b</i>	CACATCGGATTTCACCTTGCAA	QIAGEN, Hilden, Germany

Plasmid	Reference
pBIIIX-luciferase vector (pB2luc)	Ghosh, May, and Kopp (1998)

2.1.7. Buffers and solutions

Type	Configuration
Blocking solution (milk)	5% dry milk (w/v) 1x TBST
Blocking solution (BSA)	5% BSA (w/v) 1x TBST
ECL (home-brew): solution A	50 mg luminol added to 200 ml 0,1 M Tris-HCl pH 8,6

ECL (home-brew): solution B	11 mg para-hydroxy coumaric acid added to 10 ml DMSO added H ₂ O ₂ for activation
HBSS	5.4 mM KCl 0.3 mM Na ₂ HPO ₄ x 7 H ₂ O 4.2 mM NaHCO ₃ 1.3 mM CaCl ₂ 0.5 mM MgCl ₂ x 6 H ₂ O 0.6 mM MgSO ₄ x 7 H ₂ O 137 mM NaCl 5.6 mM D-glucose pH 7.4
KHX	8% Sedaxylan (v/v) 12% Ketamin (v/v) 20% Heparin 5000 (IU/mL) (v/v) 60% isotonic NaCl (v/v)
Lysis buffer (protein extraction)	137 mM NaCl 0.5% NP 40 (v/v) 2 mM EDTA 50 mM Tris HCl pH 8,0 10% Glycerol (v/v)
PBS	137.9 mM NaCl 6.5 mM Na ₂ HPO ₄ x 2 H ₂ O 1.5 mM KH ₂ PO ₄ 2.7 mM KCl pH 7.4 (NaOH)
Perfusion medium (PM)	400 mg KCl 190 mg MgSO ₄ x 7 H ₂ O 190 mg MgCl ₂ x 6 H ₂ O 60 mg Na ₂ HPO ₄ x 2 H ₂ O 2.38 g HEPES 8 g NaCl 60 mg KH ₂ PO ₄ 2 g sucrose 220 mg CaCl ₂ 2 g BSA added to 1 L, pH 7.4, sterile filter 1 mg Liberase (added before use)

Ponceau S solution	1% Ponceau S (w/v) 5% acetic acid (v/v) added bi-dist H ₂ O
Pre-perfusion buffer (PPML)	400 mg KCl 58 mg KH ₂ PO ₄ 350 mg NaHCO ₃ 8.06 g NaCl 68 mg NaHPO ₄ x 2 H ₂ O 1 g glucose 190 mg EGTA 11.91 g HEPES added to 1 L, pH 7.35 (NaOH), sterile filter
Running buffer (10x)	2 M glycine 1% SDS (w/v) 2 M Tris-base added to 1L bi-dist H ₂ O
SDS-Loading buffer (4x)	250 mM Tris-base 40% glycerol (v/v) 8% SDS (w/v) 0,1% Bromophenol blue (w/v) 5% β-Mercaptoethanol (v/v), freshly added
TBS (10x)	1,5 M NaCl 100 mM Tris-Base pH 7,4 (HCl)
TBST (10x)	1x TBS 0,1% Tween-20 (v/v)
Transfer buffer (10x)	2 M glycine 250 mM Tris-base
Transfer buffer (1x)	25 mM Tris-base 200 mM glycine 20% methanol (v/v), freshly added

2.1.8. Software and online databases

Software and online databases	Supplier
GraphPad Prism 5	GraphPad Software, La Jolla, USA
Bio-Rad CFX Manager 2.0	Bio-Rad, Hercules, USA
iControl 5.0	Tecan, Crailshaim, Germany
Image Lab TM 2.0	Bio-Rad Laboratories, Inc., Hercules, USA
Mendeley Desktop	Mendeley Ltd., London, UK
Primer3	Whitehead Institute for Biomedical Research, Cambridge, USA
Mascot MS/MS Ions Search server	Matrix Science Inc., Boston, USA
Web-based PCR Array Data Analysis Software	SABiosciences, Qiagen GmbH, Hilden, Germany

2.2. Methods

2.2.1. Animals and cell lines

All mice received human care according to the guidelines of the National Institute of Health as well as to the legal requirements in Germany. They were maintained under controlled conditions (22°C, 55% humidity and 12-hour day/night rhythm) and provided with autoclaved standard laboratory chow and water *ad libitum*.

Male C57BL/6J (BL/6) and BALB/c mice were obtained from animal facilities of the University Medical Centre Hamburg-Eppendorf (UKE), female *hmox*^{+/+}BALB/c (control littermates; wt) and *hmox*^{-/-}BALB/c (*HO-1*^{-/-}) mice were kindly provided by Prof. Tsui (General, Visceral and Thoracic Surgery Department and Clinic, UKE). Male *iNOS* knock-out (*iNOS*^{-/-}) mice with C57BL/6J genetic background (MacMicking et al. 1995) were kindly provided by Dr. Lotter (Molecular Parasitology Department, Bernhard Nocht Institute). The mice were 6-16 weeks of age, except of *iNOS*^{-/-} and corresponding control wild-type mice, which were 48 weeks of age.

Hepal-6 cells, a murine hepatoma cell line, were cultured in RPMI 1640 + GlutaMAXTM-I supplemented with 10% FCS and 1% penicillin/streptomycin. Cells were cultured in a 20% O₂ and 5% CO₂-humidified atmosphere at 37°C.

2.2.2. Isolation of primary murine hepatocytes

For primary hepatocyte (PH) isolation and culture, William's E+GlutaMAXTM-I medium was supplemented with 10% FCS, 1% L-Glutamine and 1% penicillin/streptomycin. First, mice were anesthetized with KHX (2.1.7). Second, the abdomen was disinfected with 70% ethanol. Hepatocytes were isolated by the two-step collagenase perfusion method of Seglen (Seglen 1976). Briefly, the liver was perfused with 10 ml PPML buffer (2.1.7) and digested with 0.004% Liberase (w/v). The liver capsule was gently disrupted and rinsed in PM medium. Subsequently, cell

suspension was passed through a sterile 100 μm nylon mesh. Hepatocytes were allowed to settle by gravity for 15 minutes. Parenchymal cells were separated from non-parenchymal cells by Percoll gradient centrifugation. Cell viability was determined with Trypan blue staining and the cell number was ascertained via the Neubauer cell counting chamber. Primary mouse hepatocytes were plated in plates (6-well: 500,000/well/5 ml; 24-well: 200,000/well/1 ml; 96-well: 30,000/well/100 μl) in William's E Medium and cultured in 40% O_2 and 5% CO_2 -humidified atmosphere at 37°C. Medium was exchanged after four hours and cells were allowed to adhere over night.

2.2.3. Dosage and incubation protocols

All experiments with cells were carried out under sterile conditions.

Prior to cell incubation, methylene chloride (MC) was dissolved in William's E Medium by excessively vortexing in indicated concentration. Isolated primary murine hepatocytes were incubated with William's E Medium containing MC for indicated time periods in a 20% O_2 and 5% CO_2 -humidified atmosphere at 37°C. Control cells received only William's E Medium instead.

Cellular damage was induced by incubating cells with 80 nM Actinomycin D (Act.D) for 30 min followed by the addition of 40 ng/ml recombinant tumor necrosis factor alpha ($\text{TNF}\alpha$) for 18 hours in William's E Medium. Act.D was solved in DMSO as a stock solution (100 μM), aliquoted and stored at -20°C until use. Recombinant $\text{TNF}\alpha$ was solved in ddH₂O as a stock solution (1.2 mg/ml) and stored at 4°C and -80°C until use.

Cobalt protoporphyrin IX (CoPP) was solved in 0.2M NaOH, adjusted to pH 7.6 with 0.1M HCl, filled up with ddH₂O as a stock solution (1 mg/ml) and stored at -80°C. Prior to cell incubation for 6-24 hours thawed CoPP aliquot was solved in William's E Medium (10 $\mu\text{g/ml}$) under low-light conditions.

S-Nitroso-N-acetylpenicillamine (SNAP) was used as a NO donor. SNAP was dissolved in DMSO as a stock solution (10 mM) and stored at -20°C. Prior to cell incubation for 2-20 hours, thawed SNAP aliquot was dissolved in William's E Medium in indicated concentrations under low-light conditions.

Kinase inhibitors ODQ, H-8, KT5823, and SP600125 were dissolved in DMSO as stock solutions and stored at -20°C until use. Prior to cell incubation, thawed aliquots were solved in William's E Medium in indicated concentrations under low-light conditions.

When substances solved in DMSO were used, control groups received equivalent DMSO containing William's E Medium instead.

2.2.4. Cell damage measurement

Cellular damage was assessed by measurement of lactate dehydrogenase (LDH) release using the LDH kit for Cobas Mira or Cobas Integra 400 Plus according to manufacturer's instructions. LDH amounts from the supernatants (S) and lysed cells (L) were correlated by the formula $S/(S+L) \times 100$ in order to quantify the percentage of cell damage. The amount of released LDH into the supernatant is proportional to the grade of cell damage.

2.2.5. Transfection of siRNA and plasmid DNA

Transfection of primary hepatocytes or Hepa1-6 cells either with siRNA or plasmid DNA was performed with LipofectamineTM 2000 according to manufacturer's instructions. All transfection experiments were carried out under sterile and RNase-free conditions. siRNA or plasmid DNA was solved in Opti-MEM Medium in indicated concentrations prior to cell incubation over night.

2.2.6. Luciferase reporter assay

After transfecting cells with plasmid DNA pB2luc, which is a reporter plasmid for nuclear factor kappa B (NFκB) activation, they were incubated with methylene chloride. The activation of the transcription factor was measured with the Luciferase Assay System according to manufacturer's instructions via the Infinite M200 Photometer. The luciferase activity was normalized to cell protein amount determined via Bradford assay with the Protein Assay Dye Reagent Concentrate.

2.2.7. Nitric oxide (NO) measurement

NO production was determined via conversion of non-fluorescent DAF-FM to a fluorescent benzotriazole. DAF-FM was dissolved in DMSO as a stock solution (5 mM), aliquoted and stored at -20°C until use. Prior to cell incubation for 30 min at 37°C, a thawed DAF-FM aliquot was solved in HBSS buffer (2.1.7) to the final concentration of 10 μM per well under low-light conditions. Control wells contained only HBSS. After washing with HBSS, fluorescence was measured by using the Infinite M200 Photometer. Excitation wavelength was adjusted to 495 nm and emission wavelength to 515 nm. The fluorescence was normalized to cell protein amount determined by the Bradford assay with the Protein Assay Dye Reagent Concentrate.

2.2.8. Quantitative Reverse-Transcription Polymerase Chain Reaction (qRT-PCR)

First, total RNA isolation from cells was performed with TRIzol reagent according to manufacturer's instructions under RNase-free conditions.

RNA in the aqueous phase was precipitated by adding isopropanol and the RNA pellet was washed with 75% ethanol. Dry pellet was dissolved in RNase-free, distilled water. Putative DNA contamination was eliminated via the rDNase Kit by

digesting DNA according to manufacturer's instructions. After rDNase inactivation step, RNA was stored at -80°C if not used immediately. Prior to following steps, RNA concentration and quality was measured with the NanoDrop ND-1000.

Second, isolated RNA was reverse-transcribed into cDNA using the Verso™ cDNA Kit according to manufacturer's instructions.

Third, amplification of target cDNA via qRT-PCR was performed with specific oligonucleotide pairs (section 2.1.5) and Maxima SYBR green/ROX qPCR Master Mix. The reactions were performed in a volume of 10 µl using the C1000 Thermal Cycler + CFX 96 Real-Time System. Quality and specificity of the amplified product was determined per subsequent melt curve analysis. The amount of the amplified target product was normalized to the housekeeping gene mitochondrial ATP Synthase beta (*Atp5b*).

2.2.9. RT² Profiler™ PCR Array: PAMM-014D

For the array, isolated primary hepatocytes were incubated with 100 mM CO donor methylene chloride solved in William's E Medium for four hours. Control cells received only William's E Medium instead. Total RNA was isolated as described above and transcribed into cDNA (see 2.2.8). The array was performed according to manufacturer's instructions (RT² Profiler™ PCR Array: PAMM-014D). Expression profiles of the control group and MC-incubated group were normalized to five housekeeping genes, which were: Glucuronidase beta (*Gusb*), Hypoxanthine guanine phosphoribosyl transferase 1 (*Hprt1*), Heat shock protein 90 alpha (*Hsp90ab1*), Glyceraldehyde-3-phosphate dehydrogenase (*Gapdh*), and Actin, beta (*Actb*).

Analysis of revealed threshold cycle values of all genes was performed via the Web-based PCR Array Data Analysis Software according to manufacturer's instructions.

2.2.10. Protein isolation and Western Blot analysis

Whole protein lysates were isolated from cultured isolated primary mouse hepatocytes. Cells were washed with sterile PBS and lysed in lysis buffer (2.1.7) containing a protease inhibitor cocktail (1:100) and a phosphatase inhibitor (PhosSTOP; 1:10). Cell suspension was transferred in an ultrasonic bath (Sonorex RK 102H) for 1-2 min, chilled on ice for 20 min and centrifuged (10 min, 14.000 rpm, 4°C). Supernatants were aliquoted in new tubes, shock frozen, and stored at -80°C until use.

For Western Blot analysis, the protein amount was determined via Bradford assay with the Protein Assay Dye Reagent Concentrate and arranged to a concentration of 30-50 µg per slot. Protein samples were further diluted with lysis buffer and 1X SDS-Loading buffer (2.1.7) and denaturized at 95°C for 5 min. First, proteins were fractionized in a 4% stacking gel, and second, separated either in a 10% or 12% (concerning on weight of protein of interest) separating gel. The gel electrophoresis of the stacking gel was performed at 80 V for approx. for 15-20 minutes, and of the separating gel at 120 V for approx. 1 h. Separated proteins were blotted on nitrocellulose membrane by the wet blot method using transfer buffer (2.1.7) and the Blotting tank (Mini Trans-Blot® Cell) on ice with stirring for 70 min and 350 mA. After blotting, the membrane was shortly incubated in Ponceau S for succeed protein transfer control and washed with water. Afterwards, the membrane was washed with 1xTBST and incubated in blocking solution (either 5% milk/TBST or 5% BSA/TBST according to manufacturer's instructions of primary antibodies) for one hour. Membrane was incubated with the corresponding primary antibody diluted in blocking solution over night at 4°C (2.1.4). Membrane was washed 3 x 10 min with 1xTBST prior to incubation with secondary antibody and Precision Protein™ StrepTactin Conjugate (1:10,000), which was used for visualization of the Precision Plus Protein™ WesternC™ Standard, for one hour at room temperature in 1xTBST. Visualization of proteins of interest was performed with home-brew ECL

solution (2.1.7) and subsequent detection with the VersaDoc™ Imaging System 4000 MP. Following image editing was performed with the Image Lab™ Software.

2.2.11. Two-dimensional polyacrylamide gel electrophoresis (2D PAGE) and protein identification by Liquid chromatography (LC) – Electrospray Ionization (ESI) – Ion trap analysis

For the 2D PAGE, primary murine hepatocytes (C57BL/6J) were isolated and seeded in cell culture flasks (5×10^6 per flask). After an over night recovery phase, cells were incubated with MC-containing William's E Medium for indicated time periods (A: 50 mM MC for 4 h; B: 100 mM MC for 1 h). Control cells received fresh William's E Medium instead.

Whole cell protein lysates were performed as described in 2.2.10, frozen, and committed to Prof. Schlüter (Department of Clinical Chemistry, University Medical Center Hamburg-Eppendorf), who mediated the 2D PAGE and the subsequent protein identification.

The two-dimensional gel electrophoresis and subsequent Coomassie brilliant blue staining of the gel was performed as described earlier (Binder et al. 2010). Stained gels of the MC-incubated lysates and the control lysates were further handed by me. In order to visualize altered proteins an overlay of pictures of the control gel (untreated whole cell lysate) and the test gel (MC-incubated cell lysate) was performed by using the false color representation. Unmodified protein spots appeared black and were disclosed from further analysis, blue or orange proteins spots were cut out (Fig. 3.3). The protein was isolated from the gel and digested with trypsin as described earlier (Binder et al. 2010).

The team of Prof. Schlüter performed identification of digested peptides as described earlier (Binder et al. 2010) by using the LC-ESI-Ion trap analysis.

The MS/MS datasets of analyzed peptides were further identified by using the Mascot MS/MS server and the SwissProt database by comparing the spectra of *Mus musculus*.

2.2.12. Statistical analysis

All data in this study are expressed as mean \pm SEM. Statistical analysis was performed with the GraphPad Prism5 software: Two-tailed Student's *t*-test was used when two groups were compared and one-way ANOVA followed Bonferroni's Multiple Comparison test was used when multiple groups were compared. A *p* value of 0.05 was considered as significant with following ranges: * $p \leq 0.05$; ** $p \leq 0.01$; and *** $p \leq 0.0001$.

3. Results

3.1. Carbon monoxide protects primary mouse hepatocytes from induced cellular damage

In order to test the hypothesis of the protective, anti-apoptotic effect of carbon monoxide in tumor, an *in vitro* model for the induction of cellular damage (Act.D/TNF α model) was used (see section 2.2.3 for details). In this model, a combination of the transcriptional inhibitor Actinomycin D (Act.D) with the cytokine tumor necrosis factor alpha (TNF α) induces cellular damage in isolated primary hepatocytes within 18 hours of incubation (Y. M. Kim et al. 1997). To answer the question whether the HO-1 product carbon monoxide is able to protect from induced cellular damage, primary mouse hepatocytes from C57BL/6J mice were isolated. The results show that pre-incubation of hepatocytes with methylene chloride (MC), which is catabolized to CO and CO₂ (Lakkisto et al. 2010), protected cells from Act.D (80nM)/TNF α (40 ng/ml)-induced damage in a dose- and time-dependent manner (Fig. 3.1 A+B). The relative amount of cell death was measured by lactate dehydrogenase (LDH) assay.

Incubation of murine hepatocytes with Act.D/TNF α induced cellular damage, as shown by significantly elevated toxicity levels (Fig. 3.1 A, white bars). In contrast, pre-incubation of cells with rising concentrations (50-150 mM, grey bars) of the CO donor MC for 6 hours did not significantly increase toxicity levels. Pre-incubation of cells with MC prior to damage induction significantly decreased toxicity. This effect improved over time from two hours (decrease about 43%) up to six hours (decrease about 65%) of MC incubation compared to MC-untreated cells (Fig. 3.1 B).

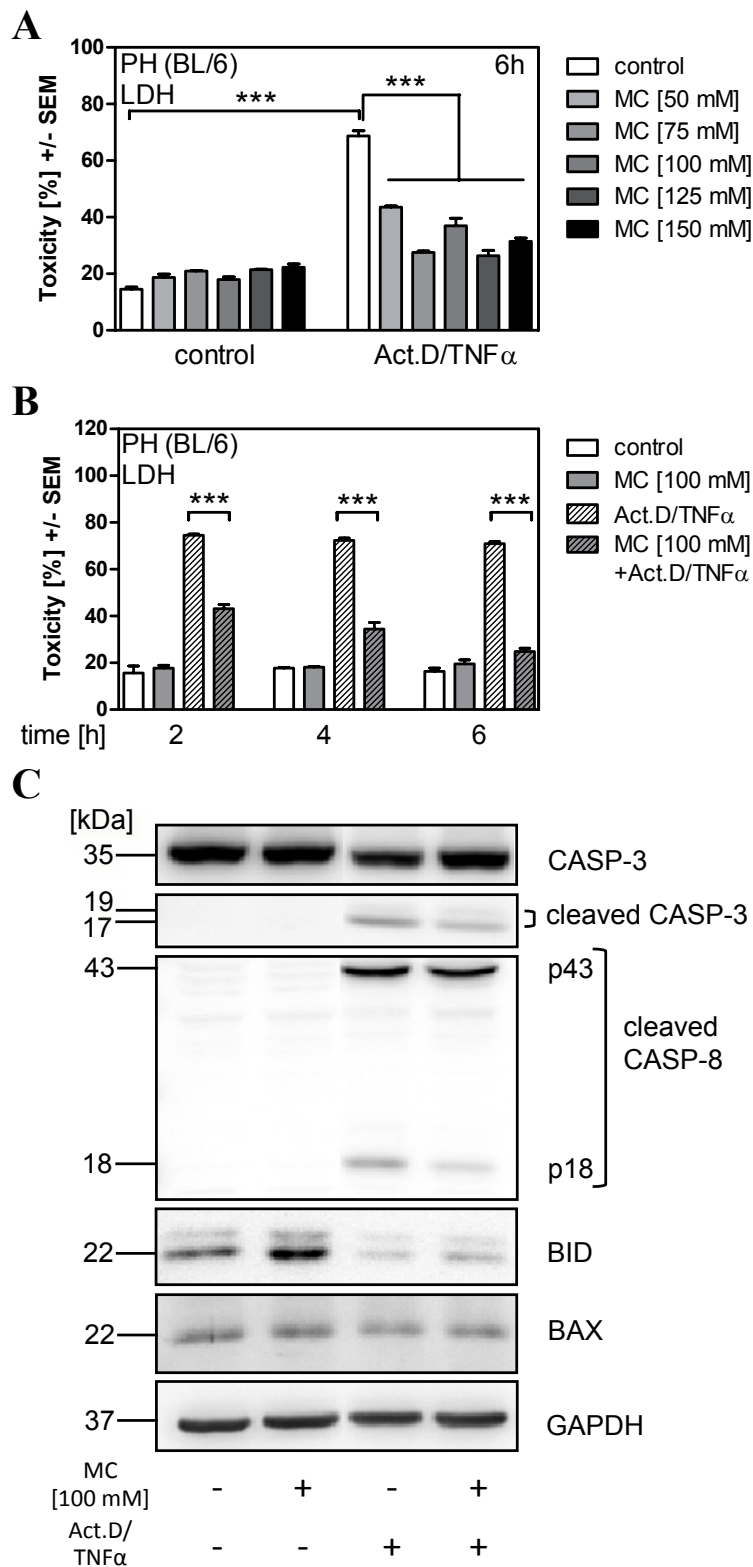


Fig. 3.1

CO-dependent protection of primary mouse hepatocytes (PH) against induced cellular damage.

Freshly isolated PHs of the C57BL/6J strain (BL/6) were incubated with methylene chloride (MC) dissolved in cell medium prior to damage induction with 80 nM Act.D and 40 ng/ml TNF α .

A: PHs were incubated with 50, 75, 100, 125, and 150 mM MC for 6 hours (grey bars) followed by damage induction for 18 hours. Control cells received fresh medium instead (white bars). Cellular damage was assessed by LDH assay.

B: PHs were incubated with 100 mM MC for 2, 4 and 6 hours followed by damage induction for 18 hours. Control cells received fresh medium instead (white bars). Cellular damage was assessed by LDH assay.

C: Western Blot analysis of PHs incubated with MC (100 mM, 6 h) alone or prior to damage induction with Act.D and TNF α for 18 hours. Detection of apoptosis associated proteins: CASP-3, cleaved CASP-3, cleaved CASP-8, BID, and BAX. GAPDH was used as a loading control.

(mean \pm SEM; *** $p \leq 0.0001$)

Western Blot analysis of apoptosis-associated proteins is a method to show anti-apoptotic effects on protein level. Incubation with 100 mM MC dissolved in cell medium did not induce apoptosis, as shown by equal amounts of Pro-CASPASE-3 and no detection of cleaved CASPASE-8 compared to untreated control cells (Fig. 3.1 C). Besides, the expression of the pro-apoptotic full-length (i.e. not activated) protein BID was increased due to MC incubation but this had no influence on cell viability (Fig. 3.1 C). Incubation with Act.D/TNF α activated the caspase cascade visible as reduced levels of non-cleaved CASPASE-3 and subsequently elevated protein levels of activated CASPASE-3 and CASPASE-8. Moreover, inactive BID was decreased compared to the untreated control, which indicates cleavage by the upstream CASPASE-8, thus demonstrating the activation of the apoptotic cascade (Fig. 3.1 C). Pre-incubation of hepatocytes with MC prior to Act.D/TNF α application decreased the activation of the caspase cascade, which depicts the protective effect of CO. This is shown by higher amounts of Pro-CASPASE-3 protein levels and by decreased cleaved CASPASE-3 and -8 protein levels compared to control (only Act.D/TNF α) sample. Similarly, the protein level of inactive full-length BID is higher after MC incubation (MC/Act.D/TNF α) indicating activation of the expression in contrast to control sample (only Act.D/TNF α). MC did not regulate the expression of pro-apoptotic protein BAX, but there is a slight reduction of band intensity after incubation with Act.D/TNF α (Fig. 3.1 C). There seems to be a moderate reduction of protein levels of BAX after cell damage induction with Act.D/TNF α , compared to untreated control sample.

These results indicate that MC-derived CO protects primary murine hepatocytes from cellular damage in a dose- and time-dependent manner.

3.2. CO protection is independent from HO-1

CO has been described to induce *Hmox1* expression in epithelial cells (Kim et al. 2007). It was therefore investigated whether protection found in this system (Fig. 3.1) is dependent on HO-1 induction or is a feature of CO alone.

In a first step, analysis of HO-1 protein expression following incubation of primary hepatocytes with MC for 6 or 24 hours was performed. The results show that MC incubation did not induce HO-1 protein expression (Fig. 3.2 A). As a positive control, cells incubated with the HO-1 inducer cobalt protoporphyrin IX (CoPP), were used (Fig. 3.2 A).

To further confirm these results knock-down and knock-out experiments were performed. The knock-down of *Hmox1* via siRNA did not attenuate the protective effect of MC in primary hepatocytes (Fig. 3.2 B). MC still showed the significant reduction of toxicity levels in siRNA-untreated control samples (toxicity reduction about 68%). Similarly, MC protected against Act.D/TNF α -induced damage in HO-1 knock-down samples (toxicity reduction about 68%) as well as in siRNA control knock-down samples (toxicity reduction about 63%).

Likewise, primary hepatocytes of *Hmox1* deficient mice (HO-1^{-/-}), pre-incubated with 100 mM MC for four hours, were protected against Act.D/TNF α -induced cell damage (toxicity reduction about 32%) (Fig. 3.2 C). In wt-samples MC significantly reduced toxicity about 45%.

In conclusion, the protective effect of CO on primary hepatocytes is independent of *de novo* HO-1 expression or its products, e.g. iron and biliverdin, but is directly caused by CO.

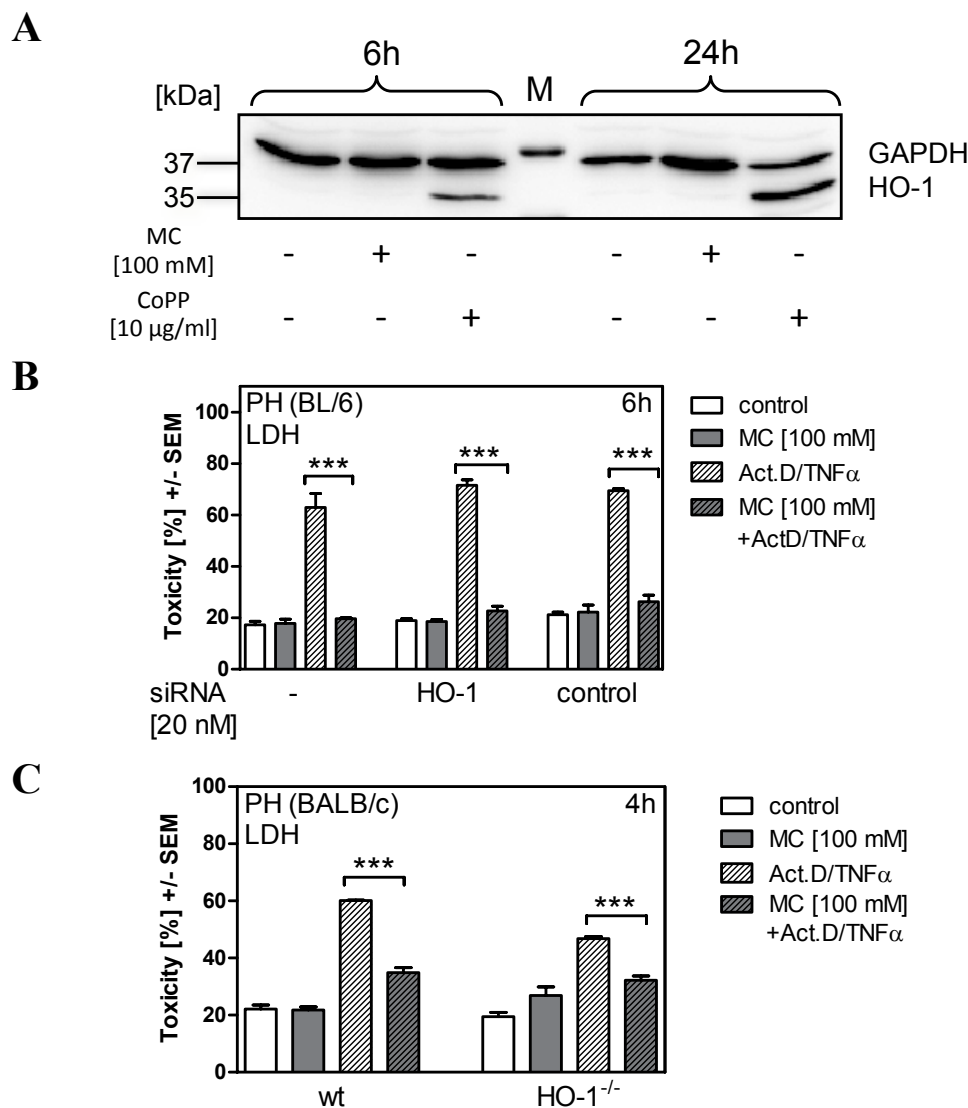


Fig. 3.2 CO-dependent protection against induced cell damage is independent from HO-1 induction in primary hepatocytes (PH).

A: Western Blot analysis of PHs (C57BL/6J), which were incubated with MC (100 mM) or cobalt protoporphyrin IX (CoPP) (10 µg/ml) for 6 or 24 h. Detection of HO-1. Detection of GAPDH was used as a loading control. (M= Precision Plus Protein™ WesternC™ Standard)

B: Knock-down of *Hmox1* or a control sequence via siRNA [20 nM] in PHs (C57BL/6J) previous to MC incubation (100 mM) for 6 h. Control cells received fresh medium instead (white bars). Cell damage induction was performed with 80 nM Act.D and 40 ng/ml TNFα for 18 h. Cellular damage was assessed by LDH assay.

C: PHs (wt or HO-1^{-/-}, BALB/c) were incubated with 100 mM MC for 4 h previous to cell damage induction with Act.D (80 nM)/TNFα (40 µg/ml) for 18 h. Control cells received fresh medium instead (white bars). Cellular damage was assessed by LDH assay.

(mean ± SEM; ***p ≤ 0.0001)

3.3. Proteomic analysis of murine primary hepatocytes upon MC via 2D PAGE

To identify mechanisms and mediators of CO-induced protection proteomic and genomic methods were used.

In a first attempt, global changes in protein expression were investigated via 2D PAGE. These experiments were performed in collaboration with Prof. Schlüter (Department of Clinical Chemistry, University Medical Center Hamburg-Eppendorf). This method identifies individual protein spots, separated by their characteristic molecular weight and isoelectric point, which are modified upon incubation with e.g. MC (for details see method section 2.2.11).

Figure 3.3 shows gel picture overlays of two approaches: incubation of primary hepatocytes with 50 mM MC for four hours (A) and incubation with 100 mM MC for one hour (B). These approaches gave the opportunity to investigate both, short and long term effects of CO incubation on protein level.

A

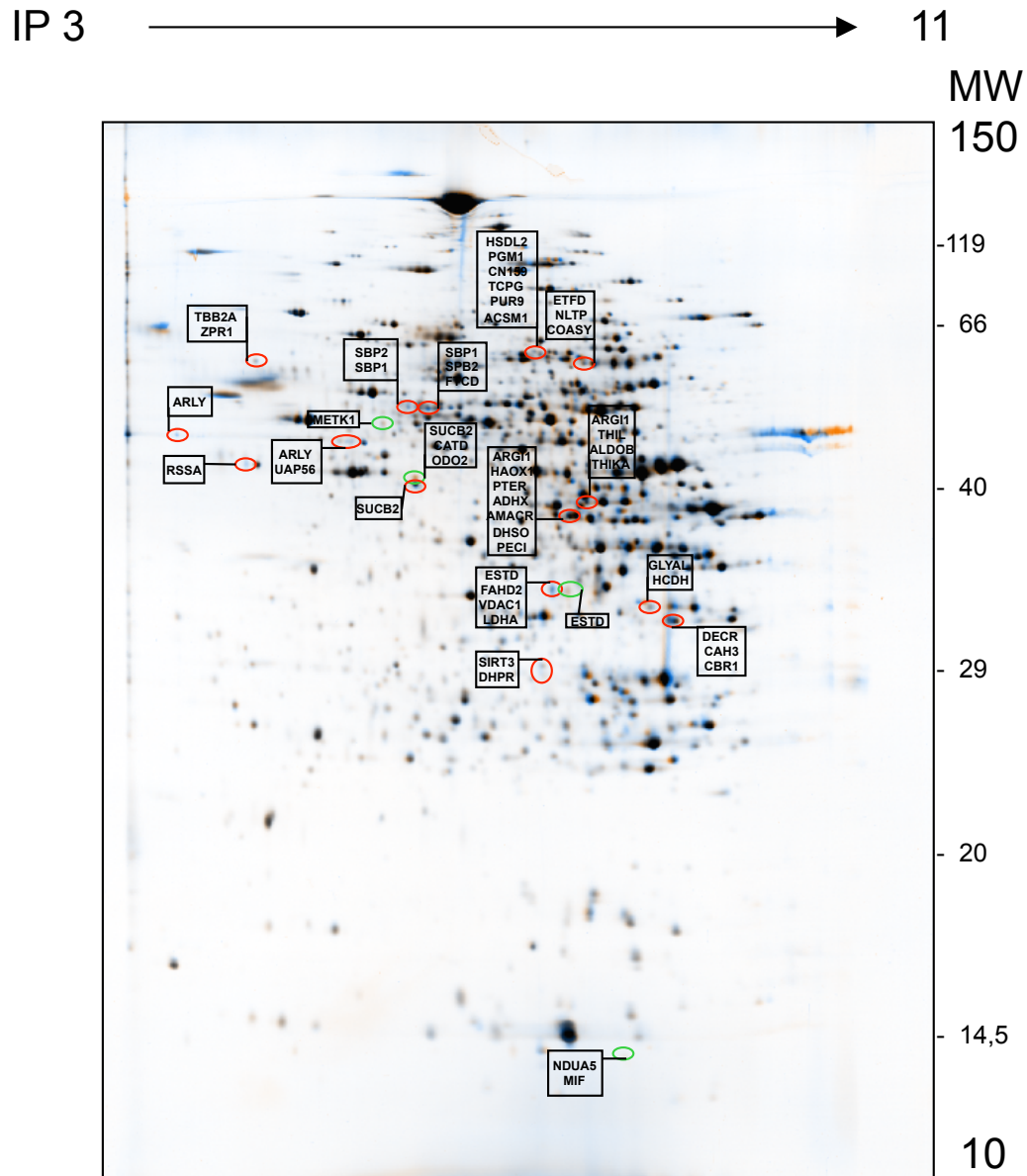


Fig. 3.3 A False color representation of overlaid pictures of the first approach of 2D-PAGE.

PHs (C57BL/6J) were incubated with 50 mM MC for 4 h. Control cells received fresh medium instead. In the first dimension (horizontal plane) proteins were separated by their characteristic isoelectric point (IP). In the second dimension (vertical lane) proteins were separated by their molecular weight (MW). Overlaying spots are black, orange spots (red circle) are from control sample gel and blue spots (green circle) are from MC-treated sample gel. Full protein names, detailed MS/MS analysis information, and rough division into cellular function are indicated in Table 3.1.

B

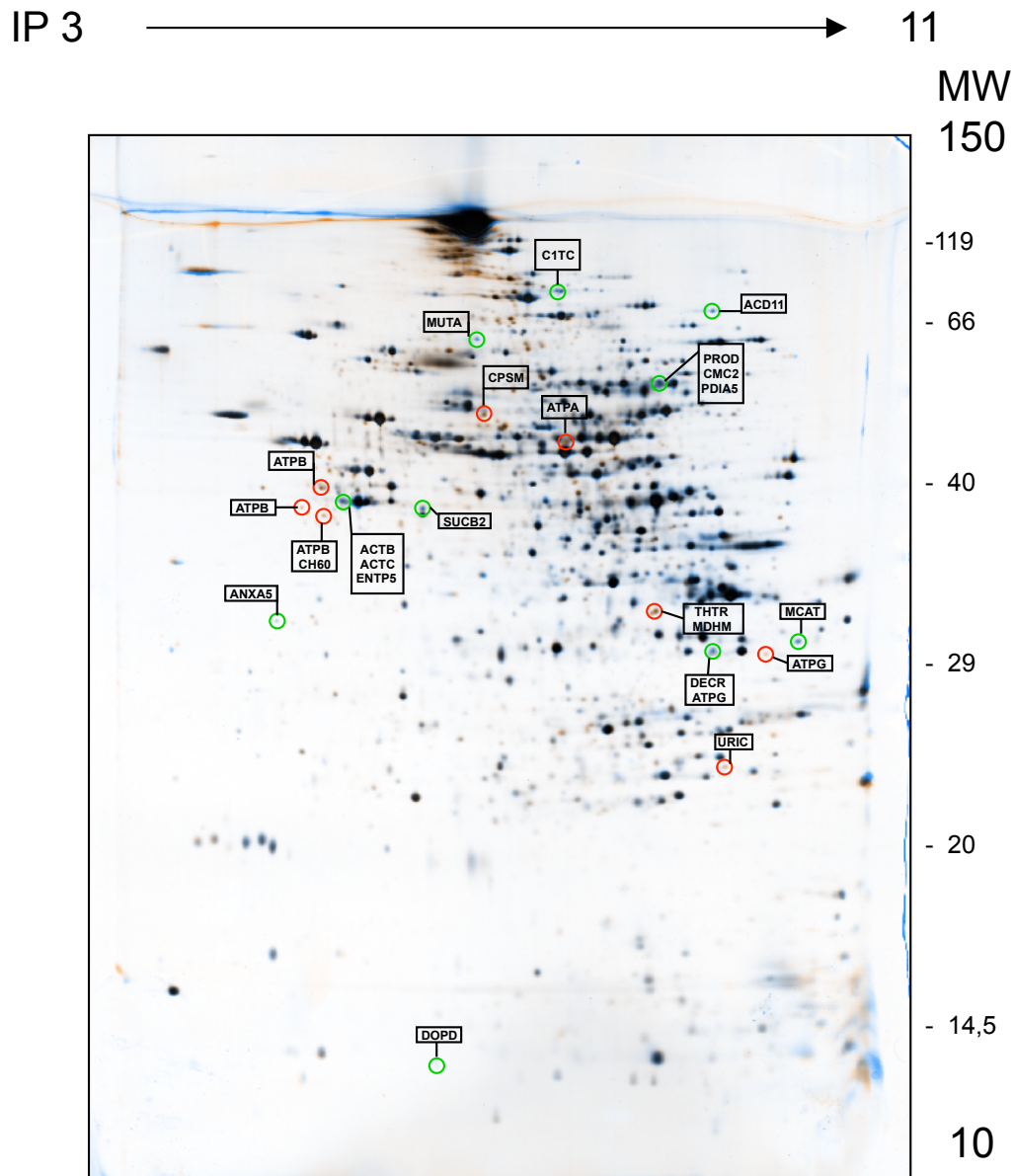


Fig. 3.2 B False color representation of overlaid pictures of the second approach of the 2D-PAGE.

PHs (C57BL/6J) were incubated with 100 mM MC for 1 h. Control cells received fresh medium instead. In the first dimension (horizontal plane) proteins were separated by their characteristic isoelectric point (IP). In the second dimension (vertical lane) proteins were separated by their molecular weight (MW). Overlaying spots are black, orange spots (red circle) are from control sample gel and blue spots (green circle) are from MC-treated sample gel. Full protein names, detailed MS/MS analysis information, and rough division into cellular function are indicated in Table 3.1.

Modified protein spots, e.g. presented as blue or orange spots in the false color representation, were isolated and analyzed via mass spectrometry (MS; see section 2.2.11.). Non-altered proteins appear black and were disclosed from the MS analysis. Table 3.1 summarizes the results.

Tab. 3.1 Proteins, identified in both approaches via 2D PAGE, of murine primary hepatocytes (C57BL/6J) incubated either with 50 or 100 mM MC for four or one hour, respectively. The proteins were further roughly arranged by their cellular function:
a) metabolism, b) energy/electron transport chain, c) signaling, d) transcription/translation, and e) other functions. MW=molecular weight; Da=Dalton; pI=isoelectric point

Approach	Spot-Nr.	Mascot abbreviation	Protein	Score	Protein MW (Da)	Protein pI	Coverage (%)	Unique peptides detected
a) metabolism								
50 mM MC 4h	2	HSDL2	Hydroxysteroid dehydrogenase-like protein	219	54174	6.31	28	12
	6	ARLY	Argininosuccinate lyase	139	51707	6.48	9	4
	7	METK1	S-adenosylmethionine synthase isoform type-1	75	43481	5.51	3	1
	8	ARLY	Argininosuccinate lyase	71	51707	6.48	9	4
	10	SUCB2	Succinyl-CoA ligase [GDP-forming] subunit beta, mitoch	574	46811	6.58	29	12
	11	ALDOC	Fructose-bisphosphate aldolase C	206	39370	6.67	20	5
	12	ARG1	Arginase-1	251	34786	6.51	33	7
	12	HAOX1	Hydroxyacid oxidase 1	236	40975	7.6	25	7
	12	PTER	Phosphotriesterase-related protein	195	39193	6.18	24	6
	12	ADHX	Alcohol dehydrogenase class-3	176	39522	6.97	32	6
	15	GLYAL	Glycine N-acyltransferase-like protein	139	34086	7.68	25	5
	16	DECR	2,4-dienoyl-CoA reductase, mitoch	228	36191	9.1	36	11
	20	SUCB2	Succinyl-CoA ligase [GDP-forming] subunit beta, mitoch	352	46811	6.58	40	17
100 mM MC 1h	1	CPSM	Carbamoyl-phosphate synthase [ammonial], mitochondrial	95	164514	6.48	7	13
	6	MDHM	Malate dehydrogenase, mitochondrial	51	35589	8.93	20	8
	8	URIC	Uricase	46	35017	8.48	25	11
	9	C1TC	C-1-tetrahydrofolate synthase, cytoplasmic	173	101136	6.7	18	18
	11	MUTA	Methylmalonyl-CoA mutase, mitochondrial	111	82792	6.42	27	19
	12	PROD	Proline dehydrogenase 1, mitochondrial	164	67992	8.5	13	7
	12	PDIA5	Protein disulfide-isomerase A5	88	59229	7.25	17	9
	14	SUCB2	Succinyl-CoA ligase [GDP-forming] subunit beta, mitoch	327	46811	6.58	43	15
	16	DECR	2,4-dienoyl-CoA reductase, mitoch	201	36191	9.1	36	17
	18	DOPD	D-dopachrome decarboxylase	51	13069	6.09	52	7

b) energy/electron transport chain								
50 mM MC 4h	3	ETFD	Electron transfer flavoprotein-ubiquinone oxidoreductase, mitoch	254	68048	7.34	15	7
	17	SIR3	NAD-dependent deacetylase sirtuin-3	46	28804	5.81	11	2
	18	THIOM	Thioredoxin, mitoch	25	18244	7.74	36	3
	19	NDUA5	NADH dehydrogenase [ubiquinone] 1 alpha subcomplex subunit 5	61	13351	7.81	31	3
100 mM MC 1h	2	ATPA	ATP synthase subunit alpha, mitoch	314	59716	9.22	31	16
	3	ATPB	ATP synthase subunit beta, mitoch	461	56265	5.19	37	17
	4	ATPB	ATP synthase subunit beta, mitoch	444	56265	5.19	33	16
	5	ATPB	ATP synthase subunit beta, mitoch	52	56265	5.19	15	9
	7	ATPG	ATP synthase subunit gamma, mitoch	80	32865	9.06	24	7
	16	ATPG	ATP synthase subunit gamma, mitoch	110	32865	9.06	26	8
c) signaling								
50 mM MC 4h	7	NHRF1	Na(+)/H(+) exchange regulatory cofactor NHE-RF1	71	38577	5.63	10	3
100 mM MC 1h	13	ENTP5	Ectonucleoside triphosphate diphosphohydrolase 5	144	47072	5.17	29	13
d) transcription/translation								
50 mM MC 4h	9	RSSA	40S ribosomal protein	154	32817	4.8	14	3
e) other functions								
50 mM MC 4h	1	TBB2A	Tubulin beta-2A chain	246	49875	4.78	28	8
	4	SBP2	Selenium-binding protein 2	292	52576	5.78	28	10
	5	SBP1	Selenium-binding protein 1	263	52480	5.87	29	12
	14	ESTD	S-formylglutathione hydrolase	129	31299	6.7	18	3
	14	FAHD2	Fumarylacetoacetate hydrolase domain-containing protein 2A	100	34668	8.42	17	3
	21	ESTD	S-formylglutathione hydrolase	101	31299	6.7	9	2
100 mM MC 1h	5	CH60	60 kDa heat shock protein, mitoch	154	60917	5.91	12	10
	6	THTR	Thiosulfate sulfurtransferase	103	33445	7.71	19	5
	10	ACD11	Acyl-CoA dehydrogenase family member 11	115	87311	8.67	14	12
	12	CMC2	Calcium-binding mitochondrial carrier protein Aralar2	337	74420	8.77	28	16
	13	ACTB	Actin, cytoplasmic 1	253	41710	5.29	46	17
	13	ACTC	Actin, alpha cardiac muscle 1	213	41992	5.23	34	15
	15	ANXA5	Annexin A5	243	35730	4.83	45	19
	17	MCAT	Mitochondrial carnitine/acylcarnitine carrier protein	56	33005	9.24	19	10

For further analysis, CO-regulated proteins were arranged by their main cellular function, e.g. metabolism, cell signaling or energy metabolism/member of electron transport chain (Fig. 3.4). Of note, 46% of proteins modified upon MC-incubation belonged to metabolism (i.e. nucleotide, amino acid, and fatty acid; 23 out of 50) and 20% to energy metabolism (10 out of 50).

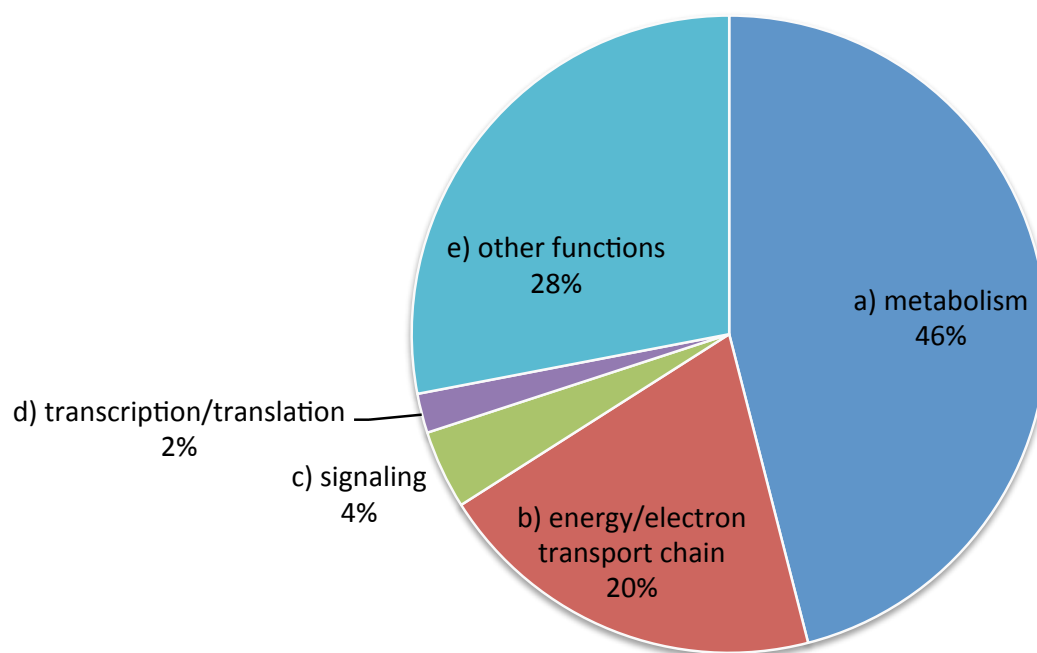


Fig. 3.4 CO-regulated proteins, which were identified by 2D PAGE, were further summarized from both approaches (A+B) and categorized by their cellular function (see also Tab. 3.1).

3.4. CO-incubation induced the nitric oxide pathway

As the 2D PAGE analysis has shown, CO influenced a high number of metabolic proteins. Thus, the further investigation was focused on this part of proteins, in particular, on members of the urea cycle: arginase 1 (ARG1; *Arg1*) and argininosuccinate lyase (ARLY/ASL; *Asl*) (Tab. 3.1). As mentioned in the introduction section 1.4, within the urea cycle the NO-cycle can be activated when the enzyme nitric oxide synthase (NOS) is expressed (Morris 2002), which was also analyzed in regard to CO.

Indeed, qRT-PCR analysis showed that incubation with MC for 1-6 hours significantly induced the expression of *Asl*, *Arg1* and *Nos2* (iNOS) (Fig. 3.5 A). *Asl* was slightly induced (1.5-fold) upon 100 mM MC incubation after 4 hours. *Arg1* expression peaked after 2 hours and dropped to baseline afterwards. The strongest influence of MC incubation could be detected at the *Nos2* expression levels: after two hours of incubation with 100 mM MC the expression level rose 2.7-fold; after four hours 3.5-fold; and after six hours 4-fold. These changes were significant. Additionally, the production of nitric oxide (NO), the catalytic product of iNOS, was already detectable after one hour of MC incubation (Fig. 3.5 B). To rule out the possibility that NO was produced by the constitutively active endothelial isoform of NOS (eNOS) mRNA analysis was performed (Fig. 3.5 C). After two and six hours of MC incubation no changes of *Nos3* (eNOS) expression could be detected, thus, leading to the conclusion that the measured NO increase was rather produced by iNOS than by eNOS.

Since expression of *Nos2* is regulated by various transcription factors, effects of CO on NFκB, AP-1, and hypoxia induced factor 1 alpha (HIF-1α; *Hif1a*) activity or expression were determined by using a luciferase reporter assay and qRT-PCR, respectively.

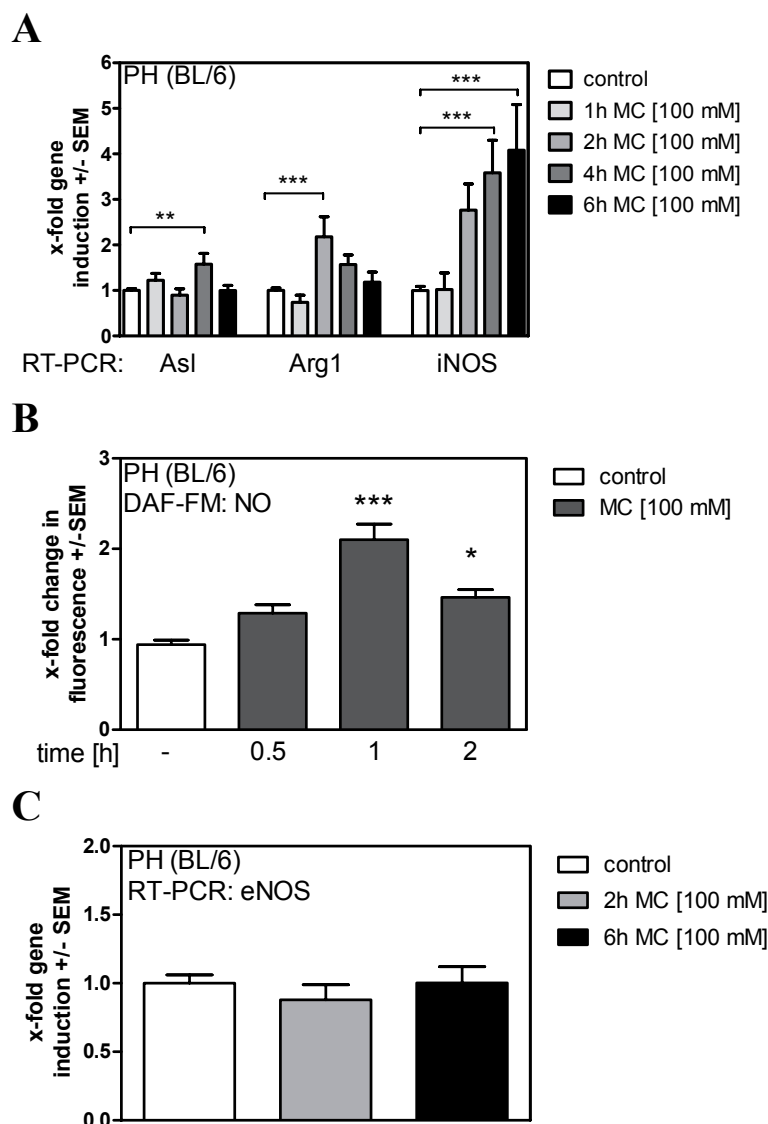


Fig. 3.5

MC interacts with the urea/NO cycle.

A: PHs (C57BL/6J) were incubated with 100 mM MC for 1, 2, 4, and 6 h. Control cells received fresh medium instead (white bars). mRNA expression levels of *Asl*, *Arg1* and *Nos2* (iNOS) were measured by qRT-PCR.

B: PHs (C57BL/6J) were incubated with 100 mM MC for 0.5, 1, and 2 hours. Control cells received fresh medium instead (white bars). Production of nitric oxide (NO) was measured via fluorescent probe (DAF-FM) transformation.

C: PHs (C57BL/6J) were incubated with 100 mM MC for 2 and 6 hours. Control cells received fresh medium instead (white bars). mRNA expression levels of *Nos3* (eNOS) were measured by qRT-PCR.

(mean \pm SEM; * $p \leq 0.05$; ** $p \leq 0.01$; *** $p \leq 0.0001$)

Unexpectedly, CO did not activate NF κ B and was not able to induce the expression of *Hif1a* (Fig. 3.6 A and B). On the other hand, mRNA expression levels of *Jun* and *Fos*, which form the heterodimeric transcription factor AP-1, were strongly induced by 100 mM MC (Fig. 3.6 B). *Jun* was significantly induced after two and four hours of MC incubation (5.2-fold and 3-fold, respectively). *Fos* was significantly induced after two hours (2.5-fold), four hours (2.3-fold), and remained slightly induced after six hours (1.9-fold).

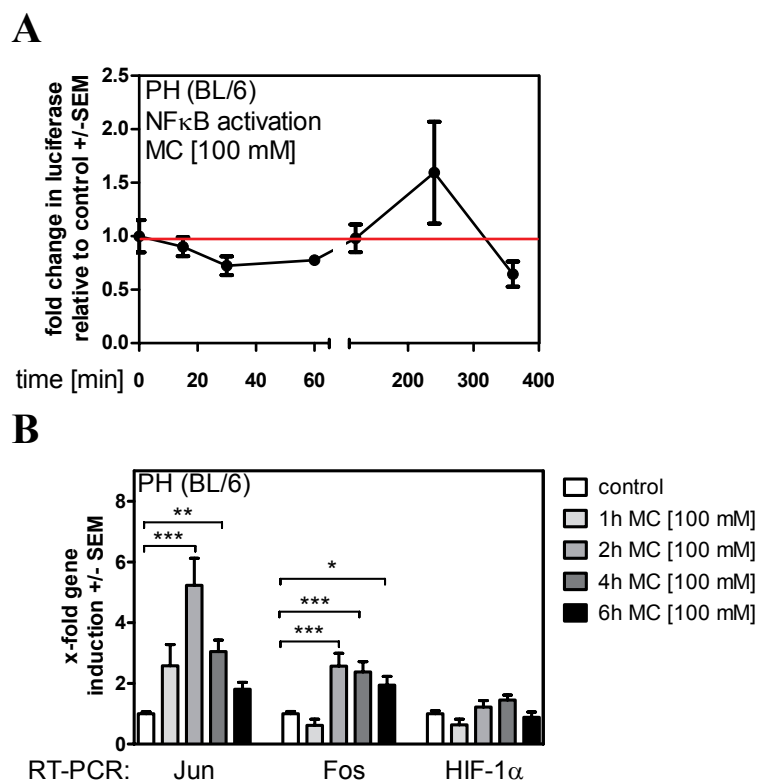


Fig. 3.6

Influence of MC on activation and expression of transcription factors (i.e. NFκB, AP-1, and Hif-1α) of iNOS.

A: PHs (C57BL/6J) were incubated with 100 mM MC for 15-360 minutes. NFκB activation was measured via luciferase reporter assay by using pB2luc reporter vector.

B: PHs (C57BL/6J) were incubated with 100 mM MC for 1, 2, 4, and 6 hours. Control cells received fresh medium instead (white bars). mRNA expression levels of *Jun*, *Fos*, and *Hif1a* were measured by qRT-PCR.

(mean ± SEM; *p ≤ 0.05; **p ≤ 0.01; ***p ≤ 0.0001)

These results indicate that activation of the transcription factor AP-1 by CO might contribute to *Nos2* expression.

NO, like CO, is a monoxidic gas with comparable physiological properties. Both gases act similar concerning vasorelaxation, neurotransmission, platelet aggregation and apoptosis (Hoetzel and Schmidt 2006). Therefore, the effects of NO incubation on cellular damage of murine hepatocytes using the NO donor S-Nitroso-N-Acetyl-D,L-Penicillamine (SNAP) were investigated.

The results show that SNAP protected hepatocytes from Act.D/TNFα-induced cellular damage in a dose- and time-dependent manner (Fig. 3.7). SNAP significantly reduced toxicity levels from 57% to 23% in SNAP/Act.D/TNFα-incubated cells. Protection was most efficient after 20 hours of pre-incubation with SNAP (750 μM), showing a toxicity level reduction about 45% (Fig. 3.7 B).

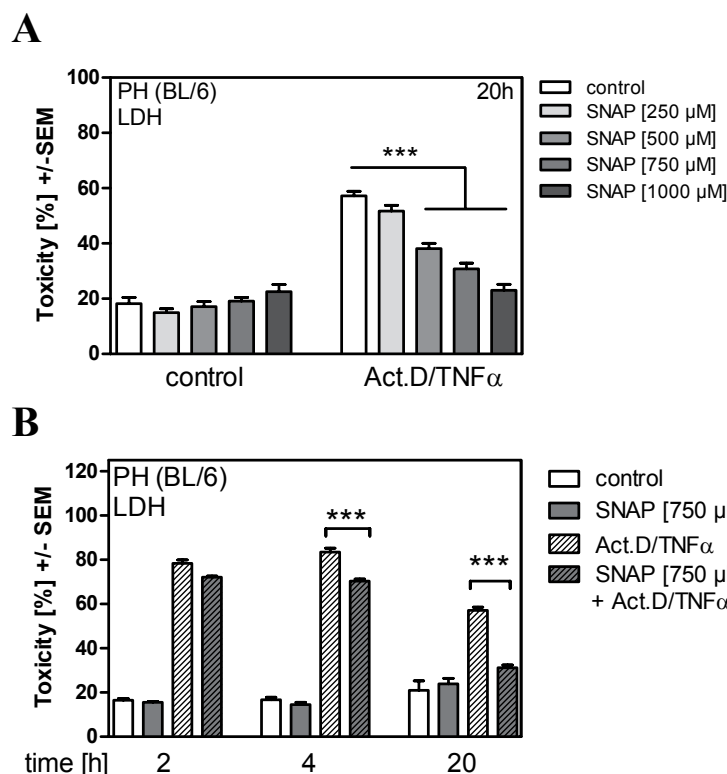


Fig. 3.7

NO-dependent protection of PHs against Act.D/TNF α -induced cellular damage.

Freshly isolated PH of the C57BL/6J strain (BL/6) were incubated with the NO donor SNAP dissolved in cell medium previously to damage induction by 80 nM Act.D and 40 ng/ml TNF α .

A: PHs were incubated with 250, 500, 750, and 1000 μ M SNAP for 20 hours followed by damage induction.

Control cells received fresh medium instead (white bars). Cellular damage was assessed by LDH assay.

B: PHs were incubated with 750 μ M SNAP for 2, 4 and 20 hours followed by damage induction. Control cells received fresh medium instead (white bars). Cellular damage was assessed by LDH assay.

(mean \pm SEM; *** $p \leq 0.0001$)

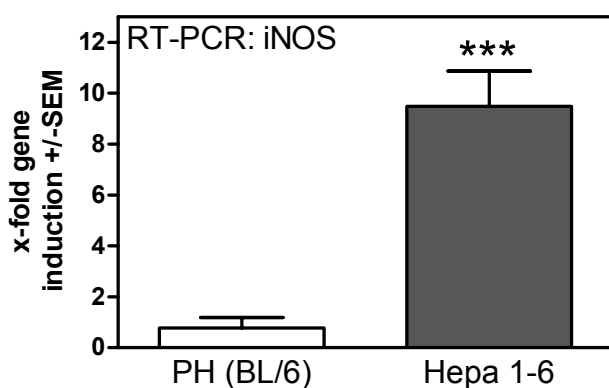
Since CO induced production of NO and in turn NO protected hepatocytes from Act.D/TNF α -induced damage *in vitro*, it was further investigated whether this molecule is important for CO-induced protection. For this purpose, knock-down and knock-out experiments of *Nos2* were performed.

To test the efficacy of two siRNAs directed against *Nos2* the mouse hepatoma cell line Hepa1-6 was used. Compared to primary hepatocytes, Hepa1-6 cells express high amounts of *Nos2* (Fig. 3.8 A). The results show that knock-down of *Nos2* in Hepa1-6 cells was 85% efficient for iNOS-a siRNA and 92% for iNOS-b siRNA (Fig. 3.8 B).

For the experiments in primary murine hepatocytes siRNA iNOS-b was used, which apparently showed higher knock-down efficacy. 24 hours after siRNA transfection hepatocytes were incubated with 100 mM MC for six hours and cell damage was induced by incubation with Act.D/TNF α (Fig. 3.9 A). MC significantly protected

cells from Act.D/TNF α -induced damage although *Nos2* expression was down regulated by siRNA. MC effectively reduced the toxicity levels about 65% in samples with down regulated *Nos2* expression. This result could also be achieved in siRNA control sample, where MC reduced the toxicity levels about 63% (Fig. 3.9 A).

A



B

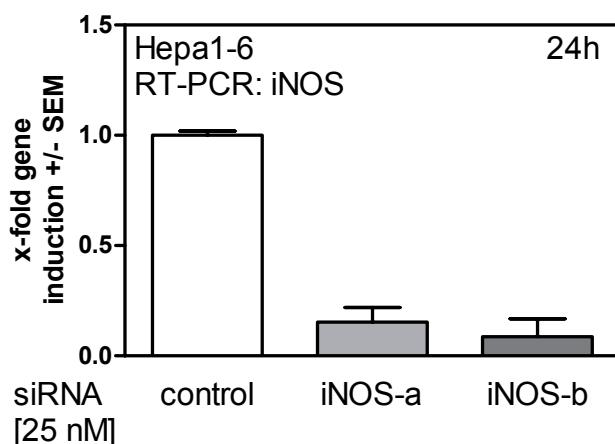


Fig. 3.8

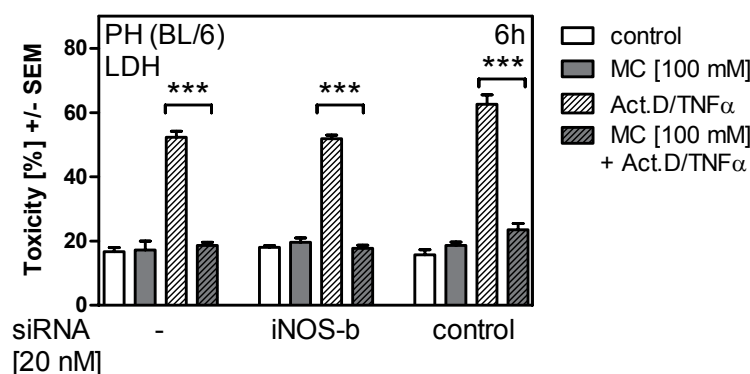
Efficiency test of siRNA (iNOS-a and iNOS-b) in the murine Hepatoma cell line Hepa1-6.

A: Measurement of *Nos2* mRNA expression level in Hepa1-6 cells (grey bar) and primary mouse hepatocytes (C57BL/6J) (white bar) via qRT-PCR.

B: Hepa1-6 cells were transfected with 25 nM siRNA (*Nos2*-a, *Nos2*-b, and control sequence). After 24 h mRNA expression levels of *Nos2* were measured to test siRNA efficacy by qRT-PCR.

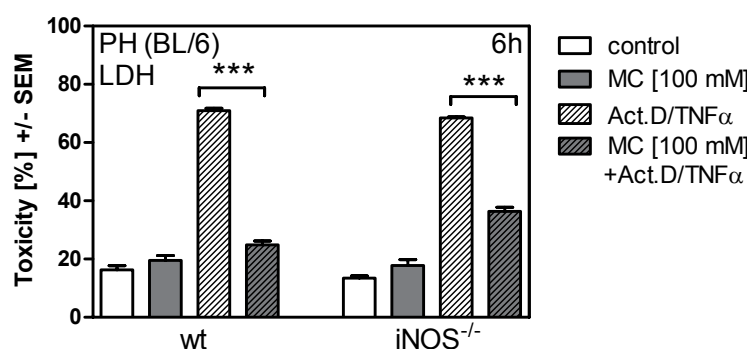
(mean \pm SEM; *** $p \leq 0.0001$)

To confirm this result, hepatocytes from mice deficient in *Nos2* expression (iNOS^{-/-}) were used. MC protected primary hepatocytes of wildtype as well as of iNOS^{-/-} mice against Act.D/TNF α -induced cell damage (Fig. 3.9 B). In the control wt mice MC reduced the Act.D/TNF α -induced toxicity about 65%. Similarly, in iNOS^{-/-} mice MC decreased toxicity levels about 48%. Obviously, the MC-dependent reduction of toxicity in wt mice was higher than in iNOS^{-/-} mice.

A**Fig. 3.9**

CO-dependent protection against Act.D/TNFα-induced cell damage is independent from NO as assessed by knock-down and knock-out experiments.

A: Knock-down of *Nos2* or a control sequence via siRNA [20 nM] in PHs (C57BL/6J) previous to MC incubation (100 mM) for 6 h. Control cells received fresh medium instead (white bars). Cell damage was induced with 80 nM Act.D and 40 ng/ml TNFα for 18h. Cellular damage was assessed by LDH assay.

B

B: PHs (wt or iNOS^{-/-}, C57BL/6J) were incubated with 100 mM MC for 6 h previous to cell damage induction by Act.D (80 nM)/TNFα (40 ng/ml). Control cells received fresh medium instead (white bars). Cellular damage was assessed by LDH assay.

(mean ± SEM; ***p ≤ 0.0001)

In conclusion, these results show that CO-mediated protection against Act.D/TNFα-induced damage was independent from *Nos2* expression and NO. NO seems to support the protective effect.

3.5. NO induced *Hmox1* expression

Since NO, like CO, protected primary hepatocytes from Act.D/TNFα-induced damage underlying mechanisms were further elucidated (Fig. 3.7). As NO was found to induce *Hmox1* in other systems (Chung et al. 2008), the HO-1 expression following incubation with the NO donor SNAP on mRNA as well as on the protein level was investigated (Fig. 3.10).

The results show that SNAP (750 μ M) induced protein expression of HO-1 in primary murine hepatocytes after 6 and 20 hours of incubation, respectively (Fig. 3.10 A+C). CoPP (10 μ g/ml) was again used as a positive control. Similarly, induction of *Hmox1* mRNA expression could be detected after SNAP and CoPP incubation (Fig. 3.10 B), while incubation with MC (100 and 150 mM for 6 hours) failed to induce HO-1 (Fig. 3.10 C).

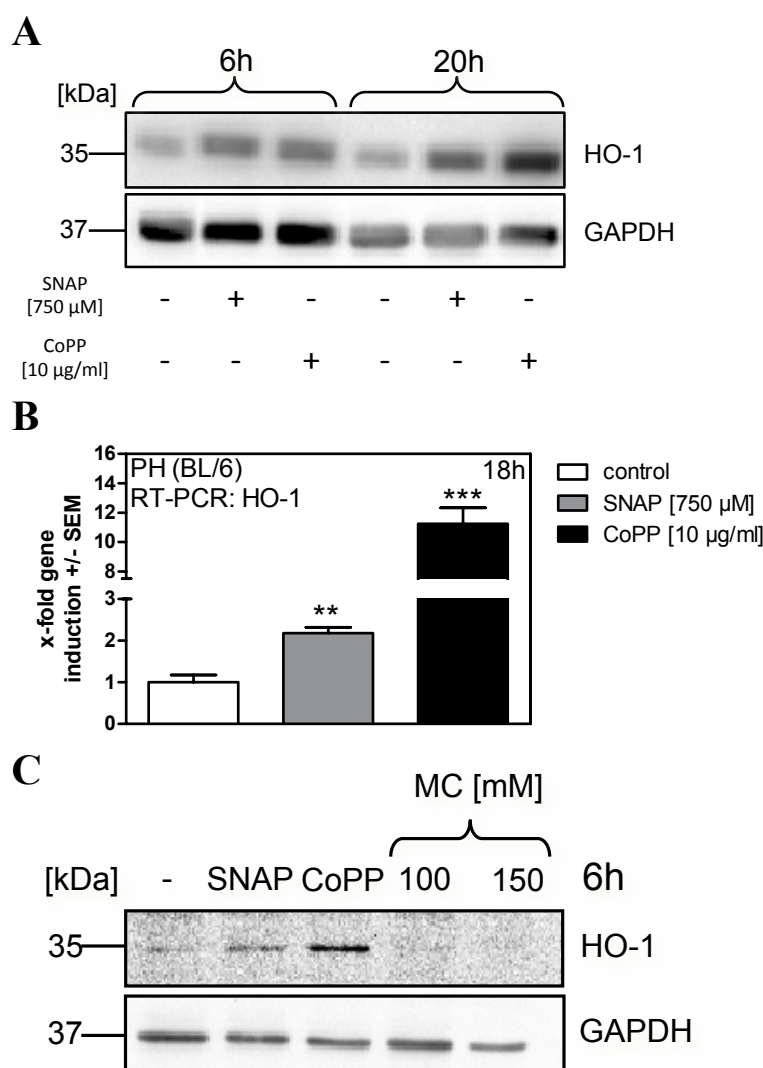


Fig. 3.10

Nitric oxide induced the expression of HO-1.

A: Western Blot analysis of PHs (C57BL/6J) incubated either with SNAP (750 μ M) or with CoPP (10 μ g/ml) for 6 or 20 h. Detection of HO-1. Detection of GAPDH was performed as a loading control.

B: PHs (C57BL/6J) were incubated with SNAP (750 μ M) or CoPP (10 μ g/ml) for 18 h. Control cells received fresh medium instead (white bar). *Hmox1* mRNA levels were detected via qRT-PCR.

C: Western Blot analysis of PHs (C57BL/6J) incubated either with SNAP (750 μ M), CoPP (10 μ g/ml), or MC (100 and 150 mM) for 6 h. Detection of HO-1. Detection of GAPDH was performed as a loading control.

(mean \pm SEM; **p \leq 0.01; ***p \leq 0.0001)

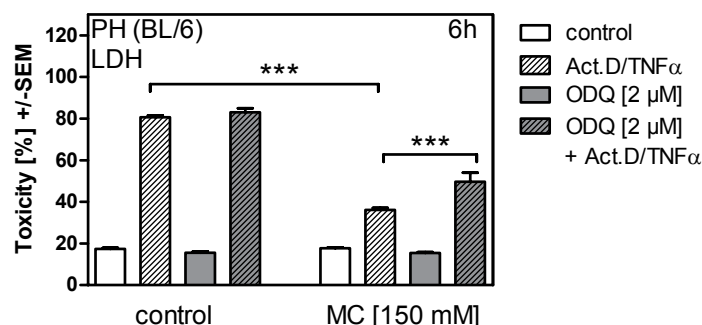
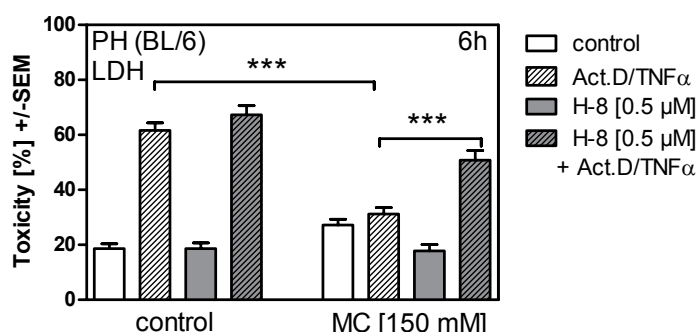
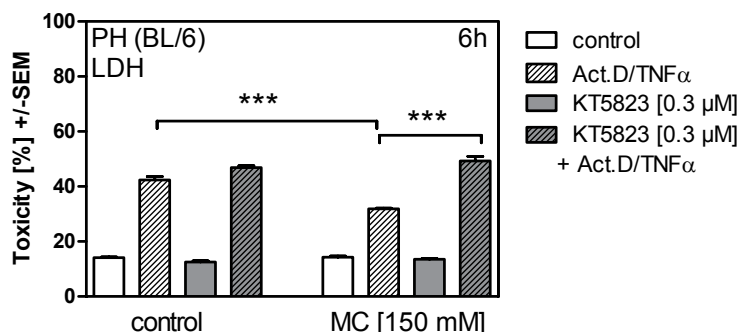
The results indicate that SNAP-released NO might protect primary hepatocytes by inducing HO-1.

3.6. Carbon monoxide activates the anti-apoptotic sGC-PKG cascade

To further elucidate pathways involved in CO-induced protection the advantage of the fact that CO and NO share some physiological properties was taken. It was investigated whether CO, like NO, might be able to activate soluble guanylyl cyclase (sGC) and its downstream target cGMP-dependent protein kinase G (PKG). For this purpose, the specific sGC inhibitor ODQ as well as two inhibitors of PKG, H-8 and KT5823, were used. At higher concentrations H-8 inhibits PKG, but also other protein kinases such as PKA and PKC. Therefore, these experiments were reproduced with the second inhibitor KT5823, which is more potent and selective for PKG. Primary hepatocytes were co-incubated with the inhibitors and 150 mM MC for six hours in order to stop the occurring anti-apoptotic mechanisms initiated by CO. Hepatocytes incubated only with 150 mM MC prior to Act.D/TNF α -induced damage reduced cell damage levels about 55% (Fig. 3.11 A). The co-incubation of MC with 2 μ M ODQ prior to cell damage induction partly abrogated the protective MC effect. The toxicity levels were elevated from 36% (only MC) up to 50% (ODQ+MC). This result indicates that sGC might be important for CO-dependent cell protection.

Similar results were obtained when PKG was inhibited with either 0.5 μ M H-8 or 0.3 μ M KT5823 (Fig. 3.11 B+C). In both cases, 150 mM MC alone significantly decreased toxicity levels (white striped bars: reduction about 50% (B) and about 24% (C)) in Act.D/TNF α -incubated cells. This protective effect was partly abrogated by H-8 (Grey striped bar: elevation about 65%) as well as by KT5823 (grey striped bar: elevation about 56%) when co-incubated with MC. The abrogation of the MC-dependent decrease in toxicity levels suggests possible anti-apoptotic effects of PKG.

Notably, neither H-8 nor KT5823 showed any toxicity when incubated alone or with MC without cell damage induction (B: H-8 shows 19% toxicity, and 18% H-8+MC; C: KT5823 shows 13% toxicity, and 14% when co-incubated with MC).

A**B****C****Fig. 3.11**

Inhibitors of sGC and PKG abrogated MC-dependent protective effect against induced cellular damage with 80 nM Act.D and 40 ng/ml TNF α in primary murine hepatocytes.

A: PHs (C57BL/6J) were incubated either alone with 150 mM MC or with 2 μ M ODQ and MC for 6 h prior to cell damage induction. Control cells received fresh medium instead (white bars). Cellular damage was assessed by LDH assay.

B: PHs (C57BL/6J) were incubated either alone with 150 mM MC or with 0.5 μ M H-8 and MC for 6 h prior to cell damage induction. Control cells received fresh medium instead (white bars). Cellular damage was assessed by LDH assay.

C: PHs (C57BL/6J) were incubated either alone with 150 mM MC or with 0.3 μ M KT5823 and MC for 6 h previous to cell damage induction. Control cells received fresh medium instead (white bars). Cellular damage was assessed by LDH assay.

(mean \pm SEM; *** $p \leq 0.0001$)

In conclusion, activation of the sGC-PKG cascade seems to contribute to CO-mediated protection of primary mouse hepatocytes against Act.D/TNF α -induced cellular damage.

In the next step, PKG-dependent anti-apoptotic effects were investigated. PKG is involved in cellular processes, such as calcium homeostasis, platelet activation and

adhesion, regulation of gene expression, and smooth muscle contraction (Francis et al. 2010). Additionally, PKG was found to regulate anti-apoptotic processes resulting in protection from ischemia-reperfusion-induced cardiac and neuronal damage (Das et al. 2006; Fiscus 2002; Francis et al. 2010). Among these protective processes are:

- phosphorylation of the pro-apoptotic protein BAD,
- activation of survival signaling cascades,
e.g. phosphorylation of ERK, p38, JNK, and GSK-3 β kinases,
- induction of the anti-apoptotic protein BCL-2,
- inhibition of opening of the mitochondrial permeability transition pore.

To determine possible downstream mechanisms the phosphorylation status of the kinases ERK1/2 and GSK3- β was investigated (Fig. 3.12).

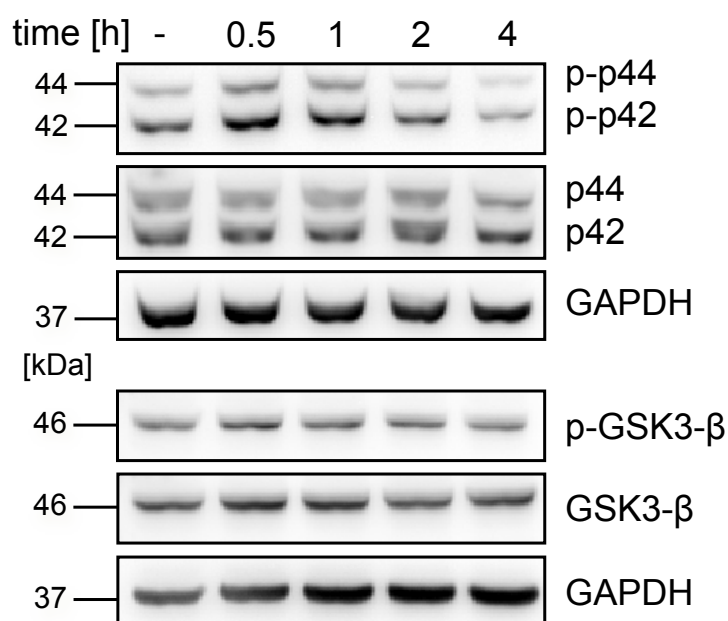


Fig. 3.12 Phosphorylation status of ERK1/2 and GSK3- β upon MC incubation in primary hepatocytes.

Western Blot analysis of PHs (C57BL/6J) incubated with 100 mM MC for 0.5, 1, 2, and 4 hours. Detection of phosphorylated and non-phosphorylated ERK1/2 (p44/p42) and GSK3- β , respectively. Detection of GAPDH was used as a loading control.

Western Blot analysis shows a strong phosphorylation, i.e. activation, of p44/p42 (ERK1/2) within the first 60 minutes of MC incubation (100 mM) compared to the non-phosphorylated p44/p42, where no change in band intensity was detectable upon MC incubation. This result indicates that CO is able to rapidly induce ERK1/2 activation.

MC (100 mM) did not cause GSK3- β phosphorylation, i.e. inactivation, in the first four hours of incubation. Regarding the detection of non-phosphorylated GSK3- β , there is also no change in band intensity after MC incubation (Fig. 3.12).

To investigate the contribution of JNK to the protective effect, this enzyme was specifically inhibited with SP600125 (Fig. 3.13 A). Primary murine hepatocytes were co-incubated with the inhibitor (1 μ M) and 150 mM MC for six hours prior to cell damage induction by Act.D/TNF α . SP600125 alone shows only a slight and not significant toxic effect in control samples (white bar: 13% toxicity; grey bar: 21% toxicity). Pre-treatment with 150 mM MC alone for six hours significantly decreased Act.D/TNF α -induced cell damage about 58%. This protective effect was also observed in samples co-incubated with MC and SP600125 (toxicity level averages 25%) (Fig. 3.13 A). The result indicates that the kinase JNK is probably not responsible for MC-dependent protection.

Finally, the expression of the anti-apoptotic gene *Bcl2* was analyzed because of reported PKG-dependent induction of *Bcl2* expression in a model of myocardial ischemia-reperfusion injury (Das, Xi, and Kukreja 2008). Figure 3.13 B depicts significantly increased mRNA expression levels of *Bcl2* upon incubation with 100 mM MC for six hours (2.6-fold) indicating a probable contribution of BCL-2 to the anti-apoptotic effect of CO.

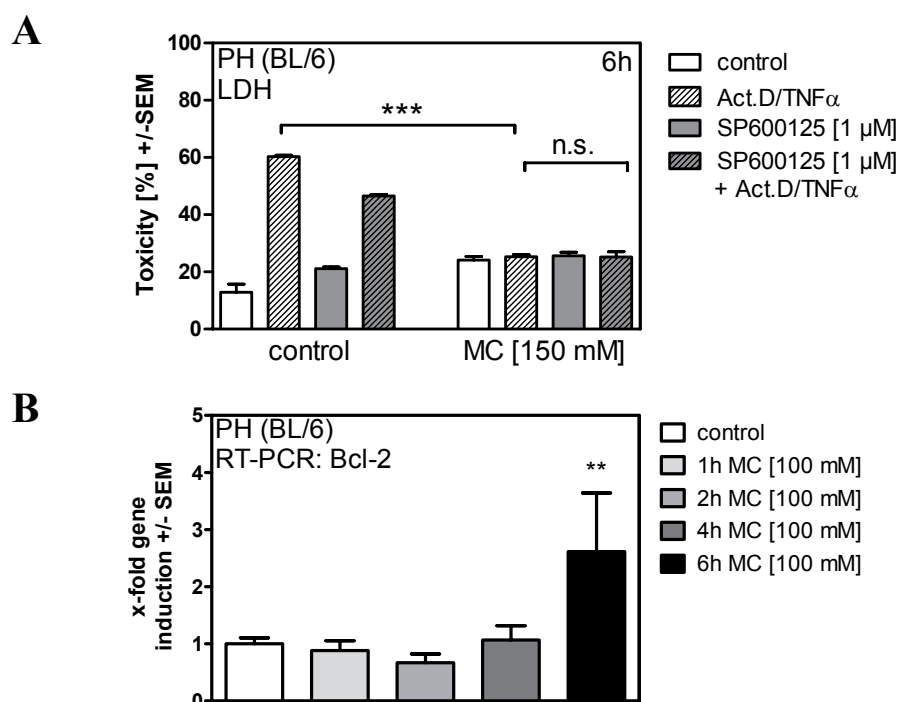


Fig. 3.13 Possible anti-apoptotic effects of MC concerning the kinase JNK and Bcl-2 in primary hepatocytes.

A: PHs (C57BL/6J) were incubated either alone with 150 mM MC or with 1 μ M SP600125 (JNK inhibitor) and MC for 6 h prior to cell damage induction with 80 nM Act.D/40 ng/ml TNF α . Control cells received fresh medium instead (white bars). Cellular damage was assessed by LDH assay.

B: PHs (C57BL/6J) were incubated with 100 mM MC for 1, 2, 4, and 6 hours. mRNA expression levels of *Bcl2* (Bcl-2) were measured by qRT-PCR.

(mean \pm SEM; ** $p \leq 0.01$; *** $p \leq 0.0001$; n.s. = not significant)

3.7. RT² ProfilerTM PCR Array

CO effects on regulatory cellular processes can be measured on the one hand via modified protein signature, as performed in section 3.3, and on the other hand via modified mRNA expression levels of target genes of distinct signaling pathways. For this purpose a PCR-based screen of 84 genes representative for 18 different transduction pathways was performed. Here, expression profiles of control primary hepatocytes were compared to profiles of MC-incubated hepatocytes (100 mM for four hours).

In Fig. 3.14 A, expression profiles of 58 genes are represented as x-fold change relative to control, which is indicated as a red line. Distinct genes, indicated by red arrows, were regarded as good candidates for further investigations because of their previously described contribution to tumor development or their altered regulation in tumorous tissue as described in the introduction section 1.2. Their expression profiles were re-evaluated by qRT-PCR (Fig. 3.14 B).

These results demonstrate that MC-derived CO exerted a strong effect on the expression of immediate early genes, e.g. FBJ (Finkel–Biskis–Jinkins) osteosarcoma oncogene (*Fos*), Jun oncogene (*Jun*), and Myelocytomatosis oncogene (*Myc*), which are transcription factors modulating among others the expression of genes responsible for cell proliferation, for example. Reproduced results illustrate that MC significantly induced the expression of *Fos* after two hours of incubation (2h: 2.6-fold; 4h: 2.4-fold; 6h: 2-fold increase). MC significantly induced *Jun* expression after one hour of incubation (2.6-fold), peaked after two hours (5.2-fold), and was still elevated after four hours (1.8-fold). Finally, the expression of *Myc* significantly increased 3.2-fold after two hours of MC incubation and slowly decreased to 2.6-fold after four hours (Fig. 3.14 B).

MC also significantly induced expression of vascular endothelial growth factor A (*Vegfa*). The increase lasted from two to four hours (2.9-fold) and slightly decreased after six hours (2.3-fold) (Fig. 3.14 B). As VEGFA is an important factor for proliferation, in particular for proliferation of endothelial cells, MC-derived CO may play a role in angiogenesis. In fact, this was previously shown in vascular smooth muscle cells and endothelial cells (Dulak et al. 2008).

The significantly increased expression of the cyclin-dependent kinase inhibitor 1A (*Cdkn1a*; p21) (after 2h: 2.8-fold increase; after 4h: 2.6-fold increase), which is a direct target gene of tumor suppressor p53, indicates a probable activation of this transcription factor (Fig. 3.14 B). On the one hand, p21 is responsible for the cell cycle arrest in G₁ phase and cellular senescence, on the other hand, p21 can

promote proliferation and an oncogenic phenotype (El-Deiry et al. 1993; Warfel and El-Deiry 2013).

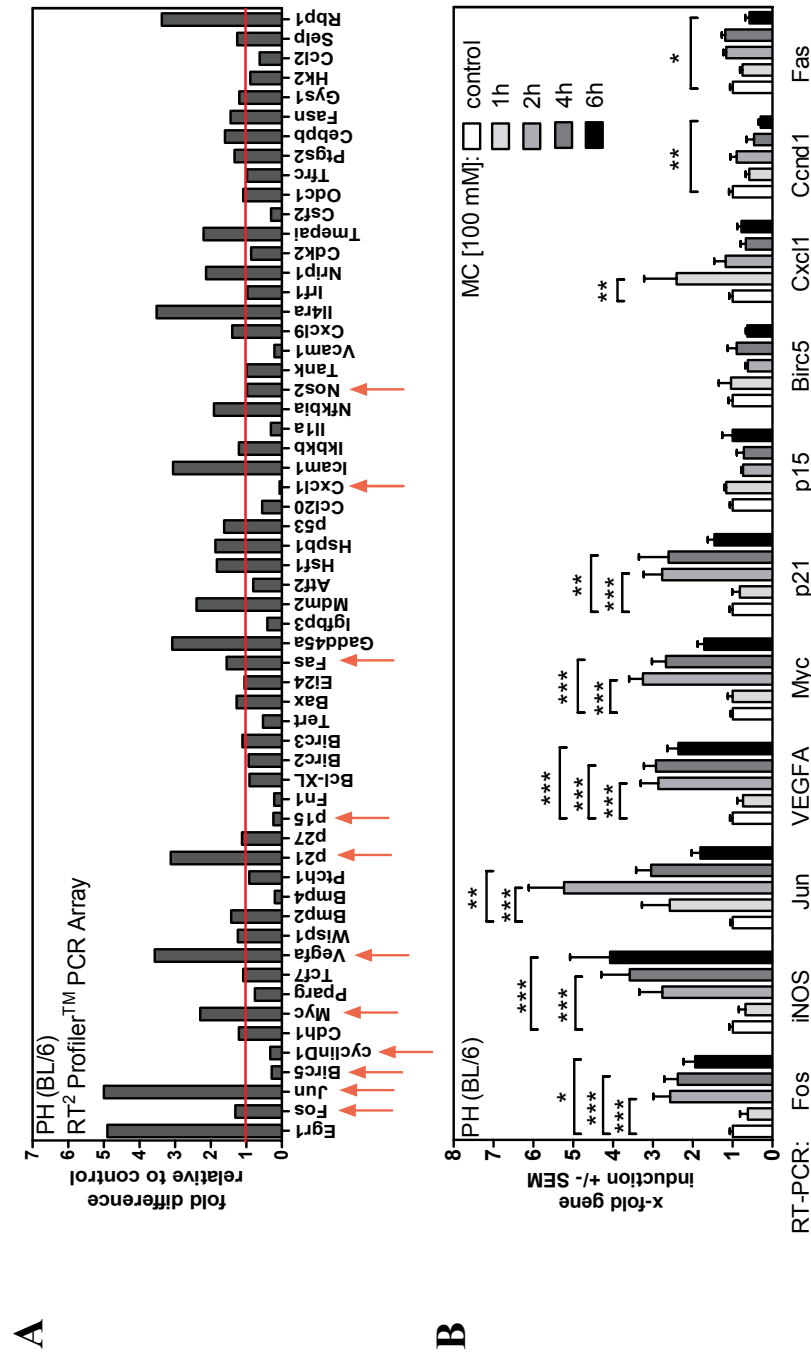


Fig. 3.14 RT² Profiler™ PCR Array and verification.

A: PHs (C57BL/6J) were either untreated (control) or incubated with 100 mM MC for 4 h. Analysis of fold difference mRNA expression levels of MC-incubated hepatocytes relative to control and housekeeping genes (*Gusb*, *Hprt1*, *Hsp90ab1*, *Gapdh*, *Actb*); red line indicates 1 (expression in untreated control cells); red arrows indicate further investigated genes in (B).

B: PHs (C57BL/6J) were incubated with 100 mM MC for 1, 2, 4, and 6 hours. Control cells received fresh medium instead (white bars). Re-evaluation of mRNA expression levels of indicated genes in (A). (mean ± SEM; *p ≤ 0.05; **p ≤ 0.01; ***p ≤ 0.0001)

A further supporting hint for the interaction of MC with p53 shows Figure 3.1 C. The protein expression of BID, which is a target gene of p53, is visibly induced upon MC incubation. Despite induced protein expression of BID, which is a pro-apoptotic Bcl-2-family member, primary hepatocytes incubated only with MC did not show enhanced apoptotic rates or activated effector caspases (Fig. 3.1 C).

Several genes were found decreased in their expression levels upon MC incubation in the Profiler array. Four of them were regarded as promising candidates as they are reported to positively or negatively correlate either with tumor development or with progression. The mRNA expression levels of Baculoviral IAP repeat-containing 5 (*Birc5*), cyclin D1 (*Ccnd1*), Cyclin-dependent kinase inhibitor 2B (*Cdkn2b*; p15), and Chemokine (C-X-C motif) ligand 1 (*Cxcl1*) were analyzed (Fig. 3.14 B).

Expression of *Birc5*, which belongs to the inhibitor of apoptosis protein (IAP) family, showed a slight tendency to down-regulation (Fig. 3.14 B). This result is unexpected as *BIRC5* was frequently found to be over-expressed in HCC cell lines and tissues (Fabregat 2009).

Similarly, p15 (*Cdkn2b*) expression was barely influenced by MC (Fig. 3.14 B).

The expression of *Cxcl1* was significantly induced (2.4-fold) after one hour of MC treatment, but dropped to the basal level afterwards, which is contrary to the finding in the PCR array (Fig. 3.14). *Cxcl1*, also called GRO α or melanoma growth-stimulatory activity (MGSA), is a chemokine which is secreted by melanoma cells and possesses among other pro-angiogenic and tumorigenic properties (Dhawan and Richmond 2002; Haskill et al. 1990).

However, the expression of cyclin D1 (*Ccnd1*) was significantly decreased after MC incubation (after 4h: 0.5-fold expression relative to control; after 6h: 0.3-fold; Fig. 3.14 B). Notably, cyclin D1 is responsible for the G₁/S cell cycle transition and therefore for cell replication. Negative regulation of cyclin D1 conceivably arrests the cell cycle. On the contrary, the expression of p21 (*Cdkn1a*), which is a natural inhibitor of cyclin D and E, is induced upon MC. It was reported that induction of HO-1 results in increased p21 and decreased Cyclin D1 expression levels in

hypertensive rat vascular smooth muscle cells (VSMC) (Jeon et al. 2009). Although the results may lead to the conclusion that MC inhibits proliferation, a recently published study reports similar observations. The authors ascertained decreased Cyclin D1 expression in 66% of HCC cases, which could not be correlated with any clinicopathological variables in HCC (Lu et al. 2013).

The expression of two more genes of the PCR array was shown to be disproved during reproduction, e.g. of *Nos2*, which was found to be induced upon MC incubation (Fig. 3.5 A), and of the Fas receptor (*Fas*). Instead of a slight induction measured in the Profiler array, MC incubation for six hours significantly decreased the expression (0.6-fold) (Fig. 3.14). Down-regulated expression of *FAS* is frequently associated with deregulated apoptosis which can be found in HCC (Fabregat 2009).

In summary, the RT² ProfilerTM PCR array provided information of numerous genes with corresponding signaling pathways simultaneously. Achieved findings indicate that MC-derived CO influences a variety of signaling pathways. Apart from the sGC-PKG pathway, which appears to be responsible for the anti-apoptotic effect of CO, also other CO-dependent tumor-promoting signaling seems to be important. These are pathways regulating the proliferation of the cells.

3.8. CO activates the STAT3 signaling pathway

The JAK-STAT3 signaling pathway plays a crucial role in cell proliferation processes during partial hepatectomy (Kurinna and Barton 2011; Taub 1996). Surprisingly, isolated primary hepatocytes incubated with 100 mM MC exhibited an activation of the transcription factor STAT3 after 30 minutes of incubation as shown by Western Blot analysis (Fig. 3.15 A).

In addition, known target genes of STAT3 were found induced upon MC incubation, e.g. *Myc*, *Jun*, and *Fos*, but also plasminogen activator, urokinase (*Plau*), and the serine/threonine kinase *Pim3* (Dauer et al. 2005). Because of previous studies, which connect these genes with carcinogenesis, they were regarded as promising candidates for investigation of CO-induced tumor cell protection.

PLAU is associated with angiogenesis and metastasis when expressed in a pathological context (Alfano et al. 2005). CO was able to significantly induce *Plau* (2-fold after two and four hours, respectively) (Fig. 3.15 B).

Pim3, a proto-oncogene with serine/threonine kinase activity, showed significantly enhanced (4.8-fold) mRNA expression levels upon MC incubation (Fig. 3.15 B). *PIM3* was found to be induced in HCC tissues (Fujii et al. 2005). Furthermore, it was reported that *Pim3*-transgenic mouse-derived hepatocytes exhibited accelerated cell cycle progression and promoted HCC development (Wu et al. 2010). PIM3 regulates signal transduction pathways, contributing to both cell proliferation and survival of healthy as well as malignant cells (Mukaida, Wang, and Li 2011).

The oncogene *Ptk6* was found highly expressed in hepatocytes when incubated with 100 mM MC for two hours and longer. MC incubation significantly induced (7.7-fold) its expression after two hours, 6-fold after four hours, and 4.2-fold after six hours (Fig. 3.15 B). *PTK6* has been found overexpressed in breast tumors and induces activation of STAT3 as well as STAT5 signaling. It also enhances the interaction between epithelial growth factor receptor (EGFR) and PI3K, resulting in potentiated PI3K/Akt signaling (Ostrander, Daniel, and Lange 2010).

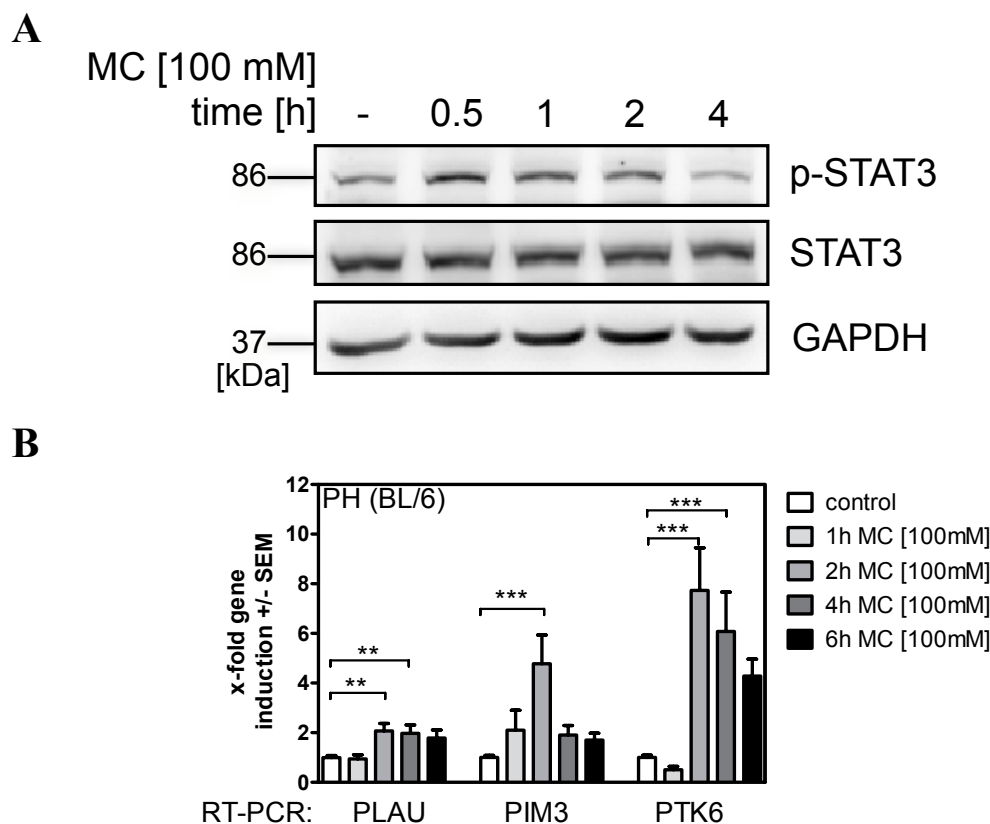


Fig. 3.15 Activation of STAT3 signaling upon MC incubation.

A: Western Blot analysis of PHs (C57BL/6J) incubated with 100 mM MC for 0.5, 1, 2, and 4 hours. Detection of phosphorylated and non-phosphorylated STAT3. Detection of GAPDH was used as a loading control.

B: PHs (C57BL/6J) were incubated with 100 mM MC for 1, 2, 4, and 6 hours. Control cells received fresh medium instead (white bars). mRNA expression levels of *Plau*, *Pim3*, and *Ptk6* were measured by qRT-PCR.

(mean ± SEM; ** $p \leq 0.01$; *** $p \leq 0.0001$)

Together, these results indicate a crucial role for CO-mediated STAT3 activation at very early time points, e.g. 30 minutes, of incubation with MC. Induced genes either activate STAT3 (in case of PTK6) or are target genes of the transcription factor, which induce angiogenesis, cell proliferation, and survival. These factors can push a healthy cell towards a malignant phenotype and therefore may represent the first step for malignant transformation.

4. Discussion

The liver is an organ with a unique regenerative potential. During a healthy state, hepatocytes are quiescent (G_0 -arrested), however, under certain circumstances these cells can be forced to enter the cell cycle. This process is initiated by the loss of tissue mass, for example, due to liver damage in case of chronic inflammation. Chronic liver damage induces a persistent cycle of necro-inflammation and hepatocyte regeneration, increasing the risk to accumulate genetic mutations in hepatocytes, leading to uncontrolled expansion of transformed cells and HCC development (Nakagawa and Maeda 2012).

The anti-inflammatory, anti-viral, and anti-apoptotic protein HO-1 is frequently induced in tumors (Jozkowicz, Was, and Dulak 2007; Was, Dulak, and Jozkowicz 2010) including HCC (Abdel Aziz et al. 2008; Calvisi et al. 2007; Sass et al. 2008). Inhibition of *Hmox1* by siRNA application in a mouse model of orthotopic HCC reduced tumor growth and increased tumor cell apoptosis (Sass et al. 2008). On the other hand, induction of HO-1 interferes with viral replication (Lehmann et al. 2010; Protzer et al. 2007; Schmidt, Mathahs, and Zhu 2012), acute and chronic inflammation (Paine et al. 2010), and reduces fibrosis progression (Barikbin et al. 2012; Lundvig, Immenschuh, and Wagener 2012). These studies depict the double-edged role of HO-1. In the early steps of acute hepatitis and fibrosis HO-1 induction is beneficial in order to reduce the virus amount (e.g. HCV or HBV) and to attenuate the overshooting reaction of the immune system. As HO-1 possesses anti-viral and anti-inflammatory properties, this might prevent carcinogenesis at its very beginning - during chronic hepatitis.

Notably, the anti-apoptotic HO-1 product CO induces protection from apoptosis (Bilban et al. 2008; Sass et al. 2003; Wegiel et al. 2013), leading to the conclusion that in already existing tumors over-expression of HO-1 would contribute to protection of malignant cells.

To elucidate the mediators and pathways of tumor cell protection the scenario of a CO-flushed hepatocyte had to be transferred to an *in vitro* system. Indeed, I was able to show that exogenous CO protected primary hepatocytes from induced damage and inhibited the apoptotic cascade (Fig. 3.1). This mechanism is independent from *de novo* HO-1 induction (Fig. 3.2).

Using two kinds of arrays based on either protein or RNA level, I observed CO-dependent regulation of several genes and signaling pathways (Tab. 4.1), which are responsible for the protection against induced cellular damage *in vitro*.

Tab. 4.1 Summary of CO-modulated key components in primary murine hepatocytes.
 ↓ = decrease; ↑ = increase

direct apoptosis-related signaling	inhibition of Caspase-3 activation inhibition of Caspase-8 activation <i>Fas</i> expression ↓ <i>Bcl2</i> expression ↑
activation of survival and proliferative signaling	urea cycle/L-Arginine metabolism iNOS/NO sGC/PKG ERK1/2 STAT3
expression of tumor-promoting genes	immediate early genes (<i>Jun</i> , <i>Fos</i> , <i>Myc</i>) ↑ <i>VEGFA</i> ↑ <i>p21</i> ↑ <i>Cyclin D1</i> ↓ <i>Cxcl1</i> ↑ <i>Plau</i> ↑ <i>Pim3</i> ↑ <i>Ptk6</i> ↑

The anti-apoptotic effect of CO was most obvious in inhibition of the activity of executor CASPASES-3 and -8 (Fig. 3.1 C). Furthermore, incubation of hepatocytes

with MC led on the one hand to decreased expression of *Fas* (Fig. 3.14 B) and on the other hand to increased expression of the anti-apoptotic *Bcl2* (Fig. 3.13 B). Down-regulation of the Fas receptor results in inhibited Fas-mediated apoptosis, which belongs to the extrinsic pathway. An expressional down-regulation of Fas ligand and/or receptor is frequently associated with HCC (Fabregat et al. 2007; Fabregat 2009). Concurrent increased expression of *Bcl2*, as observed here, shifts the cellular balance towards anti-apoptotic and protective signaling, thus favoring the escape from regulatory mechanisms (Fabregat et al. 2007).

The anti-apoptotic effects of CO on cell signaling level are divers and include CO-dependent modulations within the broad cellular metabolism as well as the activation of survival signaling, e.g. activation of sGC/PKG and ERK1/2 pathways. The finding that CO influenced broad cellular metabolism (Fig. 3.3 and Tab. 3.1) is in line with a study of Xu and colleagues, investigating the proteome of murine hepatocytes in an ischemia-reperfusion model (Xu et al. 2009). Cell incubation with MC mimics the ischemic injury by interrupting the electron transport chain and initiating cell-protective, conditioning-like mechanisms (Bilban et al. 2008). Several publications show connections between metabolism, in particular the urea cycle, and cell protection, elucidating some distinct metabolic proteins as promising candidates for further investigation (Lind 2004; Mori 2007; Nagasaki et al. 1996), for example, arginase 1 (ARG1) and argininosuccinate lyase (ARLY/ASL), which were also altered upon MC (Tab. 3.1). Within the urea cycle, these two enzymes degrade the amino acid L-Arginine (L-Arg) to urea and recycle the by-product L-Citrulline to L-Arg (Morris 2002). As mentioned in the introduction section 1.5, within the urea cycle the NO-cycle can be activated, when the enzyme nitric oxide synthase (NOS) is expressed (Morris 2002). It was shown that the CO donor induced *Asl* and *Argl* expression, which clearly indicates an interaction of CO with the urea cycle. These proteins are two out of five enzymes, which are responsible for clearing nitrogenous waste, such as ammonia, by incorporating this group into harmless urea

(Morris 2002). In more detail, ASL and ARG1 are part of the L-Arg metabolism. While ASL recycles together with argininosuccinate synthase (ASS) the amino acid L-Arg from L-Citrulline, ARG1 degrades L-Arg to L-Ornithine and urea (Morris 2002; Ye et al. 2007). NOS enzymes also utilize L-Arg as substrate for NO production and when ARG1 and iNOS are simultaneously induced, they compete for this amino acid (Morris 2002). Moreover, it has been shown that ASL can be co-induced with iNOS in various cell types (Mori 2007). This finding is consistent with observation obtained in primary mouse hepatocytes incubated with MC in present study (Fig. 3.5).

Transcription of *Nos2* is regulated by multiple transcription factors, e.g. NFκB, STAT1, AP-1, C/EBP, HIF-1, inteferon response factor 1 (IRF-1), and CREB, depending on stimulus and cell type (Aktan 2004; Lowenstein and Padalko 2004). In case of primary murine hepatocytes, incubation with CO induced *Nos2* transcription rather by the activation of the transcription factor AP-1 than of NFκB (Fig. 3.6). This finding is in line with a study of Conde de la Rosa *et al.* who similarly investigated the protective effect of HO-1 and in particular of CO in primary culture of rat hepatocytes. They also observed induction of iNOS upon CO exposure, and showed, that the CO-dependent protective effect was independent of NFκB (Conde de la Rosa et al. 2008).

Consequently to iNOS induction, the activity was proved by measuring its degradation product NO (Fig. 3.5). Depending on the amount of produced NO, it exerts the potency either to protect cells from damage or to activate the apoptosis cascade. ARG1 decreases the level of L-Arg and thus limits the main factor for NO production. This results in low NO levels, which rather promote protective signaling pathways, whereas high NO levels induce apoptosis (Abu-Amara et al. 2012).

NO is able to induce anti-apoptotic and cell-protecting mechanisms, e.g., induction of heat shock protein 70, suppression of the pro-apoptotic BAX expression, activation of soluble guanylyl cyclase (sGC), up-regulation of antioxidant systems and S-nitrosylation of CASPASE-3 protein (Kim et al. 1997; Maejima et al 2005;

Olson and Garbán 2008). Due to the fact that CO and NO share similar physiologic properties, I hypothesized that CO and NO might also share some anti-apoptotic mechanisms. Therefore, the focus was directed on the activation of sGC and its downstream target PKG. Indeed, it was reported among others in nervous and vascular systems that CO is able to activate sGC, but to a lower degree than NO does (Evgenov et al. 2006; Hartsfield 2002).

In fact, it was shown that sGC-PKG signaling was activated by CO and at least partly protects primary hepatocytes from induced damage (Fig. 3.12 and 3.13). Inhibition of sGC and PKG with their respective specific inhibitor, i.e. ODQ, H-8, and KT5823, partly abrogated CO-dependent protection of primary hepatocytes from Act.D/TNF α -induced cellular damage. These findings are in line with a report describing that the anti-apoptotic effects of CO are, in part, dependent on sGC activation in vascular smooth muscle cells (Liu et al. 2002).

The activation of PKG by cGMP, product of sGC, leads to phosphorylation of numerous intracellular proteins, which in turn regulate many important physiological functions such as control of vascular tone, cell differentiation, proliferation, and platelet aggregation (Hofmann, Ammendola, and Schlossmann 2000). Furthermore, Das *et al.* reported that in cardiomyocytes the PKG-dependent protective mechanism is based on activation of the MAP kinases Akt, ERK1/2, JNK and the increase in *Bcl2*, *Nos3*, and *Nos2* expression levels (Das et al. 2006).

By investigating these mechanisms in primary murine hepatocytes similarities were determined, e.g. activation of ERK1/2, increased expression of *Bcl2* and *Nos2*, but also discrepancies, e.g. JNK activation and GSK3- β inactivation (Fig. 3.12, 3.13 and 3.14). The Act.D/TNF α model was probably not the most advantageous one to analyze the activation of JNK, as this experiment does not show the possible activation of the kinase in the first incubation periods (30-60 minutes). The investigation of possible transcription factors of iNOS clearly demonstrated an induction of *Jun* in the first four hours (Fig. 3.6 B, 3.14 B), which is a target gene of JNK (Eferl and Wagner 2003). Even more, it appears that the sustained activation of

JNK is associated with apoptosis, whereas the acute and transient activation of JNK, which might be possible in context of endogenous CO production, is involved in cell proliferative or survival pathways (Dhanasekaran and Reddy 2008).

The results from protein and RNA arrays further indicate that CO activates not only anti-apoptotic signaling, but also induces proliferation (Tab. 4.1). While it was previously reported that CO acts in a cell-protective manner in many experimental models *in vivo* and *in vitro*, the induction of proliferation signaling pathways in non-endothelial cells was quite unexpected and contradictory to previous studies (Bauer and Pannen 2009; Wegiel et al. 2008).

Recently, our group detected, that CO induced the expression of two growth-stimulating factors: *Vegfa* and *Angpt2* (Fig. 3.14 B and unpublished observations), which are both expressed in non-endothelial cells - primary hepatocytes. When induced simultaneously, both factors promote the initiation of angiogenesis and maturation of new vessels and play a role in inflammation and metastasis (Huang et al. 2010).

Similar to observations in this thesis, it was already shown that either exogenous induction of HO-1 or incubation with CO induces VEGF expression in murine endothelial cells and vascular smooth muscle cells (VSMC) (Volti et al. 2005) and thus stimulates angiogenesis.

As normal healthy hepatocytes are quiescent and highly differentiated, external stimuli, such as cytokines, are necessary to push the cell into mitosis. In case of liver regeneration, cytokines activate a variety of transcription factors including nuclear factor kappa B (NF κ B), signal transducer and activator of transcription 3 (STAT3), CCAAT enhancer-binding protein beta (C/EBP β), and activator protein 1 (AP-1) (Stepniak et al. 2006). Notably, STAT3 and two subunits of AP-1 (i.e. *Jun* and *Fos*) were found activated upon CO incubation on protein and mRNA levels, respectively (Fig. 3.14 B and 3.15 A).

Contradiction results were observed in the expression profiles of the cyclin-dependent kinase inhibitor p21 (*Cdkn1a*) and Cyclin D1 (*Ccnd1*) (Fig. 3.14 B). MC increased p21 and decreased Cyclin D1 expression levels, respectively. As p21 is an inhibitor of the G₁/S-cyclins (i.e. cyclin D1 and E), its increased expression results in Cyclin D1 inhibition (Alberts, Johnson, and Lewis 2002). This may lead to the conclusion that CO also acts in an anti-proliferative way, but studies analyzing human HCC samples indicated down-regulation of Cyclin D1 in tumor tissue in comparison to non-tumor tissue in 66% of HCC cases (Lu et al. 2013; Xu et al. 2001). Another study demonstrated an overexpression of Cyclin D1 in 32-58% of HCCs leading to an unregulated cell proliferation (Lu et al. 2013). These studies indicate the heterogeneity of HCC.

A further evidence for induction of proliferation provides the increased expression level of the chemokine *Cxcl1* (Fig. 3.14 B). Alternatively, it is called GRO α (growth-related oncogene alpha), as it can be induced either by the growth-related serum response pathway or by the chemokine-induced (i.e. IL-1 and TNF α) pathway (Haskill et al. 1990). *Cxcl1* was initially discovered as a chemokine up-regulated in melanoma, however, since then it was also found induced in other cancer types, such as pancreatic, lung, and breast cancer (Dhawan and Richmond 2002; Wu et al. 2009). Even more, Wu *et al.* proposed the measurement of *Cxcl1* level as a potential serological marker for HCC (Wu et al. 2009). According to the literature, there is no reported connection of HO-1, CO and hypoxia with the chemokine *Cxcl1*. This result demonstrates for the first time the induction of the oncogenic chemokine *Cxcl1* upon CO.

CO induced the expression of immediate early genes, e.g. *Myc*, *Jun*, and *Fos*, within short incubation periods in primary murine hepatocytes (Fig. 3.14 B). A preceding study, which analyzed the expression of immediate early genes under hypoxic conditions *in vivo*, demonstrated that these genes are highly elevated in liver confirming the results in the present study (Gess et al. 1997).

Furthermore, these genes are regarded as oncogenes because of their elevated expression in many malignancies, although until now, no activating mutations, deletions or amplifications of any *JUN* or *FOS* gene have been identified in human tumors (Eferl and Wagner 2003). These genes and other members of their protein family form a dimeric transcription factor AP-1. The AP-1 complex exerts its oncogenic or anti-oncogenic effects by regulating genes involved in cell proliferation, differentiation, apoptosis, angiogenesis and tumor invasion (Eferl and Wagner 2003). In contrast to AP-1, many studies explain the mutation of the *MYC* oncogene as a main reason for the development, progression and poor prognosis of HCC (Lin et al. 2010). Even more, *MYC* is among others the most frequently over-expressed gene in human cancer. So far investigated, as many as 15%-20% of human genes can be regulated directly or indirectly by this transcription factor. These genes are associated with the regulation of cell cycle control, protein synthesis, cytoskeleton and cell motility, and cell metabolism (Lin et al. 2010).

Among other transcription factors, STAT3 can induce the expression of *Jun*, *Fos*, and *Myc* (Dauer et al. 2005), and was shown to be activated by CO in the first two hours of incubation (Fig. 3.15 A). This result is quite unexpected, since a culture of isolated primary hepatocytes contains approximately only 5% of non-parenchymal cells, such as Kupffer cells, which are known to produce the main ligand for the cytokine receptor: interleukin 6 (IL-6) (Seglen 1976; Taub 2003). Besides cytokine receptors, STAT3 is activated by various growth factor receptors, such as epidermal growth factor receptors (EGFR), hepatocyte growth factor receptor (HGFR), and VEGF receptor (VEGFR) (Yu, Kortylewski, and Pardoll 2007), whose ligand, *Vegfa*, was induced upon MC incubation (Fig. 3.14). This might be the reason for STAT3 activation in the culture of isolated primary hepatocytes.

Besides the reported role of STAT3 in liver regeneration (Stepniak et al. 2006), Taub described its no less important role in hepatoprotection against Fas-mediated apoptotic liver damage (Taub 2003). Haga *et al.* demonstrated *in vivo* that STAT3

activates anti-apoptotic and anti-oxidative proteins, which results in decreased apoptotic rates and lower production of ROS in the liver (Haga et al. 2003).

From an immunological point of view, STAT3 signaling plays a crucial role in the crosstalk between tumor and its immunological microenvironment, which was already mentioned in the introduction section 1.2. As STAT3 is also important for tumor-cell proliferation and survival, angiogenesis and invasion, the underlying pathway represents a direct link between carcinogenesis and immunosuppression (Yu et al. 2007).

During the investigation of STAT3 signaling, further associated genes were found induced upon CO incubation, e.g. *Plau*, *Pim3*, and *Ptk6* (Fig. 3.15 B), whose expression was shown altered in malignancies.

The urinary-type plasminogen activator (PLAU) controls matrix degradation through the conversion of plasminogen into plasmin. Under physiological and pathological conditions, such as cancer metastasis, it is thought to be the critical trigger for plasmin generation during cell migration and invasion (Alfano et al. 2005). Indeed, PLAU has the ability to support the malignant phenotype through several mechanisms. First, PLAU has matrix degrading activity, which favors tumor dissemination; second, PLAU stimulates cell motility through the control of cytoskeleton and focal adhesion formation; third, it also stimulates cell proliferation; and fourth, PLAU protects cells from apoptosis, thus enhancing tumor cell survival (Alfano et al. 2005).

A further analyzed target gene of STAT3 is *Pim3*. It is a member of the Provirus-integrating site Moloney murine leukemia virus (Pim) family, which belongs to the Ca^{2+} /calmodulin-dependent protein kinase (CaMK) group and exhibits serine/threonine kinase activity (Mukaida et al. 2011). Furthermore, Mukaida *et al.* revealed that Pim3 protein is barely detected in normal adult endoderm-derived organs, such as the liver, pancreas, colon, and stomach; however, its expression is augmented in pre-malignant and malignant lesions of these organs (Mukaida et al. 2011). For this reason, it was quite surprising to find this kinase up-regulated

upon CO incubation in primary hepatocytes (Fig. 3.15 B). Pim3 may contribute to carcinogenesis through four main activities: (i) delivery of survival signaling through phosphorylation of Bad; (ii) regulation of cell cycle progression; (iii) regulation of protein synthesis; and (iv) regulation of Myc transcriptional activity (Mukaida et al. 2011).

Finally, Ptk6, also termed breast cancer kinase (Brk), is a novel non-receptor tyrosine kinase with limited homology to the c-src kinase family and which was initially discovered in breast cancer cell lines (Harvey and Crompton 2004; Ostrander et al. 2010). Thereafter, *PTK6* expression was found deregulated in various cancer types, such as human ovarian tumor cells, in primary and metastasized colon tumors, head and neck squamous cell carcinoma (SCC), and others (Brauer and Tyner 2010). Ptk6 appears to participate in a variety of signaling pathways, e.g. STAT3/5, depending on the context in which it is expressed. For example, tissue type, hormonal milieu, physiologic status (i.e. normal or cancer) and the expression levels of related signaling molecules may dictate the specificity of Ptk6 action. However, in malignant settings Ptk6 is reported to contribute to cancer progression by sensitizing cells to mitogenic signals and enhancing proliferation, anchorage-independent survival, and migration/invasion (Ostrander et al. 2010). To best of my knowledge, Ptk6 expression is not reported induced in liver or in HCC to date. Furthermore, Ptk6 is not associated with HO-1 or CO in any other kind of malignancy. Thus, the discovery that CO induced the *Ptk6* expression represents the first link between the gas and this novel kinase (Fig. 3.15 B).

While investigating the protective mechanisms of CO it became obvious that CO activates a positive feedback loop. This feedback loop might be responsible for a sustained CO level in hepatocytes and induces, as previously mentioned, the production of NO also bearing cytoprotective properties (Fig. 4.1).

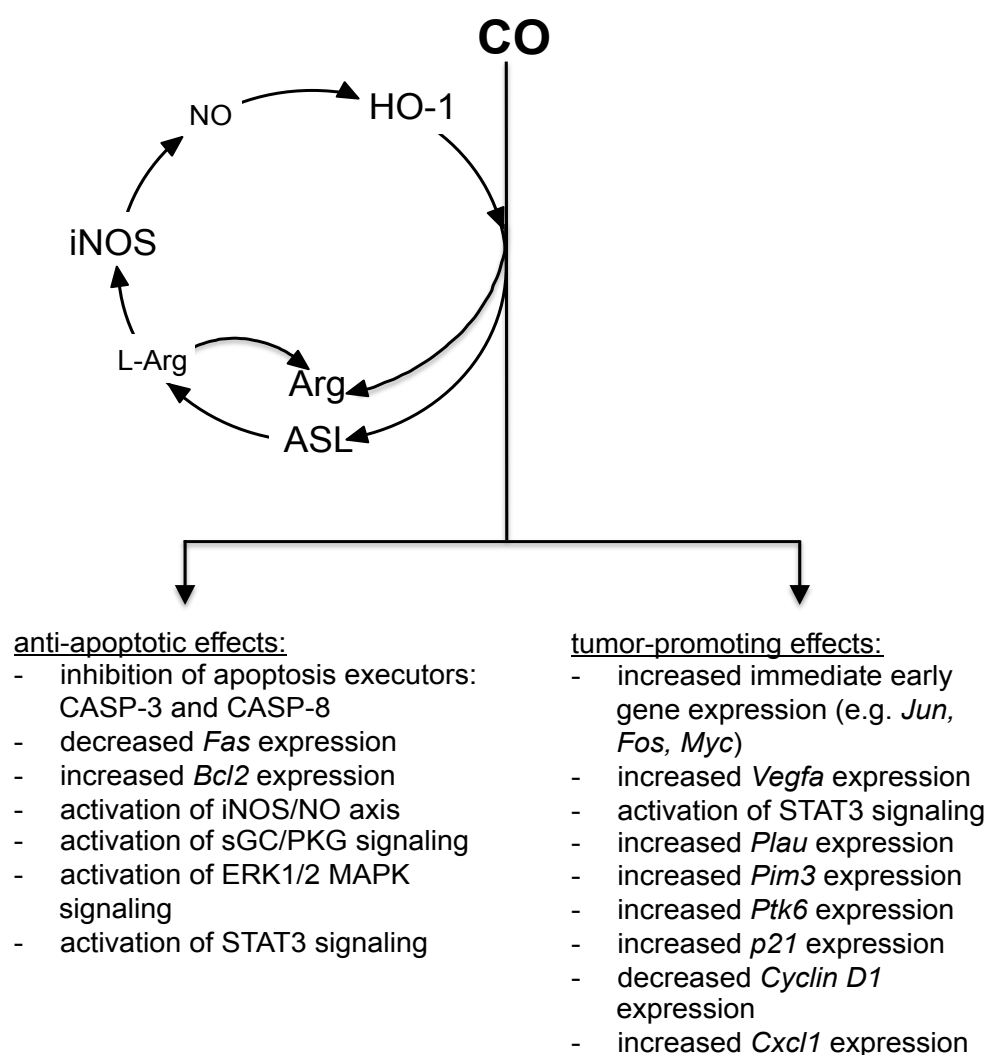


Fig. 4.1 Scheme of CO-dependent anti-apoptotic and tumor-promoting mechanisms and the positive feedback loop.

CO induced the mRNA expression of *Arg*, *Asl*, and *Nos2*. NO produced by iNOS induced *Hmox1*, which was again responsible for a sustained CO level.

Evidence for the feedback loop presents the discrepancy of the time duration for the significant protective effect of CO and NO. When comparing CO-dependent (Fig. 3.1 A+B) and NO-dependent protection (Fig. 3.7 A+B), the required time duration for a significant effect becomes evident. CO acted faster, i.e. within first two hours of incubation. MC protected primary hepatocytes significantly (reduction of toxicity about 43%) against Act.D/TNF α -induced damage. In contrast, protective

effects of NO were not observed before at least four hours of incubation with the NO donor SNAP and were less pronounced (reduction about 16%). It seems that CO acts more directly than NO. One of the protective mechanisms of NO is the induction of HO-1 (Chung et al. 2008), which was also observed in this study (Fig. 3.10).

The results show that CO induced the expression of *Asl*, leading to higher L-Arg levels in the cells, which were subsequently metabolized by CO-induced iNOS. In order to keep the NO level under cell-damaging threshold, *Arg1* was induced and thus a protective mechanism, i.e. *Hmox1* expression, was initiated (Fig. 3.5 A + 3.10). The protective effect of NO could be demonstrated by SNAP, which dose- and time-dependently reduced cytotoxicity levels in the Act.D/TNF α model (Fig. 3.7). Furthermore, SNAP-dependent protection of primary rat hepatocytes was previously described (Kim et al. 1997). This finding is in line with the observations in primary mouse hepatocytes in this study (Fig. 3.7). Although, CO seems to induce HO-1 via iNOS/NO loop, CO was able to protect hepatocytes independently from NO and *de novo* HO-1 synthesis (Fig. 3.2 and 3.9 A+B). These results indicate that the iNOS/NO pathway plays only a minor and rather supporting role in CO-dependent cell protection against induced damage.

In summary, results of this thesis, which are based on experiments performed in the *in vitro* system of isolated mouse hepatocytes, depict three main investigations (Fig. 4.1):

- (i) CO-dependent anti-apoptotic mechanisms, such as activation of the sGC-PKG axis with possible protective downstream targets, are described.
- (ii) Activation of multiple CO-mediated proliferative and tumor-promoting signaling pathways and genes is demonstrated.
- (iii) Formation of an enhancing positive feedback-loop for sustained HO-1 expression and CO production is illustrated.

This leads to the assumption that CO possesses a carcinogenic character, which provides cells with anti-apoptotic and proliferative properties, thus rendering HO-1-overexpressing HCC cells resistant against apoptotic signaling and therapy.

5. Outlook

The thesis provides many insights into the protective and tumor-promoting mechanisms of CO. On the one hand, there are activated signaling pathways (e.g. ERK1/2, STAT3, and sGC/PKG), which are responsible for proliferation and resistance towards apoptosis. On the other hand, CO induced expression of several genes (e.g. *Pkt6*, *Pim3*, *Plau*, and *Cxcl1*), which were already associated with tumor development and spreading, although in organs other than the liver. These findings underline the heterogeneity of HCC and depict the necessity for complex chemotherapeutic treatment for this kind of cancer.

Further work aspires the knock-down of identified potentially tumor protective genes *in vitro* and *in vivo*, either by transfection of siRNA or by transferring shRNA by use of a modified oncolytic vaccinavirus. Specific inhibition of CO-dependent anti-apoptotic and tumor-providing mediators would sensitize a tumor cell for apoptotic stimuli, e.g. chemotherapy or Sorafenib, and would thereby improve the therapeutic effect. This approach has two benefits: (i) healthy cells, which do not show activation of a distinct mediator, remain unaffected by the knock-down and apoptosis induction, and (ii) HO-1, in general, can still mediate its anti-inflammatory, anti-viral and anti-oxidative effects and thus support therapy.

6. References

- Abdel Aziz, Mohamed T. et al. 2008. "Molecular evaluation of apoptotic versus antiapoptotic angiogenic markers in hepatocellular carcinoma." *Clinical biochemistry* 41(12):1008–14.
- Abraham, Nader G., and Attallah Kappas. 2008. "Pharmacological and Clinical Aspects of Heme Oxygenase." *PHARMACOLOGICAL REVIEWS* 60:79–127.
- Abu-Amara, Mahmoud, Shi Yu Yang, Alexander Seifalian, Brian Davidson, and Barry Fuller. 2012. "The nitric oxide pathway--evidence and mechanisms for protection against liver ischaemia reperfusion injury." *Liver international : official journal of the International Association for the Study of the Liver* 32(4):531–43.
- Aktan, Fugen. 2004. "iNOS-mediated nitric oxide production and its regulation." *Life sciences* 75(6):639–53.
- Alberts, B., A. Johnson, and J. Lewis. 2002. "Intracellular Control of Cell-Cycle Events." in *Molecular Biology of the Cell*. New York, NY: Garland Science.
- Alfano, Daniela et al. 2005. "The urokinase plasminogen activator and its receptor Role in cell growth and apoptosis." *Thromb Haemost* 93:205–11.
- Allen, Barry W., Ivan T. Demchenko, and Claude a Piantadosi. 2009. "Two faces of nitric oxide: implications for cellular mechanisms of oxygen toxicity." *Journal of applied physiology (Bethesda, Md. : 1985)* 106(2):662–67.
- Balkwill, F., and a Mantovani. 2001. "Inflammation and cancer: back to Virchow?" *Lancet* 357(9255):539–45.
- Barikbin, Roja et al. 2012. "Induction of heme oxygenase 1 prevents progression of liver fibrosis in Mdr2 knockout mice." *Hepatology (Baltimore, Md.)* 55(2):553–62.
- Bauer, Inge, and Benedikt H. J. Pannen. 2009. "Bench-to-bedside review: Carbon monoxide--from mitochondrial poisoning to therapeutic use." *Critical care (London, England)* 13(4):220.
- Bilban, Martin et al. 2008. "Heme oxygenase and carbon monoxide initiate homeostatic signaling." *Journal of molecular medicine (Berlin, Germany)* 86(3):267–79.

- Binder, Mascha et al. 2010. "Stereotypical chronic lymphocytic leukemia B-cell receptors recognize survival promoting antigens on stromal cells." *PloS one* 5(12):e15992.
- Brauer, Patrick M., and Angela L. Tyner. 2010. "Building a better understanding of the intracellular tyrosine kinase PTK6 - BRK by BRK." *Biochimica et biophysica acta* 1806(1):66–73.
- Calvisi, Diego F. et al. 2007. "Mechanistic and prognostic significance of aberrant methylation in the molecular pathogenesis of human hepatocellular carcinoma." *The Journal of clinical investigation* 117(9).
- Campbell, N. A. 2000. *Biology*. 4. ed. Heidelberg; Berlin; Oxford: Spektrum Akademischer Verlag GmbH.
- Chung, Hun-Taeg, Byung-Min Choi, Young-Guen Kwon, and Young-Myeong Kim. 2008. "Interactive relations between nitric oxide (NO) and carbon monoxide (CO): heme oxygenase-1/CO pathway is a key modulator in NO-mediated antiapoptosis and anti-inflammation." *Methods in enzymology* 441(08):329–38.
- Conde de la Rosa, Laura et al. 2008. "Carbon monoxide blocks oxidative stress-induced hepatocyte apoptosis via inhibition of the p54 JNK isoform." *Free radical biology & medicine* 44(7):1323–33.
- Das, Anindita, Albert Smolenski, Suzanne M. Lohmann, and Rakesh C. Kukreja. 2006. "Cyclic GMP-dependent protein kinase Ialpha attenuates necrosis and apoptosis following ischemia/reoxygenation in adult cardiomyocyte." *The Journal of biological chemistry* 281(50):38644–52.
- Das, Anindita, Lei Xi, and Rakesh C. Kukreja. 2008. "Protein kinase G-dependent cardioprotective mechanism of phosphodiesterase-5 inhibition involves phosphorylation of ERK and GSK3beta." *The Journal of biological chemistry* 283(43):29572–85.
- Dauer, Daniel J. et al. 2005. "Stat3 regulates genes common to both wound healing and cancer." *Oncogene* 24(21):3397–3408.
- Dhanasekaran, D. N., and E. P. Reddy. 2008. "JNK signaling in apoptosis." *Oncogene* 27(48):6245–51.
- Dhawan, Punita, and Ann Richmond. 2002. "Role of CXCL1 in tumorigenesis of melanoma." *Journal of leukocyte biology* 72(1):9–18.

- Dulak, Jozef, Jessy Deshane, Alicja Jozkowicz, and Anupam Agarwal. 2008. "Heme oxygenase-1 and carbon monoxide in vascular pathobiology: focus on angiogenesis." *Circulation* 117(2):231–41.
- Eferl, Robert, and Erwin F. Wagner. 2003. "AP-1: a double-edged sword in tumorigenesis." *Nature reviews. Cancer* 3(11):859–68.
- El-Deiry, W. S. et al. 1993. "WAF1, a potential mediator of p53 tumor suppression." *Cell* 75(4):817–25.
- El-Serag, Hashem B., and K. Lenhard Rudolph. 2007. "Hepatocellular carcinoma: epidemiology and molecular carcinogenesis." *Gastroenterology* 132(7):2557–76.
- El-Serag, Hashem B., Donna L. White, and Zhannat Nurgalieva. 2008. "Epidemiology of Hepatocellular Carcinoma." in *Gastrointestinal Oncology: A Critical Multidisciplinary Team Approach*, edited by and Y. Fong. J. Jankowski, R. Sampliner, D. Kerr. Blackwell Publishing.
- Evgenov, Oleg V et al. 2006. "NO-independent stimulators and activators of soluble guanylate cyclase: discovery and therapeutic potential." *Nature reviews. Drug discovery* 5(9):755–68.
- Fabregat, Isabel. 2009. "Dysregulation of apoptosis in hepatocellular carcinoma cells." *World Journal of Gastroenterology* 15(5):513.
- Fabregat, Isabel, Cesar Roncero, and Margarita Fernandez. 2007. "Survival and apoptosis : a dysregulated balance in liver cancer." *Liver International* 155–62.
- Fang, Ping et al. 2012. "Efficacy and safety of bevacizumab for the treatment of advanced hepatocellular carcinoma: a systematic review of phase II trials." *PloS one* 7(12):e49717.
- Fiscus, Ronald R. 2002. "Involvement of Cyclic GMP and Protein Kinase G in the Regulation of Apoptosis and Survival in Neural Cells." *Neurosignals* 11(4):175–90.
- Folkman, J. 1990. "What is the evidence that tumors are angiogenesis dependent?" *Journal of the National Cancer Institute* 82(1):4–6.

- Foresti, Roberta, Mohamed G. Bani-Hani, and Roberto Motterlini. 2008. "Use of carbon monoxide as a therapeutic agent: promises and challenges." *Intensive care medicine* 34(4):649–58.
- Francis, Sharron H., Jennifer L. Busch, and Jackie D. Corbin. 2010. "cGMP-Dependent Protein Kinases and cGMP Phosphodiesterases in Nitric Oxide and cGMP Action." *PHARMACOLOGICAL REVIEWS* 62(3):525–63.
- Fujii, Chifumi et al. 2005. "Aberrant expression of serine/threonine kinase Pim-3 in hepatocellular carcinoma development and its role in the proliferation of human hepatoma cell lines." *International journal of cancer. Journal international du cancer* 114(2):209–18.
- Gess, B., K. Wolf, M. Pfeifer, G. a Riegger, and a Kurtz. 1997. "In vivo carbon monoxide exposure and hypoxic hypoxia stimulate immediate early gene expression." *Pflügers Archiv : European journal of physiology* 434(5):568–74.
- Ghosh, S., M. J. May, and E. B. Kopp. 1998. "NF-kappa B and Rel proteins: evolutionarily conserved mediators of immune responses." *Annual review of immunology* 16:225–60.
- Glazer, Evan S., Warnar D. Kaluarachchi, Katheryn L. Massey, Cihui Zhu, and Steven a Curley. 2010. "Bioengineered arginase I increases caspase-3 expression of hepatocellular and pancreatic carcinoma cells despite induction of argininosuccinate synthetase-1." *Surgery* 148(2):310–18.
- Gozzelino, Raffaella, Viktoria Jeney, and Miguel P. Soares. 2010. "Mechanisms of cell protection by heme oxygenase-1." *Annual review of pharmacology and toxicology* 50:323–54.
- Graca-Souza, A. V. 2005. "Hematophagy and Heme Toxicity: What can we learn from natural-born vampires?" in *Heme Oxygenase*, edited by L E Otterbein and Brian S Zuckerbraun. Nova Science Publishers, Inc.
- Gray, Henry. 1918. "The Liver." in *Anatomy of the Human Body*. Philadelphia: Lea & Febiger, 1918; on-line published May 2000 by Bartleby.com.
- Haga, Sanae et al. 2003. "Stat3 protects against Fas-induced liver injury by redox-dependent and -independent mechanisms." *J. Clin. Invest* 112:989–98.
- Hanahan, Douglas, and Robert a Weinberg. 2011. "Hallmarks of cancer: the next generation." *Cell* 144(5):646–74.

- Hartsfield, Cynthia L. 2002. "Cross Talk Between Carbon Monoxide and Nitric Oxide." *ANTIOXIDANTS & REDOX SIGNALING* 4(2):301-7.
- Harvey, Amanda J., and Mark R. Crompton. 2004. "The Brk protein tyrosine kinase as a therapeutic target in cancer : opportunities and challenges." *Anti-Cancer Drugs* 15:107–11.
- Hashizume, Hiroya et al. 2010. "Complementary actions of inhibitors of angiopoietin-2 and VEGF on tumor angiogenesis and growth." *Cancer research* 70(6):2213–23.
- Haskill, S. et al. 1990. "Identification of three related human GRO genes encoding cytokine functions." *Proceedings of the National Academy of Sciences of the United States of America* 87(19):7732–36.
- Hoetzel, A., and R. Schmidt. 2006. "[Carbon monoxide--poison or potential therapeutic?]." *Der Anaesthetist* 55(10):1068–79.
- Hofmann, F., a Ammendola, and J. Schlossmann. 2000. "Rising behind NO: cGMP-dependent protein kinases." *Journal of cell science* 113 (Pt 10):1671–76.
- Huang, Hanhua, Abhijit Bhat, Gary Woodnutt, and Rodney Lappe. 2010. "Targeting the ANGPT-TIE2 pathway in malignancy." *Nature reviews. Cancer* 10(8):575–85.
- Jeon, Eun Mi, Hyoung Chul Choi, Kwang Youn Lee, Ki Churl Chang, and Young Jin Kang. 2009. "Hemin inhibits hypertensive rat vascular smooth muscle cell proliferation through regulation of cyclin D and p21." *Archives of pharmacal research* 32(3):375–82.
- Jozkowicz, Alicija, Halina Was, and Jozef Dulak. 2007. "Heme Oxygenase-1 in Tumors: Is It a False Friend?" *Antioxid Redox Signal.* 9(12):2099–2117.
- Kim, Hoe Suk, Patricia a Loughran, Peter K. Kim, Timothy R. Billiar, and Brian S. Zuckerbraun. 2006. "Carbon monoxide protects hepatocytes from TNF- α /Actinomycin D by inhibition of the caspase-8-mediated apoptotic pathway." *Biochemical and biophysical research communications* 344(4):1172–78.

- Kim, Hoe Suk, Patricia a Loughran, Jayashree Rao, Timothy R. Billiar, and Brian S. Zuckerbraun. 2008. "Carbon monoxide activates NF-kappaB via ROS generation and Akt pathways to protect against cell death of hepatocytes." *American journal of physiology. Gastrointestinal and liver physiology* 295(1):G146–G152.
- Kim, Ki Mo et al. 2007. "Carbon monoxide induces heme oxygenase-1 via activation of protein kinase R-like endoplasmic reticulum kinase and inhibits endothelial cell apoptosis triggered by endoplasmic reticulum stress." *Circulation research* 101(9):919–27.
- Kim, Y. M., M. E. de Vera, S. C. Watkins, and T. R. Billiar. 1997. "Nitric oxide protects cultured rat hepatocytes from tumor necrosis factor-alpha-induced apoptosis by inducing heat shock protein 70 expression." *The Journal of biological chemistry* 272(2):1402–11.
- Kimura, H. et al. 1998. "Angiogenesis in hepatocellular carcinoma as evaluated by CD34 immunohistochemistry." *Liver* 18(1):14–19.
- Krebs, H. A., and K. Hanseleit. 1932. "Studies on urea formation in the animal organism." *Hoppe-Seylers Z. Physiol. Chem* 210.
- Kuo, MT, N. Savaraj, and LG Feun. 2010. "Targeted cellular metabolism for cancer chemotherapy with recombinant arginine-degrading enzymes." *Oncotarget* 1(4):246–51.
- Kurinna, Svitlana, and Michelle Craig Barton. 2011. "Cascades of transcription regulation during liver regeneration." *Int J Biochem Cell Biol* 43(2):189–97.
- Lakkisto, Päivi et al. 2010. "Heme oxygenase-1 and carbon monoxide promote neovascularization after myocardial infarction by modulating the expression of HIF-1alpha, SDF-1alpha and VEGF-B." *European journal of pharmacology* 635(1-3):156–64.
- Lautt, W. W. 2009. "Overview." in *Hepatic Circulation: Physiology and Pathophysiology.*, edited by San Rafael (CA). Morgan & Claypool Life Sciences.
- Lee, Han Chu, Miran Kim, and Jack R. Wands. 2006. "Wnt/frizzled signaling in hepatocellular carcinoma." *Frontiers in Bioscience* 11:1901–15.

- Lehmann, Elisabeth et al. 2010. "The heme oxygenase 1 product biliverdin interferes with hepatitis C virus replication by increasing antiviral interferon response." *Hepatology (Baltimore, Md.)* 51(2):398–404.
- Lin, Che-Pin, Chien-Ru Liu, Chun-Nin Lee, Tze-Sian Chan, and H. Eugene Liu. 2010. "Targeting c-Myc as a novel approach for hepatocellular carcinoma." *World journal of hepatology* 2(1):16–20.
- Lind, D. Scott. 2004. "Arginine and cancer." *The Journal of nutrition* 134(10 Suppl):2837S–2841S; discussion 2853S.
- Liu, Xiao-ming, Gary B. Chapman, Kelly J. Peyton, Andrew I. Schafer, and William Durante. 2002. "Carbon monoxide inhibits apoptosis in vascular smooth muscle cells." *Cardiovascular Research* 55:396–405.
- Lodato, Francesca et al. 2006. "Hepatocellular carcinoma prevention: a worldwide emergence between the opulence of developed countries and the economic constraints of developing nations." *World journal of gastroenterology : WJG* 12(45):7239–49.
- Lowenstein, Charles J., and Elizaveta Padalko. 2004. "iNOS (NOS2) at a glance." *Journal of cell science* 117(Pt 14):2865–67.
- Lu, Jeng-Wei et al. 2013. "Clinical implications of deregulated CDK4 and Cyclin D1 expression in patients with human hepatocellular carcinoma." *Medical oncology (Northwood, London, England)* 30(1):379.
- Lundvig, Ditte M. S., Stephan Immenschuh, and Frank a D. T. G. Wagener. 2012. "Heme oxygenase, inflammation, and fibrosis: the good, the bad, and the ugly?" *Frontiers in pharmacology* 3(May):81.
- MacMicking, J. D. et al. 1995. "Altered responses to bacterial infection and endotoxic shock in mice lacking inducible nitric oxide synthase." *Cell* 81(4):641–50.
- Maejima, Yasuhiro, Susumu Adachi, Kino Morikawa, Hiroshi Ito, and Mitsuki Isobe. 2005. "Nitric oxide inhibits myocardial apoptosis by preventing caspase-3 activity via S-nitrosylation." *Journal of molecular and cellular cardiology* 38(1):163–74.
- Maines, MD. 1988. "Heme oxygenase: function, multiplicity, regulatory mechanisms, and clinical applications." *FASEB J* 2(10):2557–68.

- McCoubrey, W. K., T. J. Huang, and M. D. Maines. 1997. "Isolation and characterization of a cDNA from the rat brain that encodes hemoprotein heme oxygenase-3." *European journal of biochemistry / FEBS* 247(2):725–32.
- Medina, Jesús, Alicia G. Arroyo, Francisco Sánchez-Madrid, and Ricardo Moreno-Otero. 2004. "Angiogenesis in chronic inflammatory liver disease." *Hepatology (Baltimore, Md.)* 39(5):1185–95.
- Mori, Masataka. 2007. "Regulation of Nitric Oxide Synthesis and Apoptosis by Arginase and Arginine Recycling." *The Journal of Nutrition* 137:3–7.
- Morris, Sidney M. 2002. "Regulation of enzymes of the urea cycle and arginine metabolism." *Annual review of nutrition* 22(58):87–105.
- Motterlini, Roberto, and Leo E. Otterbein. 2010. "The therapeutic potential of carbon monoxide." *Nature reviews. Drug discovery* 9(9):728–43.
- Mukaida, Naofumi, Ying-Ying Wang, and Ying-Yi Li. 2011. "Roles of Pim-3, a novel survival kinase, in tumorigenesis." *Cancer science* 102(8):1437–42.
- Muntané, Jordi, and Manuel De la Mata. 2010. "Nitric oxide and cancer." *World journal of hepatology* 2(9):337–44.
- Nagasaki, Akitoshi et al. 1996. "Coinduction of Nitric Oxide Synthase , Argininosuccinate Synthetase , and Argininosuccinate Lyase in Lipopolysaccharide-treated Rats." *The Journal of biological chemistry* 271(5):2658–62.
- Nakagawa, Hayato, and Shin Maeda. 2012. "Inflammation- and stress-related signaling pathways in hepatocarcinogenesis." *World journal of gastroenterology : WJG* 18(31):4071–81.
- Nishida, Naoshi, and Ajay Goel. 2011. "Genetic and epigenetic signatures in human hepatocellular carcinoma: a systematic review." *Current genomics* 12(2):130–37.
- Oliner, Jonathan et al. 2004. "Suppression of angiogenesis and tumor growth by selective inhibition of angiotensin-2." *Cancer cell* 6(5):507–16.
- Olson, SY, and HJ Garbán. 2008. "Regulation of Apoptosis-Related Genes by Nitric Oxide in Cancer." *Nitric Oxide* 19(2):170–76.

- Ostrander, Julie H., Andrea R. Daniel, and Carol a Lange. 2010. "Brk/PTK6 signaling in normal and cancer cell models." *Current opinion in pharmacology* 10(6):662–69.
- Paine, Ananta, Britta Eiz-Vesper, Rainer Blasczyk, and Stephan Immenschuh. 2010. "Signaling to heme oxygenase-1 and its anti-inflammatory therapeutic potential." *Biochemical pharmacology* 80(12):1895–1903.
- Parkin, D. Maxwell. 2001. "Global cancer statistics in the year 2000." *lancet oncol* 2(0):533–43.
- Paternostro, Claudia. 2010. "Hypoxia, angiogenesis and liver fibrogenesis in the progression of chronic liver diseases." *World Journal of Gastroenterology* 16(3):281.
- Protzer, Ulrike et al. 2007. "Antiviral activity and hepatoprotection by heme oxygenase-1 in hepatitis B virus infection." *Gastroenterology* 133(4):1156–65.
- Ryter, Stefan W., Jawed Alam, and Augustine M. K. Choi. 2006. "Heme Oxygenase-1 / Carbon Monoxide : From Basic Science to Therapeutic Applications." *Physiol Rev.* 86:583–650.
- Sass, G., R. Barikbin, and G. Tiegs. 2012. "The multiple functions of heme oxygenase-1 in the liver." *Z Gastroenterol* 50(1):34–40.
- Sass, Gabriele et al. 2003. "Heme oxygenase-1 and its reaction product, carbon monoxide, prevent inflammation-related apoptotic liver damage in mice." *Hepatology (Baltimore, Md.)* 38(4):909–18.
- Sass, Gabriele et al. 2008. "Inhibition of heme oxygenase 1 expression by small interfering RNA decreases orthotopic tumor growth in livers of mice." *International journal of cancer. Journal international du cancer* 123(6):1269–77.
- Sato, T. et al. 2001. "Sinusoidal endothelial cell proliferation and expression of angiopoietin/Tie family in regenerating rat liver." *Journal of hepatology* 34(5):690–98.
- Schmidt, Warren N., M. Meleah Mathahs, and Zhaowen Zhu. 2012. "Heme and HO-1 Inhibition of HCV, HBV, and HIV." *Frontiers in pharmacology* 4:3:129.

- Seglen, P. O. 1976. "Preparation of Isolated Rat Liver Cells." in *Methods in cell biology*, edited by D. M. Prescott. Academic Press, Inc. (London) LTD.
- Shambaugh, GE. 1977. "Urea biosynthesis I. The urea cycle and relationships to the citric acid cycle." *Am J Clin Nutr.* (December):2083–87.
- Smollin, Craig, and Kent Olson. 2010. "Carbon monoxide poisoning (acute)." *Clin Evid (Online)* (June):1–12.
- Stepniak, Ewa et al. 2006. "c-Jun / AP-1 controls liver regeneration by repressing p53 / p21 and p38 MAPK activity." *GENES & DEVELOPMENT* 20:2306–14.
- Taub, R. 1996. "Liver regeneration 4: Transcriptional control of liver regeneration." *FASEB J* 10:413–27.
- Taub, Rebecca. 2003. "Hepatoprotection via the IL-6 / Stat3 pathway." *Journal of Clinical Investigation* 112(October):978–80.
- Taura, Kojiro et al. 2008. "Hepatic stellate cells secrete angiopoietin 1 that induces angiogenesis in liver fibrosis." *Gastroenterology* 135(5):1729–38.
- Tenhunen, Raimo, Harvey S. Marver, and Rudi Schmid. 1969. "Microsomal Heme Oxygenase: CHARACTERIZATION OF THE ENZYME." *J. Biol. Chem.* 244.
- Tso, Patrick, and James McGill. 2004. "The Physiology of the Liver." P. 896 in *Medical Physiology*, edited by Rodney A Rhoades and George A Tanner. Lippincott Williams & Wilkins.
- Virchow, Rudolf. 1863. *Die krankhaften Geschwülste*. Berlin: Verlag von August Hirschwald.
- Volti, Giovanni L. I. et al. 2005. "Carbon Monoxide Signaling in Promoting Angiogenesis in Human Microvessel Endothelial Cells." *ANTIOXIDANTS & REDOX SIGNALING* 7(5):704–11.
- Warfel, Noel a, and Wafik S. El-Deiry. 2013. "p21WAF1 and tumourigenesis: 20 years after." *Current opinion in oncology* 25(1):52–58.
- Was, Halina, Jozef Dulak, and Alicja Jozkowicz. 2010. "Heme oxygenase-1 in tumor biology and therapy." *Current drug targets* 11(12):1551–70.

- Wegiel, Barbara, Beek Y. Chin, and Leo E. Otterbein. 2008. "Inhale to survive, cycle or die? Carbon monoxide and cellular proliferation." *Cell Cycle* 7(May):1379–84.
- Wegiel, Barbara, Douglas W. Hanto, and Leo E. Otterbein. 2013. "The social network of carbon monoxide in medicine." *Trends in molecular medicine* 19(1):3–11.
- Wen, Zongmei, Yan Liu, Feng Li, and Tao Wen. 2012. "Low dose of carbon monoxide intraperitoneal injection provides potent protection against GalN/LPS-induced acute liver injury in mice." *Journal of applied toxicology : JAT* Dec;33(12):1424–32.
- Wong, Chun-Ming, and Irene O. L. Ng. 2008. "Molecular pathogenesis of hepatocellular carcinoma." *Liver international : official journal of the International Association for the Study of the Liver* 28(2):160–74.
- Wu, Fei-Xiang et al. 2009. "Identifying serological biomarkers of hepatocellular carcinoma using surface-enhanced laser desorption/ionization-time-of-flight mass spectroscopy." *Cancer letters* 279(2):163–70.
- Wu, G., and S. M. Morris. 1998. "Arginine metabolism: nitric oxide and beyond." *The Biochemical journal* 336 (Pt 1):1–17.
- Wu, Y. et al. 2010. "Accelerated hepatocellular carcinoma development in mice expressing the Pim-3 transgene selectively in the liver." *Oncogene* 29(15):2228–37.
- Xu, Chengfu et al. 2009. "Proteomic analysis of hepatic ischemia/reperfusion injury and ischemic preconditioning in mice revealed the protective role of ATP5beta." *Proteomics* 9(2):409–19.
- Xu, X. R. et al. 2001. "Insight into hepatocellular carcinogenesis at transcriptome level by comparing gene expression profiles of hepatocellular carcinoma with those of corresponding noncancerous liver." *Proceedings of the National Academy of Sciences of the United States of America* 98(26):15089–94.
- Ye, Xiaoying, Won-Suk Kim, Stanislav S. Rubakhin, and Jonathan V Sweedler. 2007. "Ubiquitous presence of argininosuccinate at millimolar levels in the central nervous system of *Aplysia californica*." *Journal of neurochemistry* 101(3):632–40.

- Yu, Hua, Marcin Kortylewski, and Drew Pardoll. 2007. "Crosstalk between cancer and immune cells: role of STAT3 in the tumour microenvironment." *Nature reviews. Immunology* 7(1):41–51.
- Zulehner, Gudrun et al. 2010. "Nuclear beta-catenin induces an early liver progenitor phenotype in hepatocellular carcinoma and promotes tumor recurrence." *The American journal of pathology* 176(1):472–81.

Eidesstattliche Versicherung

Hiermit erkläre ich an Eides statt, dass ich die vorliegende Dissertationsschrift selbst verfasst und keine anderen als die angegebenen Quellen und Hilfsmittel benutzt habe.

A handwritten signature in blue ink, appearing to read 'Schulze', is written on a light gray rectangular background.

Hamburg, Januar 2014

Danksagung

Zuerst möchte ich mich bei Frau Prof. Dr. Tiegs für die Chance bedanken, diese herausfordernde und packende Doktorarbeit in Ihrem Team anzufertigen zu können. Die Möglichkeit an Kongressen teilzunehmen hat meinen beruflichen Erfahrungsschatz sehr bereichert, wofür ich ihr ebenfalls sehr danke. Gleichfalls bedanke ich mich bei Prof. Tiegs für die Möglichkeit und Unterstützung dabei, Familie und Beruf im Rahmen dieser Dissertation erfolgreich vereinen zu können.

Gleichzeitig bedanke ich mich auch bei meiner Betreuerin Frau Prof. Dr. Sass, die mir das spannende Feld der Krebsforschung und Therapie näher gebracht hat. Ich danke ihr für die kreativen Diskussionen, Motivation und ihr Vertrauen in mich, meine Ideen und Experimente.

Diese Dissertation wurde im Rahmen eines integrierten Graduiertenkollegs angefertigt, welches die notwendigen finanziellen und wissenschaftlichen Mittel bereitstellte. Dafür bedanke ich mich bei den Vorsitzenden des SFB841 "Leberentzündung: Infektion, Immunregulation und Konsequenzen". Besonderer Dank gilt hier meinen Betreuern Frau Dr. Dandri und Herr Dr. Wege, die mein Projekt mit ihren fruchtbaren Diskussionen und hilfreichen Tipps anregten.

Selbstverständlich danke ich auch meinen Kollegen, unter denen ich auch Freunde gefunden habe, für ihre Hilfe nicht nur im Labor, sondern auch am Schreibtisch und in der Diskussionsrunde. Ohne sie hätte die Arbeit an dieser Dissertation nur halb so viel Spaß bedeutet. Elena Tassika gilt besonderer Dank für die Isolation primärer Hepatozyten und dafür, dass sie immer einen Termin und eine Maus für mich parat hatte. Auch Christine Loscher danke ich für ihre exzellente technische und moralische Unterstützung am PC sowie der Bench.

Im Weiteren bedanke ich mich für die tolle und ergebnisreiche Kollaboration mit Herrn Prof. Dr. Schlüter und seinem Team (Institut für Klinische Chemie, UKE). Die Arbeit mit Dr. Maria Trusch an der 2D PAGE und am Massenspektrometer hat mich fasziniert und meinen Erfahrungsschatz um eine technisch anspruchsvolle Methode sowie gleichermaßen eine innovative Sicht auf die Biologie bereichert.

Ohne alle helfenden Hände namentlich nennen zu können, bedanke ich mich auch bei allen weiteren Kollaborationspartnern für das Bereitstellen von Materialien und Versuchstieren, die eine Reihe meiner Experimente erst ermöglichten.

Herzlich danken möchte ich auch Frau Dr. Lauke-Wettwer, der Gleichstellungsbeauftragten des UKE, die immer ein offenes Ohr für meine beruflichen und privaten Anliegen hatte und mir mit Rat und vor allem Tat zur Seite stand.

Zum Schluss danke ich den wichtigsten Menschen - meiner Familie und meinen Freunden. Meinem Mann Markus gilt besonderer Dank für seine unendliche Unterstützung, seine treibende Kraft, nicht aufzugeben, und seine selbstverständliche Hilfe. Meiner Tochter Zoe danke ich für die große Herausforderung, Beruf und Familie zu vereinbaren, durch die ich als Mensch gewachsen bin und die ich nicht missen möchte. Meinen Eltern und meiner Schwester danke ich für ihren Ansporn, Geduld, Vertrauen und die vielen guten Zusprüche, die mir auch in schweren Zeiten geholfen haben. Meinen Freunden Nina und Rüdiger danke ich für die moralische Unterstützung und ihre Motivation, auch fernab von Hamburg.

Julia Schildgen
Entenweg 41
22549 Hamburg
Tel.: 0170-8183779
Email: j.solomentsew@uke.de